Spatial and Temporal Distribution of a Marine Microbial Parasite, Syndiniales MALV I and II, within St Helena Bay.

Shani Fourie

Thesis presented for the Masters' degree

in the Department of Biological Sciences

Faculty of Science

University of Cape Town

2025

Supervisor: Dr Emma Rocke

Declaration

I, … Shani Fourie…, hereby declare that the work on which this thesis is based is my original work (except where acknowledgements indicate otherwise) and that neither the whole work nor any part of it has been, is being, or is to be submitted for another degree in this or any other university. I empower the university to reproduce for the purpose of research either the whole or any portion of the contents in any manner whatsoever.

Signature: Signed by candidate

Date: ……12/02/2025……..

Table of Contents

Abstract

MALV I and II are globally distributed marine microbial parasites that infect and kill a wide range of phytoplankton hosts. These organisms play an important role in bloom dynamics, are suspected to terminate algal blooms, and contribute significantly to carbon fluxes, an important process required to lock away greenhouse gases. The study aims to investigate the spatial and temporal distribution of MALV I and II and their hosts in the Benguela upwelling system, one of the four major Eastern Boundary Upwelling Systems (EBUS). A Fluorescent In Situ Hybridization (FISH) technique was used to identify and quantify MALV I and II in samples taken at 0m and 10m respectively over the course of 10 consecutive days during an upwelling event in December of 2016, and in samples taken at 1m and 25m respectively over the course of 5 consecutive days during a stratified period in April 2019 within St Helena Bay. Microscopy observations revealed a distinct difference in their infection dynamics between an active upwelling season (austral spring and summer) and a stratified period (austral autumn and winter), with distinctly different phytoplankton communities present in the water column between these two seasons. Whilst temperature and silicate were significant factors correlating with the infection rates at the surface during an upwelling period, biological factors (presence of MALV I and II hosts) appeared to be the most important contributor. Furthermore, 18S rRNA data confirmed that MALV I and II dominated the water column, with group I exhibiting the highest relative abundance, contradicting microscopy observations which showed no significant difference in infection rates between MALV I and II. This shed light on the realities of amplicon data, especially with high gene copy numbers present in MALV rRNA. This study applies a holistic approach to understanding the infection dynamics of MALV I and II and in doing so revealed a transition from diatom hosts during an active upwelling period to dinoflagellate hosts during a stratified period in the same region. Ultimately, the MALV I and II populations are dependent upon available hosts to infect, and the infection rates are driven by multiple environmental and biotic factors.

Chapter 1: Introduction

Marine microbes and their lifestyles

Marine microbes are unicellular organisms that occupy virtually all marine environments (Caron et al., 2012), from the surface waters of the eutrophic zone to the dark oxygen poor waters of the deep sea known as the abyssopelagic (3000-6000m below sea level) and hadalpelagic (6000-11000m below sea level) zones. Microbes inhabit even the most extreme environments such as boiling hydrothermal vents to the freezing waters of underground lakes within the Antarctic. Marine microbes include bacteria, archaea, viruses and single-celled eukaryotes (also known as protists) and are categorized according to a logarithmic scale that include picoplankton (0.2-2µm), nanoplankton (2-20µm), microplankton (20-200µm), and mesoplankton (>200µm) (Sieburth, 1979; Lévêque, 2001). The size fractions that contribute most to the total biomass of the lower trophic levels are the pico- and nanoplankton (Vaulot et al., 2008; Worden and Not, 2008; Jardillier et al., 2010; Massana, 2011). The word plankton refers to microorganisms that have no means of propulsion and passively drift within the water column (Newell and Newell, 1970).

Microbes employ several lifestyles such as autotrophy (generating their own food via carbon fixation in photosynthetic processes), heterotrophy (obtaining food and energy via the consumption of organic carbon), or mixotrophy (switching between autotrophic and heterotrophic processes) (Willey et al., 2011; Mitra et al., 2014). In the ocean, there is an intricate balance between the production of organic material by the autotrophs and the respiration by the heterotrophs, mainly by bacteria, recycling the organic material back into an inorganic state via a process called remineralization (Kaiser, 2011).

Primary production begins with phototrophic organisms such as dinoflagellates and diatoms (Fenchel, 1988) in addition to Chroococcoid cyanobacteria which arguably represent the largest fraction of photosynthetic activity in surface waters (Johnson and Sieburth, 1979; Iturriaga and Mitchell, 1986; Stockner and Antia, 1986; Li and Platt, 1987). These organisms use sunlight to fix atmospheric carbon which can then be consumed by heterotrophic nanoflagellates, phagotrophic microplankton, and zooplankton such as copepods, which in turn get consumed by fish and predators higher up the food chain (Fenchel, 1988).

The ocean's primary production is dependent on four major factors which include light, nutrient availability, stability, and mixing (Falkowski et al., 1998). Available light is by far the most important factor, as it will determine the rate of photosynthetic activity of phytoplankton (Kirk, 1994). It is both the quantity and quality of light that controls the rate of photosynthesis. Typically, light does not penetrate deep and is restricted to the upper 50m of the water column, depending on the amount of

particulate or dissolved organic matter, bacteria, plankton, and sediment within the water that contribute to the scattering of light, limiting primary production to the upper few meters of the eutrophic zone. In clear waters, however, light can penetrate up to 200m, but even in the clearest of waters, no light penetrates below 1000m. The photosynthetic rate is linearly proportional to the irradiance up to a specific point known as P_{max} where photosynthesis is saturated. At too high irradiances, photoinhibition can occur due to damaged electron transport chains or cellular membranes crippling photosynthesis (Kaiser, 2011). Some astonishing adaptations have evolved in algal cells to prevent this damage by rearranging their chlorophyll within the chloroplasts and arranging the chloroplasts around the nucleus (Kaiser, 2011).

The next factor influencing the rate of photosynthesis is the availability of nutrients. The main limiting nutrients are found in various chemical species of nitrogen (NO_3^-, NO_2^-, NH_4^+, NH_3, N_2, and urea), phosphorus (HPO_4^{2-}, PO_4^{3-}, and $H_2PO_4^-$), and sulphur (SO_4^{2-}, and H_2S). Trace elements such as iron or manganese, amongst other metals, should not be overlooked, as they can be the rate-limiting factor in primary production within the Southern Ocean (Kaiser, 2011). Organisms will compete with one another for these essential resources, which limits the total biodiversity, and ultimately influences the structural community composition within the euphotic zone (Dutta et al., 2014; Ryabov and Blasius, 2011; Tilman, 1982)

Inorganic carbon in the marine environment is rarely a rate limiting nutrient and is part of the major pools of carbon within the world's oceans. These pools of carbon are largely controlled by the so called carbon pump and are in the forms of: dissolved inorganic carbon or DIC (~3200 pentamoles of carbon (Pmol-C), Dittmar and Stubbins, 2014); dissolved organic carbon or DOC (~55 Pmol-C, Williams and Druffel, 1987); particulate organic carbon or POC (~1-2 Pmol-C, Eglington and Repeta, 2013); and deposits of biogenic carbon in marine sediments (~1 000 000 Pmol-C, Sundquist and Visser Ackerman, 2013).

The last two abiotic factors that play a role in primary production are water stability and mixing. Stability is essential to allow for enough time for algae to grow whereas water mixing is required to replenish nutrients in the surface waters with those from deeper cooler waters. It is ultimately these physical processes that will influence the rate of primary production.

The microbial loop

The traditional food chain is more complex than previously thought. It is found that most of the primary production isn't consumed by heterotrophs, but rather the photosynthate of the primary producers gets shuttled via dissolved and particulate organic matter (DOM and POM) to bacteria. Bacteria directly incorporate DOM and POM, making the organic carbon once again available to

heterotrophic organisms, particularly nanoflagellates (Fenchel 1982; Caron et al., 1985), as bacteria are too miniscule for most filter feeding zooplankton (Johson, P., 1982; Fenchel, 1984). The DOM is composed out of amino acids, humic acids, and aromatic hydrocarbon polymers (Ma et al., 2021) and serves as an energy source for phytoplankton (Minor and Oyler, 2023) which once again can contribute to the photosynthate exudates. This shunt of DOM between photosynthetic pico- and nanoplankton and heterotrophic picoplankton that nanoplankton graze upon forms the so-called microbial loop (Figure 1). Zooplankton grazes upon nanoflagellates, bacteria, and phytoplankton, controlling their community composition and abundance (Azam et al., 1983; Hahn and Höfle, 2001) and in turn the zooplankton feeds fish and larger predators. Viruses also play a large role in the microbial loop and are the most abundant microbial group within the ocean (Vincent and Vardi, 2023). The viral loop consists of the lysis process of autotrophic and heterotrophic plankton and bacteria, which directly contributes to the release of DOM from the host cells' inner contents. The released DOM promotes further heterotrophic picoplankton and bacterial growth which heterotrophic nanoflagellates can graze upon (Fuhrman and Suttle, 1993; Suttle, 1994, 2007).

The DOM contents are regulated via sources like pico-, nano-, and microplankton secretion and viral lysis and sinks such as biological uptake or photodegradation (Thornton et al., 2014; Cory et al., 2015; Duan et al., 2022). DOM that are not shuttled back in the microbial loop, and POM that aggregates and sinks to the sea floor contribute to the biological carbon pump (Legendre et al., 2015; Stukel and Ducklow, 2017).

According to the data collected via the TARA expedition that sampled from 68 stations across the global oceans, more than half of the richness and abundance of sequences within the nanopicoplankton category were composed of parasites (de Vargas et al., 2015). Marine microbial parasites are ubiquitous in the global oceans and comprise of prokaryotes and eukaryotes (de Vargas et al., 2015; Anderson and Harvey, 2020). They are typically categorised by short generation times, small size, high reproduction rates, and a simple life cycle usually within a single host. Using co-occurrence analyses made from operational taxonomic unit (OTU) abundance data, parasite-host pairs can be inferred, as was done in the TARA Oceans study, which suggested that parasitism was the most abundant taxon-taxon interaction recorded (Lima-mendez et al., 2015). Increased water temperatures have been linked to increased parasite prevalence and is considered to play an important role during warmer conditions (Rohde 1984). The role of parasites within the microbial loop has been understudied and to fully understand parasite infection dynamics and how they contribute to carbon and nutrient cycling within the microbial loop it is important to take a holistic approach and

to investigate time series data as marine communities are dynamic over time, especially in coastal regions with varying environmental factors.

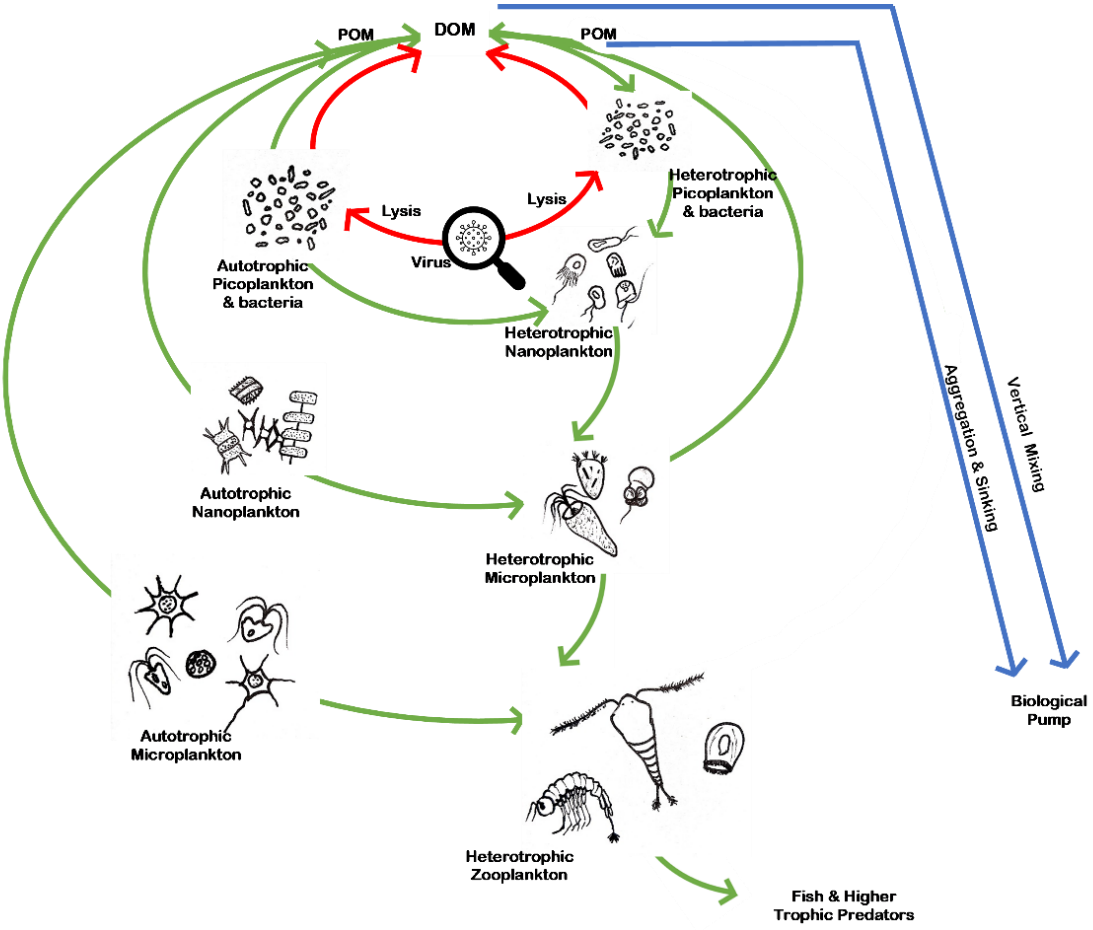

Figure 1: A schematic representation of the microbial loop between autotrophic and heterotrophic microbes (green), the role of viruses within the microbial loop (red), and the biological pump (blue). Adapted from Fenchel, 1988.

Determinants of microbial community compositions

Studying community composition dynamics and environmental parameters can provide insight into which organisms have close interactions and how these interactions occur (Fuhrman et al., 2015). The composition, diversity, and abundance of protists are subject to processes that either induce growth, such as upwelling events that supplement large quantities of nutrients to oligotrophic waters, or promote mortality, such as predator-prey or parasite-host interactions (Decelle et al., 2015; Fuhrman et al., 2015; Rose and Caron, 2007).

Thermal Stratification in Water Bodies

The ocean water column is divided into distinct layers namely the surface mixed layer, the thermocline, and the deep-water layer, formed by differences in salinity, temperature due to solar radiation and density (Jamshidi and Yousefi, 2021). Warmer temperatures are found at the surface (0 to 100/200m) and decline in the intermediate layer (100/200m to 1000/1500m) after which it is relatively constant (less than 4°C) in the deep layer (1000/1500m and deeper). Water density is a mirror image of the water temperature profile as density is largely determined by temperature. The salinity is variable within the surface and intermediate layers due to precipitation, evaporation, and river runoff, but is uniform in the deep layers (34.5 to 35 ppt (parts per thousand)). The surface layer experiences water mixing via surface winds, currents, and waves, however during warmer seasons such as spring and summer, the surface layer can heat up and become less dense, forming a thermocline (a sudden change in temperature over a small depth) as well as a pycnocline. The extent of the pycnocline will determine the stability of the water, with a large density difference resulting in higher stability (Castro and Huber, 2010). Water stability and water mixing will influence the microbial community dynamics in the surface layer (Wang et al., 2021).

The Benguela current

The Benguela Upwelling System, located off the west coast of South Africa, is one of the world's four major Eastern Boundary Upwelling Systems (EBUS) and is considered one of the most productive marine regions, playing a vital role in supporting ocean ecosystems (Pitcher and Louw, 2021). This current is a body of water that flows parallel to the southeastern coast of Africa in a North to North-westward direction (Nelson and Hutchings, 1983). Upwelling on the western coast of South Africa occurs when the south-easterly winds from the South Atlantic Anticyclone push the surface water away from the shore via Ekman transport. The wind causes friction on the surface waters transferring energy to the underlaying water layers which causes the water layer to move. This movement deviates at an angle of 20-40° due to the earth's movement known as the Coriolis effect. Each water layer causes the underlaying water layer to move again at this deviated angle from the one above, and the energy transported decreases with each layer due to friction resulting in a net water movement of 90° west from the wind direction in the southern hemisphere (and 90° east in the northern hemisphere). This is known as Ekman transport, named after Vagn Walfrid Ekman who investigated wind driven ocean currents in 1902. The movement of the surface water away from the coast forces cold nutrient-rich but oxygen poor water from the depths to rise to the well-lit surface where it rapidly gets oxygenated via phytoplankton growth and oxygen diffusion (Nelson and Hutchings, 1983).

These nutrient-rich upwelled waters originating below the pycnocline support a diverse range of marine life as well as commercial fisheries which are important for the coastal communities.

Occasionally upwelling events can have a negative impact on marine life and commercial fisheries (i.e. hypoxia when algae blooms escalate beyond control of grazers) (Pitcher and Louw, 2021). Amongst the nutrients such as phosphorus, nitrogen, and iron, which are vital for phytoplankton, dinoflagellate cysts that have accumulated in the sediment (Belmonte and Rubino, 2019) also rise to the surface and cause algal blooms, including harmful algal blooms (HABs), oxygen-depleted waters, and a change in the ocean chemistry (Anderson et al., 2003; Garcés et al., 2004).

Diatoms are the first algae to colonize and dominate the eutrophic waters post upwelling (Lamont et al., 2014). Due to their small size and ability to rapidly multiply under favourable conditions, diatoms showcase high standing stocks, resulting from high growth rates and productivity which is typically associated with upwelled turbulent waters (Tilstone et al., 2000). The production of diatoms allows for the allochthonous nitrogen from deeper waters to be transformed into nitrogen sources such as ammonium and dissolved organic nitrogen (DON) which upon diatom cell death is released and can readily be incorporated by dinoflagellates, ultimately causing a shift from diatom-dominated to dinoflagellate-dominated waters (Álvarez-Salgado et al. 1996, María Trigueros and Orive, 2001). With this change in succession of diatoms to dinoflagellates, there are short term changes in the genera of diatoms according to nutrient regimes and hydrography (Margalef, 1958) and are revealed in carbon fixation patterns (Gallegos, 1992; Lohrenz et al., 1994). Because diatoms such as *Skeletonema costatum* and *Thalassiosira nana* have high standing stocks they are the first to dominate freshly upwelled waters, and are succeeded by larger diatoms such as *Cerataulina, Chaetoceros, Lauderia, Coscinodiscus* and *Thalassionema* which have lower growth rates and productivity (Margalef 1958). As the water ages and becomes more stratified and nutrients such as phosphate and silicate become limiting, flagellates become the dominant phytoplankton (Legendre 1990; Painting et al., 1993; Lamont et al., 2014).

Syndiniales, a Marine Alveolate (MALV) group

There are several microbial interactions found in the surface layers of the ocean. Symbiotic interactions between planktonic organisms and protists play an important role in the marine food web as they are key players in the primary production and consumption of organic carbon, fixation of nitrogen, and the biogeochemical cycling of key elements required for growth (Karl et al., 2012; Thompson et al., 2012; Worden et al., 2015; Cabello et al., 2016). The types of plankton symbiosis identified are mutualism as seen in diatom-diazotroph associations (Vincent and Bowler, 2022), commensalism as exhibited by heterotrophic bacteria living on the surface of phytoplankton and utilizing the alga's excreted organic carbon (a paradoxical ecological relationship (Bratbak and Thingstad, 1985)), and parasitism typically seen in dinoflagellates with *Amoebophrya* being well known and widely distributed in coastal waters (Park et al., 2004). Plankton symbiosis has major

ecological roles. They aid in nutrient cycling, carbon export, primary productivity, and ecosystem stability. A long-term study done by Karl et al., (2011) found that symbiosis between nitrogen fixing cyanobacteria and diatoms contributed to a large part of carbon sequestration, and important aspects of atmospheric carbon regulation. Microbial communities' diversity and structure have been recognized to be influenced by parasitism, with parasitism being a key evolutionary pressure on their hosts (Lively, 1996; Morran et al., 2011; Toft & Karter, 1990). This influence can have both negative and positive interactions on diversity. For instance, dinoflagellate parasites can infect and kill dinoflagellate hosts, diminishing their abundance and ultimately causing a microbial community shift (Álvarez-Salgado et al. 1996; Trigueros and Orive, 2001; Zhou et al., 2017; Spilling et al., 2018). Parasitism can potentially play a role in regulating POC sinking and serve as a proxy for carbon export (Anderson et al., 2024). Symbiotic relationships are key factors required for certain organisms such as sponges, corals and many other marine invertebrates to survive (Fan et al., 2013) contributing to the ecosystem stability.

Parasitism has widespread interactions with protist communities which can at times have a much greater mortality effect on the protist composition than grazing activities by microzooplankton (Montagnes et al., 2008; Salomon and Stolte., 2010; Jephcott et al., 2016; Bjorbækmo et al., 2020). The biogeochemical cycle can be altered by parasitism through rerouting biomass away from the standard food web, supplying the microbial loop with elements such as carbon and nitrogen (Yih and Coats., 2000; Park et al., 2004; Salomon et al., 2009). It is therefore critical to study and understand which interactions are dominating in the marine environment to quantify their contributions to the biogeochemical cycle (Worden et al., 2015; Fuhrman et al., 2015). Parasitism plays a crucial ecological role in the marine environment by maintaining ecosystem balance and facilitating the transfer of biomass across different trophic levels (Johnson et al., 2013; Dougherty et al., 2016; Paseka et al., 2020).

Syndiniales is represented by five Marine Alveolate groups (MALV I-V), with the most sequences from environmental samples assigned to Syndiniales Groups I and II, with 8 and >100 clades respectively (Guillou et al., 2008; Cai et al., 2020). Group II has the most diversity (Guillou, et.al., 2008), and consists of a single described genus, *Amoebophrya* which are parasites that inhabit marine waters globally (Guillou et al., 2008, Siano et al., 2011; de Vargas et al., 2015). This group has an extensive range of hosts, from unicellular organisms such as radiolarians, ciliates, and dinoflagellates, to Metozoa (Cachon, 1987; Coats, 1999; Park et al., 2004; Guillou et al., 2008; Chambouvet et al., 2011; de Vargas et al., 2015). Several *Amoebophrya* spp. are obligatory killers of their dinoflagellate host in order to complete their life cycle (Chambouvet et al., 2011). The lysis of their hosts, specifically harmful toxic

producing dinoflagellates, can lead to the demise of HABs (Montagnes et.al., 2008, Guillou et.al., 2008). This is of ecological significance because dinoflagellates are key primary producers that can form HABs which can result in oxygen depletion at depth, and in some cases cause noxious conditions that may create illnesses for animals and humans leading to economic losses (Smayda, 1997; Zingone and Enevoldsen, 2000; Anderson et al., 2012; Wu et al., 2022). The formation of these blooms is largely controlled by abiotic conditions such as water stratification, light, salinity, and nutrient concentrations (Shilo, 1967; Smayda, 2002). However, the parasite abundance and infection rates are thought to be mainly driven by the host density, with planktonic blooms resulting in increased infections (Park et al., 2004; Coats et al., 1996).

Several studies have shown that the parasitic *Amoebophrya* spp. are responsible for the demise of noxious microalgal species, decreasing or even terminating HABs (Chambouvet et al., 2008; Park et al., 2002; Park et at., 2004; Velo-Suárez et al., 2013; Li et al., 2014; Choi et al., 2017). Given that HABs have become increasingly prevalent due to eutrophication along coasts and possibly global change (Anderson, 1997), studies on *Amoebophrya* spp. infecting dinoflagellates have received more interest to explore the potential of top-down control of HABs, stressing the need for us to study their physiology (Coats & Bockstahler, 1994; Coats et al., 1996; Kim et al., 2004; Chambouvet et al., 2008; Decelle et al., 2021), to quantify their impact on the carbon cycle, and to understand their effect on microbial diversity and coevolution (Jephcott et al., 2016).

The duration of the life cycle of *Amoebophrya* within optimal conditions is about 2-3 days. It starts with an infection process by the free-swimming biflagellate dinospore (zoospore) that are between 1 and 12 µm in diameter (Sehein et al., 2022). The dinospore attaches to the outer surface of a host and either invades the cytosol or the nucleus where it will remain for the next two phases of its life cycle, the trophont and sporont stages (Coats, 1999; Park et al., 2004). These are the endoparasitic stages in the life cycle, where growth via nuclear division and flagellar replication occurs without the completion of cytokinesis until the host volume is filled (Fritz and Nass, 1992). The parasite breaks the host membrane and a motile veriform is formed, typically identified by a “beehive” structure with multiple nuclei and a mastigocoel cavity (Fritz and Nass, 1992; Coats and Boackstahler, 1994; Coats and Park, 2002). This is a short-lived structure that will fragment into 60 to 400 dinospores which will be able to infect new host cells and begin the life cycle once more (Coats and Boackstahler, 1994; Coats and Park, 2002). It is crucial for the dinospores to find a new host as they have a short survival time of up to 10 days in the water column (Coats and Park, 2002). A study has observed that the Syndiniales parasite remained within a dormant resting stage of one of the known hosts, *Scrippsiella acuminata* within a culture (Chambouvet et al., 2011a, b), suggesting a method of survival when a bloom dies, and host

dormant spores sink to the ocean floor. Future upwelling currents will bring the dormant spores of the hosts still infected with Syndiniales to the euphotic zone, where a bloom will once again occur, and the Syndiniales parasite can once again start its life cycle.

Several studies have shown that factors such as temperature (Berdjeb et al., 2018; Yih and Coats, 2000), nutrients (Siano et al., 2011), the extent of physical water mixing (Coats and Bockstahler. 1994), and the water column depth (Coats et al., 1996), may play a role in the population dynamics of Syndiniales.

A widely distributed and abundant microalga that dominates HABs is the dinoflagellate *Alexandrium* sp., *Scripsiella acuminata* (formally *Scrippsiella trochoidea*, (Kretschmann et al., 2015)) one of Syndiniales' host organisms (Gottschling et al., 2012; Dai et al., 2012). This dinoflagellate has two distinct life cycles: clonal and sexual reproduction (Wyatt and Jenkinson, 1997). Clonal reproduction leads to a rapid increase in the population, which may lead to HABs, and sexual reproduction leads to cysts that sink to the sediment and can remain viable for several years (Wyatt and Jenkinson, 1997; Anderson, 1998; Anderson et al., 2012). Although dinoflagellates are the main hosts for Syndiniales group II, a study done by Sassenhagena et al., (2020) has hypothesised that diatoms might be a potential host for these parasites, and that the host range might be larger than previously expected. This is significant for the southern Benguela as the inshore plankton communities are largely diatom dominated during strong upwelling events (Walker and Peterson, 1991; Barlow et al., 2001). To understand the bloom dynamics of the Benguela, it is vital to understand the diatom-parasite population dynamics.

Hypotheses

Based on previous studies the theory is that the Syndiniales parasites will play a role in the degradation of an algal bloom (Coats and Bockstahler, 1994; Coats et al., 1996; Coats and Park, 2002; Park et al., 2004; Montagnes et al., 2008; Velo-Suarez et al., 2013). Infections by Syndiniales are mainly driven by the host density; it is therefore believed that planktonic blooms will result in increased infections (Park et al., 2004; Coats et al., 1996; Chambouvet et al., 2011). These infected dinoflagellates and potentially diatom host cells will ultimately die as Syndiniales completes its lifecycle and causes lysis. I hypothesize that during the termination of a bloom, the total number of infections by Syndiniales will decrease as the total number of eukaryotic protist cells decreases.

This thesis will investigate the spatial and temporal distribution and infection dynamics of Syndiniales in the Benguela upwelling system, one of the four major EBUSs. In the first experimental chapter, Chapter 2, Fluorescent In-Situ Hybridization (FISH) will be used to identify and quantify Syndiniales in samples taken at 0m and 10m respectively over the course of 10 days during an upwelling system in

Elands Bay located within St Helena Bay during an austral summer period. Furthermore, a CARD-FISH analysis will be used to validate the data obtained by the FISH procedure. In the second experimental chapter, Chapter 3, FISH samples will be analysed to identify and quantify Syndiniales in samples taken at 1m and 25m during a 5-day period in austral autumn at an anchor station in the Berg River Line Station 6 located in St Helena Bay during a stratified period.

Chapter 2: Infection dynamics of Syndiniales during an upwelling event in Elands Bay

The Benguela current during an austral spring/summer period

The topography of the Cape Peninsula and Cape Columbine regions has an impact on the Benguela upwelling system leading to spatial and temporal variation along the western coast of Southern Africa (Harris and Shannon, 1979; Nelson and Hutchings, 1983). This irregularity in upwelling was first investigated by Hart and Currie in 1950 and 1951 and published in 1960 (Hart and Currie, 1960). Further studies have shown that the shelf width of the eastern coast impacts the chlorophyll concentrations, with wider shelf regions of approximately 200m (Nelson and Hutchings, 1983) supporting higher chlorophyll concentrations, however, it is unclear if this difference is due to increased iron availability or grazing pressures (Carr and Kearns, 2003). The wider shelf assists stratification and stability which support dinoflagellate growth as they are susceptive to turbulent waters (Cullen and MacIntyre, 1998; Probyn et al., 2000). St Helena Bay is thought to receive its upwelled water from Cape Columbine via a cyclonic gyre (Holden 1985) and supports high productivity due to the stability of the system (Mitchell-Innes and Walker, 1991).

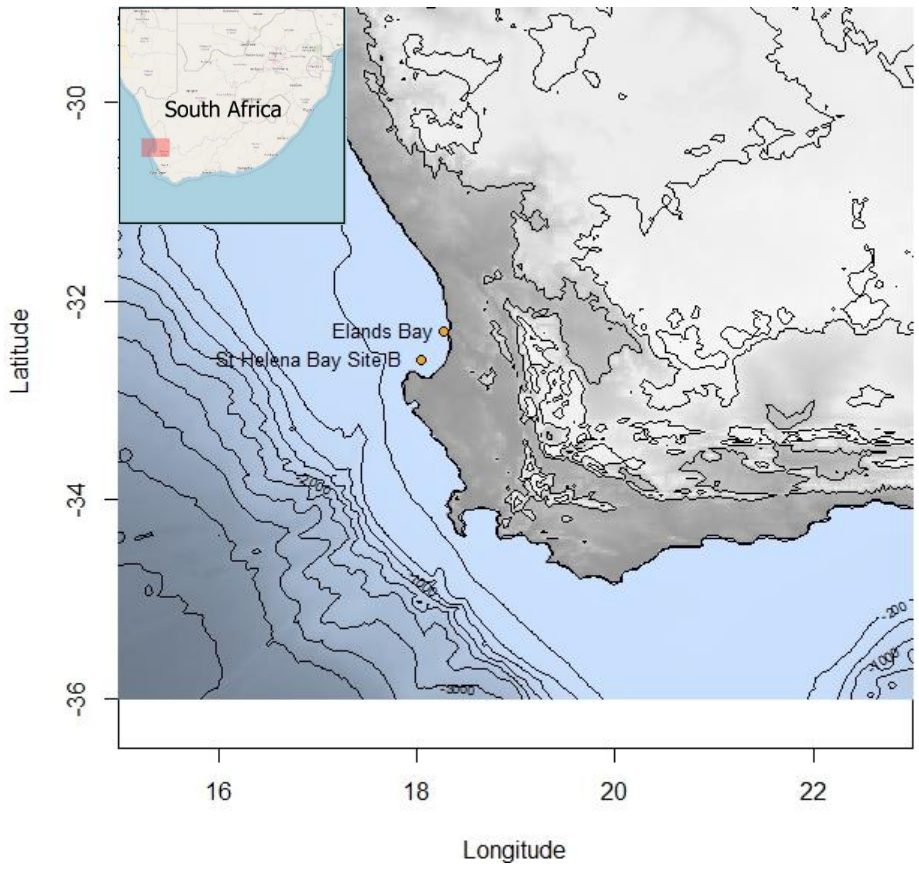

Figure 2: Map showing the study sites in St Helena Bay. The Elands Bay orange point (32.308°S; 18.275°E) indicates the fixed-point station where sampling was conducted in November/December 2016. The St Helena Bay

Site B orange point (32.596°S, 18.043°E) indicates the Berg River line fixed-point station (station 6) where sampling was conducted in April 2019.

The study site of this thesis was in Elands Bay situated within St Helena Bay (32.308°S; 18.275°E; bottom depth of ~30 m), a characteristic retention zone north of the Cape Columbine that support large quantities of primary production year-round (Brown et al., 1991). Retention zones are of ecological significance, as the body of water in these zones retain and concentrate planktonic organisms, resulting in high chlorophyl concentrations year-round (Weeks et al., 2006). The St Helena retention zone has high water stability, which allows for the large primary production found there (Mitchell-Innes and Walker, 1991). This stability is a very important characteristic required for dinoflagellates to thrive (Horstman, 1981) as they require strong stratification of the surface waters. The water residence time within St Helena Bay can be up to 25 days (Walker and Pitcher, 1991, Bailey and Chapman, 1991).

During the spring and summer months, this bay experiences "pulsed" upwelling events that last between 3 and 10 days (Nelson and Hutchings, 1983). Sampling was done during one of these "pulsed" upwelling events during the summer of 2016 from the 29th of November to the 8th of December.

Methods and Materials

Sample collection and environmental data

Five-liter water samples were collected for 10 consecutive days at around 10 am aboard the MA-RE 17.3 m Gemini inflatable craft during an upwelling event in December 2016 (Burger et al., 2020). Water samples were taken at 0m and 10m respectively and prepared for FISH by the addition of 37% formaldehyde with a final concentration of 1%. The water samples were then filtered out onto a membrane filter with a pore size of 0.2µm and 47mm diameter. Each membrane filter was placed in a Petri dish and was stored at -80°C until further processing took place in 2023.

The hydrography of the water was obtained via dispatching a handheld CTD (Sea Bird 1900 Plus) sensor from the surface to within 5m of the seafloor prior to the sampling collection (only done for days 5 to 10). The methods of obtaining the potential density anomaly of seawater ($\sigma\theta$; kg m−3) and the CTD derived salinity data are explained in more detail in the Burger et al., (2020) paper. Data for days 1 to 4 were estimated using linear regression models explained in detail in the Burger et al., (2020) paper.

Burger et.al (2020) explains how the oxygen, nutrients, and Chlorophyll *a* samples were taken and measured and how the net primary production, nitrate and ammonium uptake rates were calculated.

Laboratory and microscopy work

Fluorescent in Situ hybridization is a molecular technique that is used to identify and detect microorganisms without the use of cultures. Although a very useful tool in the microbial ecological world, some of its downfalls are insufficient sensitivity due to the limited target number of molecules in the cell, inferior probe hybridization efficiency, and low permeability of the probe into the cell (Amann et al., 1995). The sensitivity of FISH has been advanced with a technique called catalyzed reporter deposition (CARD)-FISH with 10-fold stronger fluorescent signal intensity (Kubota., 2013). CARD-FISH has been successfully used to quantify the free-living dinospores of Syndiniales in coastal and open waters (Chambouvet et al., 2011; Siano et al., 2011; Velo-Suarez et al., 2013). The disadvantage of CARD-FISH is that it is extremely expensive compared to FISH, and therefore in this thesis, FISH was used to process all the samples in triplicates, and CARD-FISH was used to validate the FISH results (no replicates were done for CARD-FISH).

The following FISH protocol was used to prepare each sample for microscope observation: Each membrane filter was divided into 9 wedges; 3 wedges were treated with the Syndiniales 1 probe 5'-TCC TCG CGT TAG ACA CGC -3' (molecular weight of 5435g/mol) and 3 wedges were treated with the Syndiniales 2 probe 5'- CAC CTC TGA CGC GTT AAT -3' (molecular weight of 5435g/mol), the remaining 3 wedges were kept for a CARD-FISH procedure. Agarose (0.2%) was heated to a liquid and pipetted and spread onto each wedge to cover the entire surface to ensure the cells don't fall off the membrane filter during processing. The wedges were then placed into an oven at 65°C to allow the agarose to dry, whereafter each wedge was placed into a proteinase K buffer solution (50µl of proteinase K into 10ml TE buffer solution) for 30 minutes at room temperature. The wedges were then placed into 0.01M HCl solution for 20 minutes at room temperature, then in PBS for 1 minute, rinsed in ethanol for a few seconds, and placed in a Petri dish to dry.

The Syndiniales probes (50ng/µl) were prepared to create the working solution in an Eppendorf tube covered with foil. A 2ml hybridization buffer was prepared for each wedge using the following substances (added in this order): 40µl of 5M Tris/HCl with a pH of 8; 360µl of 5M NaCl; 400µl of formamide; 1198µl of milliQ H_2O; 2µl of 10% SDS. The hybridization buffers were preheated to 46°C. The Syndiniales probes were then prepared using 27µl preheated hybridization buffer with 3µl of the working probe (50ng/µl) for each wedge (81µl buffer and 9µl probe Syn 1 for the first 3 wedges; and 81µl buffer and 9µl probe Syn 2 for the remaining 3 wedges). The wedges were then placed onto glass slides (three wedges on each glass slide) and 30µl probe-buffer solution was pipetted onto each wedge and spread to cover the entire wedge. The glass slides were then placed into falcon tubes and blotting paper was placed in the tube underneath the glass slide. The remaining prewarmed hybridization

buffer was then poured onto the blotting paper underneath the glass slide and the tube was closed and incubated at 46°C for 16-17 hours in the dark.

A 50ml wash buffer was prepared in a falcon tube using the following substances (added in this order): 1ml of 1M Tris/HCl with a pH of 8; 500µl of 0.5 EDTA with a pH of 8; 2150µl of 5M NaCl; milliQ H_2O filled to the 50ml mark of the falcon tube; 50µl of 10% SDS. After the required incubation time, the wash buffer was prewarmed to 48°C. The wedges were placed into the prewarmed wash buffer for 15 minutes at 48°C whilst keeping the incubation chamber covered with foil to keep the samples in the dark. Wedges were then placed into Petri dishes and covered with foil to dry in the dark whereafter a Calcofluor White stain was pipetted onto the wedges and left for 7 minutes in the dark. The wedges were then rinsed in milliQ H_2O for 1 minute and placed into Petri dishes to dry again whereafter a drop of DAPI was added to each wedge and left for 5 minutes in the dark. The wedges were once again rinsed in water for a minute and then in ethanol for an additional minute whereafter they were allowed to dry. The wedges were then placed onto glass slides (one with the hybridized Syndiniales 1 probe and one with the Syndiniales 2 probe on each glass slide). A drop of SlowFade Diamond Antifade Mountant was placed onto each wedge and a coverslip was placed on. All samples were stored in the dark at -20°C until microscope quantification took place.

The prepared microscope slides were inspected using the Zeiss Axiovert 200M inverted fluorescent Microscope. The x100 oil immersion objective was used for observations. Twenty random frames of view were observed for each wedge and images were taken with the AxioVision 4.8 software and the monochrome Zeiss AxioCam HRm. Samples were inspected under the UV (385nm) and Blue (475nm) light and the total eukaryotes, eukaryotes with the fluorescent green emissions, and total bacteria were counted. All data was then entered onto an Excel sheet and Statistical analyses and graphs were done in R studios.

After microscopy observations were done, the total number of cells per ml were estimated using equation 1.

$Field\ of\ view = 0.023\ mm\ diameter$
$Area\ of\ Field\ of\ view = 0.000415\ mm^2$
$Total\ number\ of\ field\ of\ views\ = 4178313$

The total number of cells per ml were estimated using the following equation:

$$Cells\ per\ ml = \frac{Average\ cells\ in\ field\ of\ view\ x\ Total\ number\ of\ field\ of\ views}{Total\ ml} \quad \text{.....1}$$

$$Cells\ per\ ml = \frac{Average\ cells\ in\ field\ of\ view\ x\ 4178313}{50\ ml}$$

For the statistical analyses, a Shapiro-Wilk test was done to test for the normality distribution of the data, which was followed by Mann-Whitney U tests to compare the total cell density per ml at the surface and at a 10m depth. Next the data was grouped into two cycles identified by Burger et al., (2020), namely the upwelling cycle which spanned across days 1 to 5 and a resting cycle which occurred over days 6 to 10.

To investigate the frequency of infected microeukaryotes by Syndiniales over the two cycles, the infected microeukaryote cells were divided by the total microeukaryote cells. Mann-Whitney U tests were run separately for the surface and 10m data to compare the frequency of infected cells over two cycles.

CARD-FISH Procedure

Following the sensitive FISH procedure, the CARD-FISH procedure was done to validate the findings in the FISH observations. The remaining 3 wedges were used (one for the Syndiniales 1 probe, one for the Syndiniales 2 probe, and one with a non-probe as control, 5'-ACT CCT ACG GGA GGC AGC-3'). The CARD-FISH procedure was done as follows: Agarose gel (0.2%) was heated to a liquid, pipetted onto the filter membranes and spread over the surface area. The wedges were then placed into an oven at 46°C for 15 minutes to allow the agarose to dry. Next the inactivation of endogenous peroxidases was done by incubating the filter sections in 10ml of 0.01M HCl for 10 minutes at room temperature, whereafter it was rinsed in 50ml PBS for a minute and then in 50ml ddH_2O.

The permeabilization step was done using a lysozyme solution that was prepared fresh using lysozyme and TE buffer at a concentration of 10mg/ml. The filter sections were incubated in the lysozyme solution for 60 minutes at 37°C. After incubation the filter sections were rinsed in 50ml ddH_2O then 50ml of Absolute ethanol (96%) and then in PBS. Further permeabilization was done using proteinase K. A 0.05% proteinase K solution was made using 50µl of proteinase K in 10ml TE buffer. The filter sections were incubated at 37°C for 60 minutes and then washed three times in ddH_2O. Further incubation then occurred in 0.01M HCl at room temperature for 20 minutes, rinsed twice in ddH_2O, and finally they were dehydrated in 50ml of Absolute ethanol and air dried. To prepare the hybridization buffer, a blocking reagent was made using the Blocking Reagent for nucleic acid hybridization and detection protocol by Roach Diagnostics (cat. No. 11096176001). Using a 50ml Falcon tube, the hybridization buffer was made up of 3.6ml of 5M NaCl, 0.4ml of 1M Tris HCl, 10ml ddH_2O water, with 2.0g dextran sulfate added (in this order). To ensure a homogenous solution, this mixture was heated to 50°C and shook until the dextran sulfate had dissolved. Once completely dissolved, it was allowed to cool down before adding in 4ml of formamide, 2ml of 1xblocking reagent, and 40µl of 10% SDS. The hybridization step involved mixing the hybridization buffer with

the Syndiniales probes (300:1) in a 2ml reaction vial, using 1500µl of hybridization buffer and 5µl of 50ng/µl probe and hybridized at 46°C for 2.5 hours.

The washing buffer was then prepared in a 50ml Falcon tube by adding the following chemicals in this order: 0.5ml of 0.5M EDTA, 1ml of 1M Tris HCl, 2150µl of NaCl, ddH_2O water filled to the top of the tube, and lastly 25µl of 20% SDS. The washing buffer was preheated to 48°C and the filter sections were washed in the washing buffer for 5 minutes and rinsed in PBS for 10 minutes (repeated 3 times). Next two to three drops (100-150µl) of poly-HRP-conjugated secondary antibody were added to the filter sections and incubated for 60 minutes at room temperature. The filter sections were then rinsed in PBS at room temperature for 10 minutes (repeated 2 times).

The second hybridization step was done using the Tyramide SuperBoost Kit. A tyramide working solution was prepared using 5µl of 100x Tyramide stock solution, 5µl of 100x H_2O_2 solution, and 500µl of 1x Reaction buffer. A 100µl of tyramide working solution was applied to each filter section and incubated for 8 minutes, whereafter a 100µl stop reagent (prepared fresh by diluting the stock solution 1:11 in PBS) was applied. The filter sections were rinsed three times in PBS and a drop of DAPI was added to the filter sections and incubated for 10 minutes in the dark. Finally, one drop of Antifade mountant was added to the filter sections before placing a coverslip over it. The prepared microscope slides were stored at -20°C until microscopy observations took place. The microscopy observations were done in the same manner as the FISH microscope slides.

Statistical analysis

The Shapiro Wilk test was done in R studios to inspect the normality of the total eukaryotic cell (2-100µm) density over the 10-day period. This test was followed by the non-parametric Mann-Whitney U test for the surface and 10m depth respectively for the 10 days, as well as for the surface and Depth for the two identified cycles, upwelling (Day 1-5) and resting (Day 6-10). These same tests were performed for the frequency of infected eukaryotic cells by Syndiniales. The following R packages were used in all the statistical analyses and figure creations: dplyr, stats, ggplot2, ggcorrplot, tidyr, stringr, tidyverse, vegan, psych, devtools, ggbiplot.

A Pearson correlation matrix was created using R studios for the surface and depth data respectively, incorporating all the available environmental factors to identify any linear correlations between these factors and the total cells as well as the frequency of infections.

The microscopy observations of the surface FISH data were validated using CARD-FISH for the same surface samples and a non-parametric Wilcoxon signed-rank test was performed in R studios.

Following the creation of the bar graph for the frequency of infected eukaryotic cells (2-100µm), a similar profile was detected to that of the relative abundance of *Skeletonemia costatum* in the paper written by Burger et al (2020), hence a linear regression test was performed on the microscopy counts of *S. costatum* and the frequency of infections by Syndiniales (data of the relative abundance obtained via light microscopy was provided by Burger et al. (2020)).

The map of the western coast of South Africa depicting the two study sites, Elands Bay and a second study site within St Helena Bay along the Berg River line (Station 6), was created in R studios using the marmap, mapdata, ggrepel, and fields packages.

DNA extraction, amplification, and sequencing

DNA extraction, amplification and sequencing was done by Dames (2022) and is briefly explained here. The picoplankton (0.2–3 µm size fraction) biomass was filtered via a 0.2 µm polycarbonate filter for the purposes of DNA analysis. The filters were cut into finer sections using sterile equipment and the QIAGEN® DNeasy® Blood and Tissue Kit (Qiagen, USA) was used to extract the DNA according to the manufacturers protocol. After extraction, a Nano Drop ND-Spectrophotometer (NanoDrop Technologies Inc., Wilmington, DE) and a 2% agarose gel stained with ethidium bromide was used to assess the DNA quality and quantity, whereafter 16S ribosomal RNA metabarcoding was done on the 13 samples. The metabarcoding was carried out using the 16S rRNA V3-V4 primer set 341F (5'-CCTAYGGGRBGCASCAG-3') and 806R (5'-GGACTACNNGGGTATCTAAT-3') (Muyzer et al., 1993; Caporaso et al., 2011). The 18S rRNA V4 region was amplified using the barcodes TAREUK454FWD1 (5'-CCAGCASCYGCGGTAATTCC-3') and TAREUKREV3 (5'-ACTTTCGTTCTTGATYRA-3') for 15 samples (Stoeck et al., 2010), to identify the picoeukaryote community over the course of the study period (Stoeck et al., 2010). The PCR reactions were performed using Phusion® High-Fidelity PCR Master Mix (New England Biolabs) and MID adaptor linked primers, and a 2% agarose gel stained with ethidium bromide was used to verify amplifications. A DNA mixture was created by mixing the PCR products in equidensity ratios to ensure equal representations of each PCR product and then purified with a Qiagen Gel Extraction Kit (Qiagen, USA) to isolate the DNA fragments from the agarose gels and contaminants. The DNA was then prepared for Illumina sequencing by generating DNA libraries using the TruSeq® DNA PCR-Free Sample Preparation Kit followed by a quantification step via Qbit and qPCR to sequence the DNA via next generation sequencing (NGS) using the HiSeq Illumina Platform.

The raw sequences were processed using QIIME2, undergoing a demultiplex step were all the reads in the sequence.fastq file were assigned to the barcode sequences in the barcode.fastq file, turning the single fastq file that contains all the sample sequences, into separate fastq files for each sample

(two files per sample for the paired end reads to contain the forward and the reverse read). Next the denoise step was performed using DADA2 (Callahan et al., 2016) accessible through the q2-dada2 plugin for quality filtering, removal of chimeras, as well as joining paired-end reads. Truncated parameters were set based on the sequence quality score plots. The samples that successfully passed the quality control for the 18S rRNA amplification were the surface samples from days 1, 4, 6-10, and the depth of 10m samples collected on days 1 and 4-10. The output files from DADA2 were the feature table showing the amplicon sequence variants (ASV's) observed in the data, and the feature data which contain the sequences that define each of the ASV's. The taxonomic classification was done according to the QIIME2 Taxonomy Assignment tutorial which is a machine learning classifier. The SILVA database was used for a finer resolution of taxonomy. The downstream steps were then taken using an integrated R package "microeco" that uses advance approaches in microbial community ecology research (Liu et al., 2021). All chloroplast and mitochondria related ASVs were removed prior to downstream analysis. The abundance in each sample was rarefied at the lowest sequence depth of 7400.

A further filtering step was included for the creation of the CCA plot to inspect the correlation of the environmental variables with the 18S rRNA Syndiniales sequences. The ASV's and the taxonomic table were filtered for ASV's assigned as Syndiniales at the Class level using a grep function. The subsequent data was Helliger transformed in the vegan package to investigate the changes in variability between the different Syndiniales groups over the study period and to perform a CCA plot to inspect what environmental variables are influencing the Syndiniales community distribution.

Results

Water hydrography

The hydrography of the water column during the 10-day study period is explained in detail by Burger et.al., 2020. The major water column variables measured included the potential density σ_θ (kg.m^{-3}), oxygen concentration (µmol L^{-1}), nitrate (µmol L^{-1}), ammonium (µmol L^{-1}) and chlorophyll-a (µg L^{-1}) as seen in Figure 3. In summary, the hydrography of the water indicated that the first five days active upwelling occurred, and a well-mixed water column was established. This was followed by stratification and relaxation over the next five days (Burger et al., 2020). These two cycles of upwelling and relaxation were used to separate the eukaryote cell density and frequency of infections data for further statistical analysis. The mixed layer depth present at 5m during the first five days decreased to 2.5m on days 6 and 7, whereafter it increased to 10-15m on day 8 to 10 (Burger et al., 2020). The oxygen concentrations were lower at depth (>10m) than at the surface and the nitrate concentrations were lower at the surface (2.6 to 17.4 µmol L^{-1}) than at depth (18.5 to 26.8 µmol L^{-1}). The ammonium concentrations, however, were extremely variable over the 10 days (Burger et al., 2020). There was a

consistent higher concentration of Chlorophyll *a* at the surface compared to depth with an increase in [Chl-*a*] from day 4 onwards in the 0-10m depth area and showcased a peak [Chl-*a*] at 5m on day 5 (Burger et al., 2020).

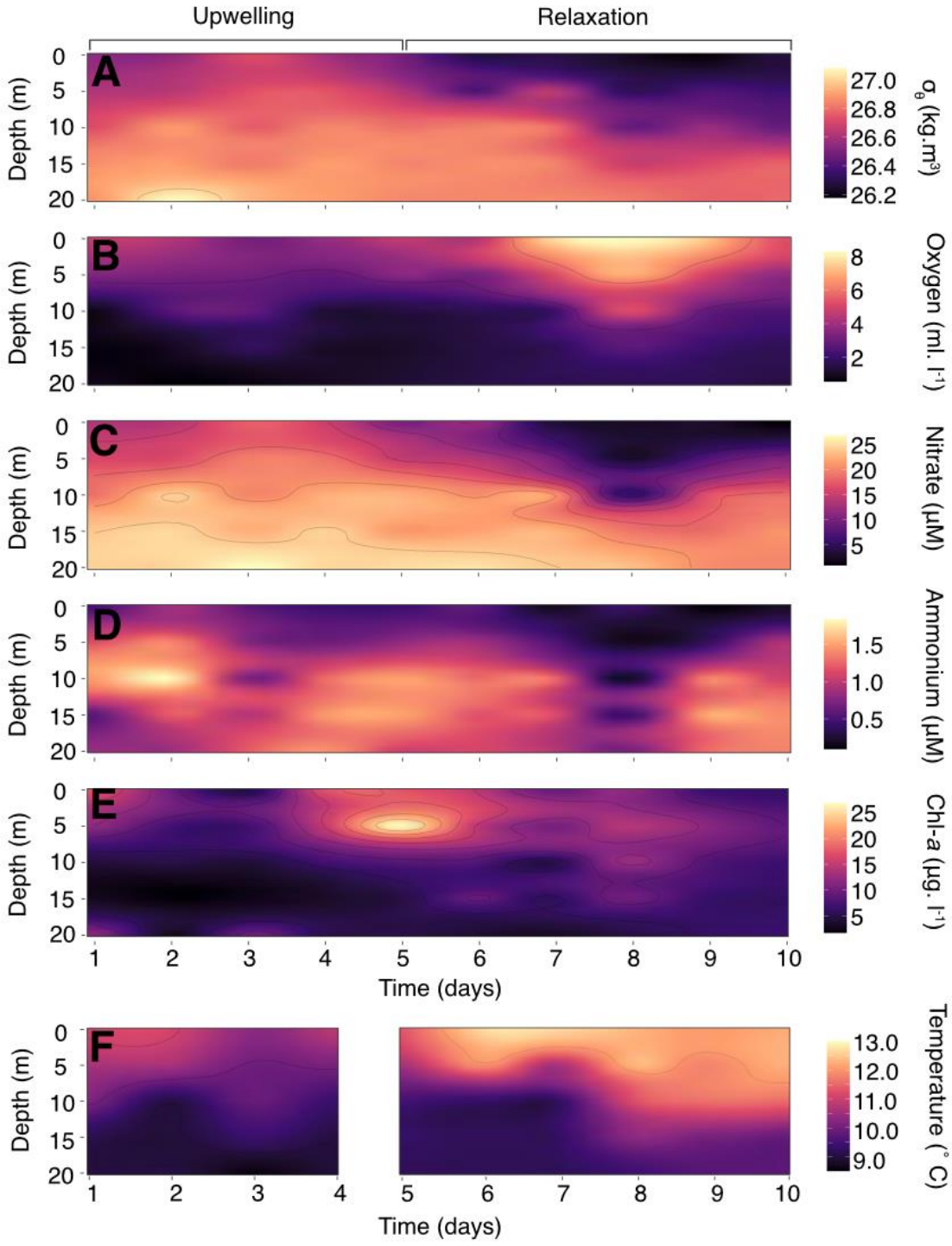

Figure 3: The hydrography of the water column over the 10 consecutive day sampling period. The major water column variables measured included the A: potential density σ_ϑ (kg.m^{-3}), B: oxygen concentration (ml.L^{-1}), C: nitrate concentration (μM), D: ammonium concentration (μM) and E: chlorophyll-a concentration (μg.L^{-1}). Day 1

to 5 showed characteristics of an upwelling period whilst day 6 to 10 showed a period of relaxation. Figure taken from Dames et al., 2022.

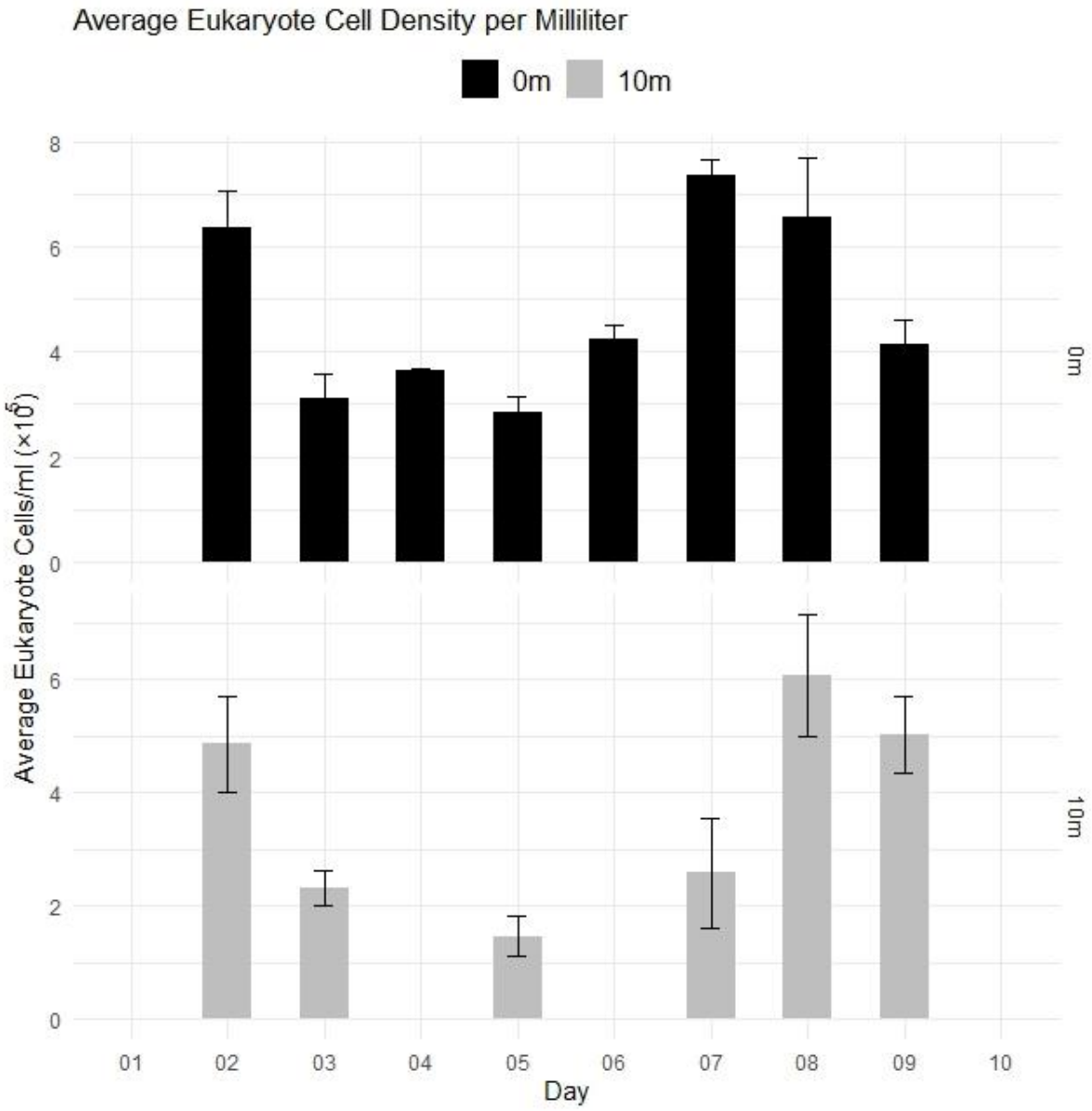

Figure 4: The average eukaryote cell density (2-100µm) per millilitre for the samples collected over 10 consecutive days from 29 Nov to 8 Dec 2016. The black depicts the cell density at the surface (0m) and the grey depicts the cell density at a depth of 10m. Missing data are indicated by the omitted bars in the graph.

Eukaryotic cell density (2-100µm)

In both the 0m and the 10m depth data, the Shapiro wilk test indicated non-normal distribution of the total cell densities per ml over the 10 days ($W = 0.79866$, p-value $< 2.2e^{-16}$ and $W = 0.7985$, p-value $< 2.2e^{-16}$ respectively). The non-parametric Mann-Whitney U test was performed to compare the mean eukaryotic cell densities between the two depths over the 10-day study period. The test

revealed a significant difference in the distribution of the total cell density between the surface and 10m depth (W = 407996, p-value = $4.931e^{-13}$, n_1=944, n_2=728).

Based on the findings in Burger et al. (2020), the data for both the surface and 10m depth were divided into two phases, namely the upwelling and resting phase. The Mann-Whitney U test was used to compare the total eukaryotic cell density per ml for the two cycles at the surface. The test gave supporting evidence of a significant difference in the total cell densities per ml at the surface for the Upwelling (Day 1-5) and Resting (Day 6-10) cycles (W = 74453, p-value < $2.2e^{-16}$, n_1=482, n_2=462). A Mann-Whitney U test comparing the total eukaryotic cells per ml at a 10m depth for the two cycles was also performed. This p-value suggested that there might be a potential difference between the total cell densities for the upwelling and resting cycles at a depth of 10 m (W=65016, p-value = 0.05021, n_1=846, n_2=826). As the p-value was essentially 0.05, the result of the Mann-Whitney U test was seen as significant. A graphical presentation of the eukaryote cell density (2-100µm) for both the surface and 10m depth data is depicted in Figure 4.

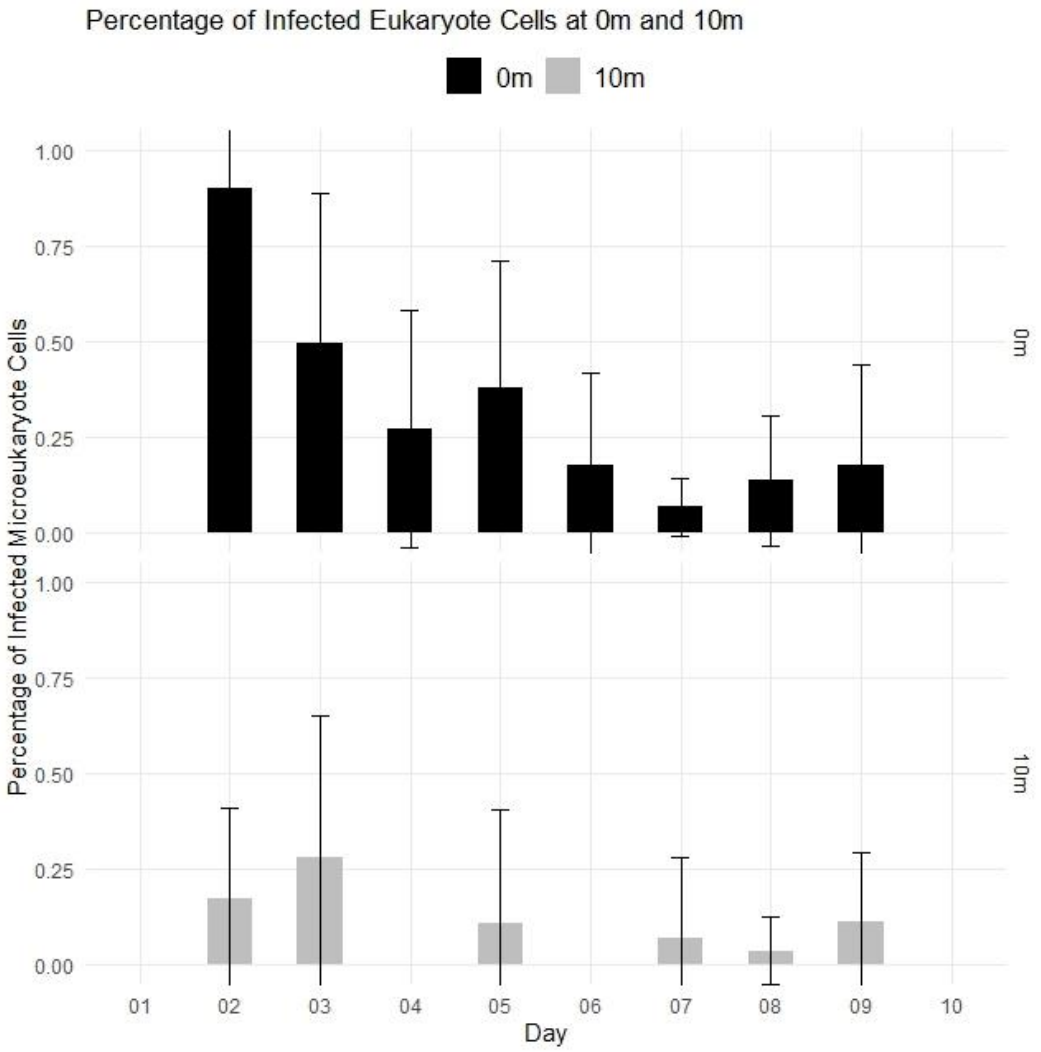

Figure 5: The percentage of eukaryote cells (2-100µm) that are infected by Syndiniales during the 10-day study period are depicted in this graph. The black depicts the percentage of infections at the surface (0m) and the grey depicts the percentage of infections at a depth of 10m. Missing data are indicated by the omitted bars in the graph.

Eukaryotic infections by Syndiniales MALV I and II

The Wilcoxon test indicated that there were no significant differences in the frequency of infections by Syndiniales I and II (W=334776, p-value=0.2815). Hereafter, no distinction was made between Syndiniales I and II for statistical analyses.

Similar to the total cell density, the non-parametric Mann-Whitney U test was used to compare the mean infections by Syndiniales between the two cycles. The test indicated that there was a significant difference in the distribution of the frequency of infected eukaryotic cells at the surface between the Upwelling and Resting cycles (W= 158338, p-value < $2.2e^{-16}$, n_1=482, n_2=462).

The same test was computed for the 10m depth data and provided evidence for a statistically significant difference in the distribution of the frequency of infected cells at a depth of 10m during

the Upwelling and Resting cycles (W = 71633, p-value = 0.002247, n1=364, n2=364). The percentage of infected eukaryotic cells (2-100µm) per ml is depicted in Figure 5.

Surface environmental factors, eukaryotic cell densities, and frequency of infections

A Pearson correlation matrix was created for the surface data, incorporating all the available environmental factors to identify any linear correlations between these factors and the total cells as well as the frequency of infections. Based on the correlation matrix, the total eukaryote cell density had a strong positive correlation with temperature (r = 0.721, p-value = 0.019) and oxygen (r = 0.753, p-value = 0.012) and a strong negative correlation with Nitrite (r= -0.689, p-value = 0.028) and Silicate (r = -0.645, p-value = 0.044). The frequency of Syndiniales infections of eukaryotic cells had a strong positive correlation with Nitrite (r = 0.949, p-value < 0.001), Phosphate (r = 0.906, p-value < 0.001), Silicate (r=0.817, p-value = 0.004), and potential density (r = 0.836, p-value = 0.003), and had a strong negative correlation with temperature (r = -0.719, p-value = 0.019) and oxygen (r = -0.675, p-value = 0.032). The results are shown in Table 1.

10m Depth environmental factors, eukaryotic cell densities, and frequency of infections

The Pearson correlation matrix created for the samples taken at 10m yielded significant negative correlations of the total eukaryotic cell densities with nitrate (r = -0.764, p-value = 0.027), phosphate (r = -0.781, p-value = 0.022), and silicate (r = -0.857, p-value = 0.007), and a weakly significant negative correlation with nitrite (r = -0.701, p-value = 0.053). A significant positive correlation with temperature was observed (r = 0.823, p-value = 0.012).

No significant correlations were noted between the environmental variables and the frequency of infected eukaryotes. The correlation matrix for the 10m samples is depicted in Table 2.

Validation of FISH results

Catalyzed reporter deposition (CARD)-FISH data was used to validate the data obtained from the FISH procedure. It was necessary to use CARD-FISH because Syndiniales is so small (Sehein et al., 2022) that using FISH might not have been sufficient. A non-parametric Wilcoxon signed-rank test was performed between the FISH and CARD-FISH microscopy observations for the surface data only due to cost constraints. No significant differences were reported for the total number of eukaryotic cells (2-100µm) between the FISH and the CARD-FISH datasets (V-value = 26, df = 6, p-value = 0.3125), nor the total number of infected eukaryotic cells (V-value = 18, df = 6, p-value = 1)

Relative abundance of eukaryotes (2-100µm)

The profile of the relative cellular abundance of *Skeletonemia costatum* depicted in Figure 6 showcased a similar trend to the total frequency of infections by Syndiniales (Figure 5). Upon further investigation, a linear regression test was done, and a scatter plot (Figure 7) was created. The linear regression test showed that the data for infections via Syndiniales Group I does not fit the model with an R^2 value of 0.1949, adjuster R^2 value of 0.1279, an F-statistic of 2.906 on 1 and 12 degrees of freedom with a p-value of 0.114, indicating that there was no statistically significant relationship between the relative abundance of *S. costatum* and the infections via Syndiniales Group I. The linear regression model also didn't significantly explain the variation in the data for Syndiniales Group II with an R^2 value of 0.1479, adjuster R^2 value of 0.0769, an F-statistic of 2.082 on 1 and 12 degrees of freedom with a p-value of 0.174, indicating that other factors also played a role in the infection dynamics of Syndiniales Group II. Furthermore, a line graph (Figure 8) was created to investigate the trend between the total *S. costatum* and the frequency of infections. The plot showed an interesting trend where the total *S. costatum* and the frequency of infections mirror each other, having a 24-hour delayed response. Understanding the infection dynamics of the Syndiniales parasite, this graph makes sense, depicting high infection rates during high host abundance leading to a decrease in total host, causing the infection rates to plummet. There was an overall higher abundance of S*. costatum* during the upwelling phase (Day 1-5) that showed an overall high frequency of infection.

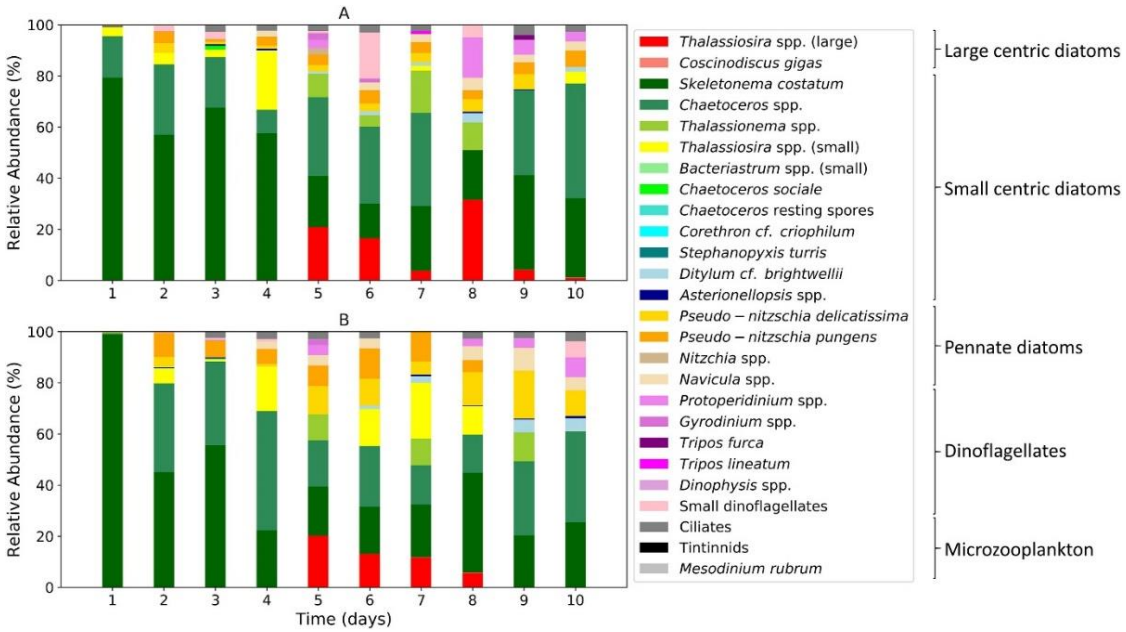

Figure 6: The relative protist species abundance identified in St Helena Bay via light microscopy at 0m (A) and 10m (B) over the 10-day study period. S. costatum (depicted in dark green) showcased a similar trend to the total infected cells at the surface (Figure 5). This is a promising find as Syndiniales are suspected to infect S. costatum (illustration taken from Burger et al 2020).

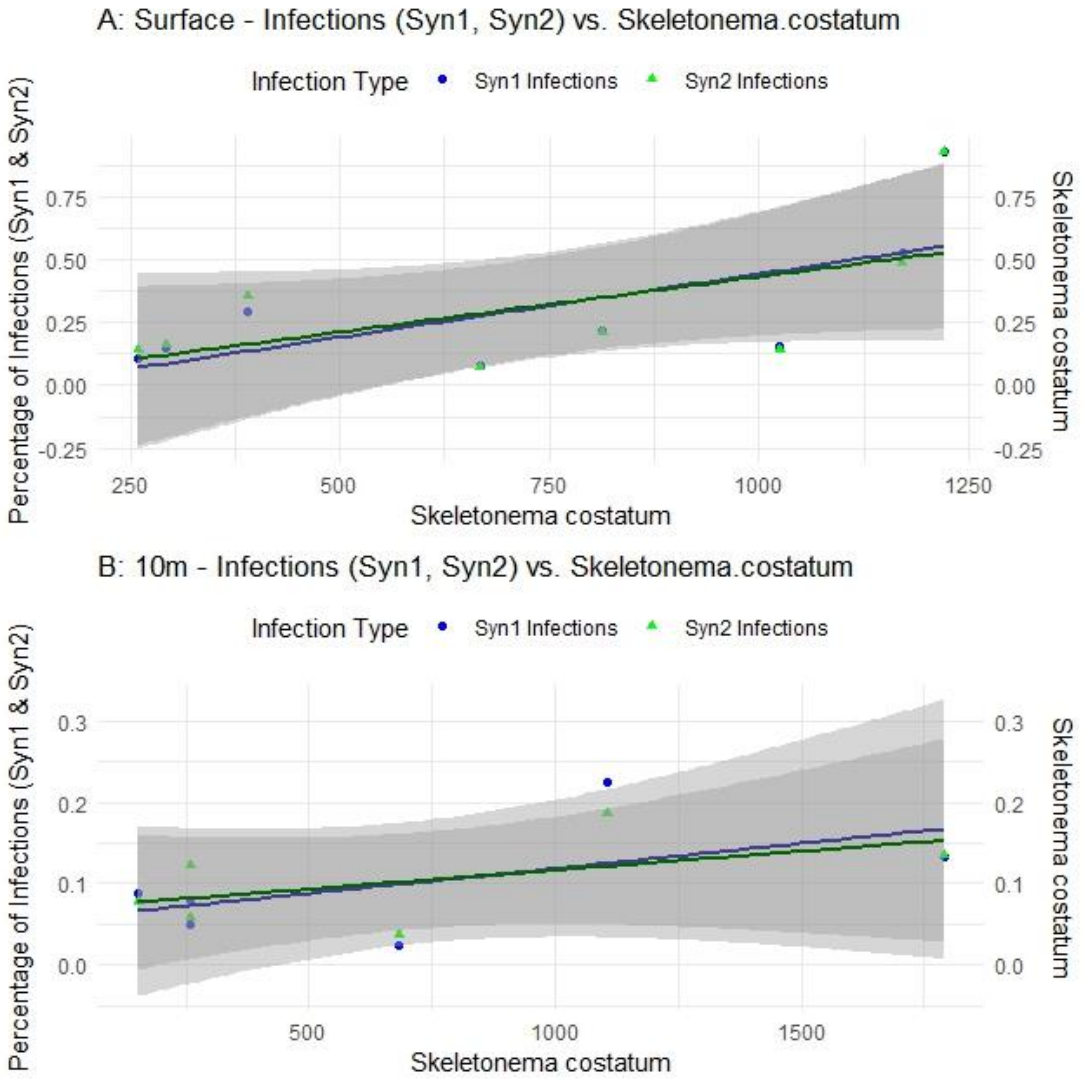

Figure 7: A scatter plot displaying the relationship between the total S. costatum *counts and the frequency of infections by Syndiniales group I (blue) and II (green) for both the surface (A) and 10m depth (B). A positive but not significant relationship exists between the frequency of infections of Syndiniales Group I and II and the total abundance of* S. costatum.

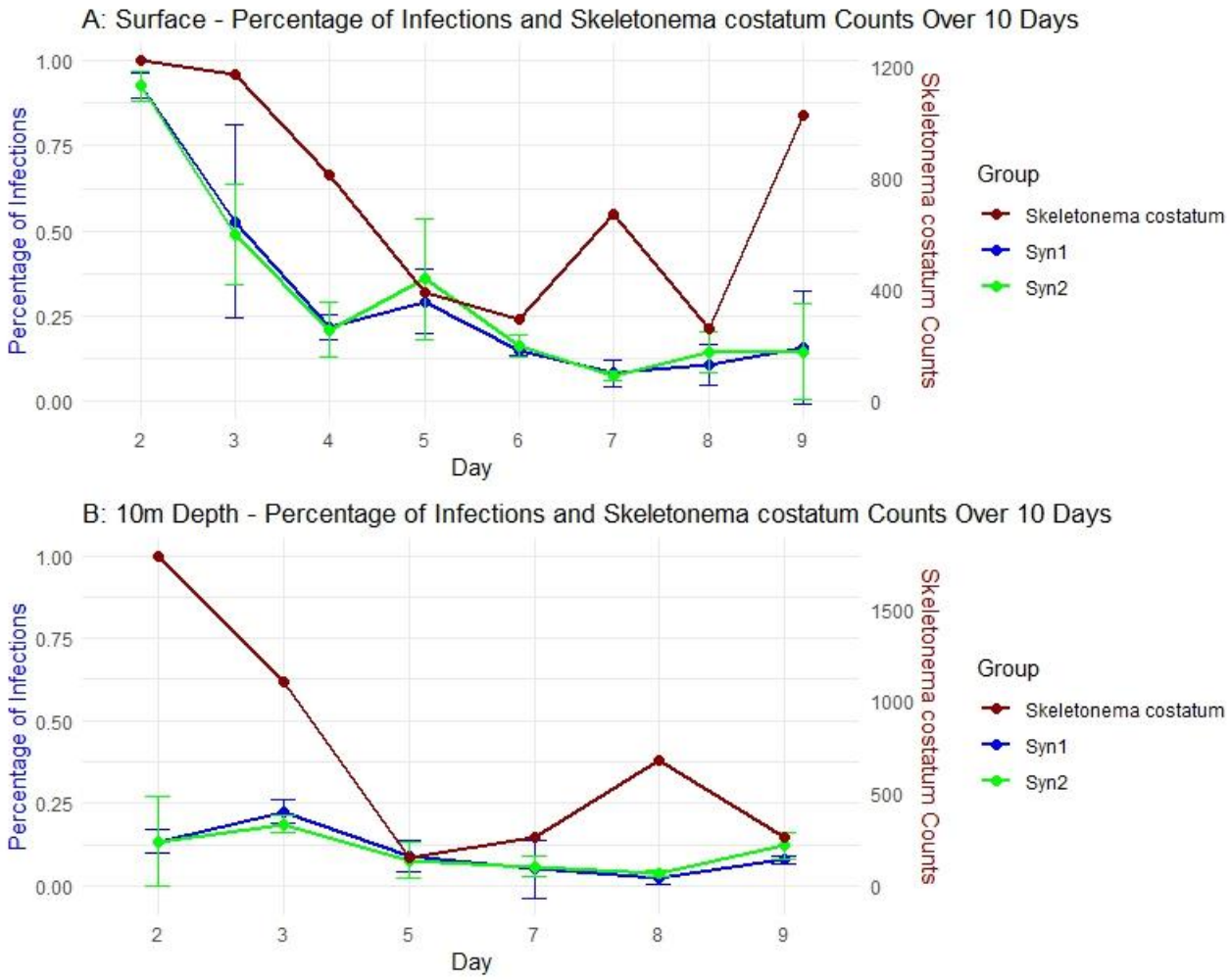

Figure 8: Trends of the total S. costatum *organisms (right axis in dark red) and the percentage of infections by Syndiniales (left axis in blue and green) observed at the surface and depth over the 10-day study period. Multiple R-squared: 0.01441, Adjusted R-squared: -0.3141, F-statistic: 0.04387 on 1 and 3 DF, p-value: 0.8475. The surface graph mirrors each other with what appears to be a 24-hour delayed response time, depicting high infection rates resulting in a decrease in total host, causing the infection rates to plummet.*

Relative abundance of 18s rRNA

The relative abundance of the 18S rRNA for the samples taken at the surface on days 1, 4, and 6-10 were dominated by Syndiniales (Figure 9). This could be attributed to the high copy number of Syndiniales which lead to an overrepresentation of this group. There was an increase in the relative abundance of Dinophyceae from day 1 to day 4 during which time the nitrate peaked on day 3 (17.6µM) and nitrite peaked on day 4 (4.485µM). On day 6, the relative abundance seemed to shift dramatically from the other days with a high proportion of fungi, mainly representatives of the class Saccharomycetes and Chytridiomycetes. The cause for this community shift is unknown, a possible explanation being that an alien intrusion occurred near the sampling site such as a seal passing by and defecating mere hours before sampling took place.

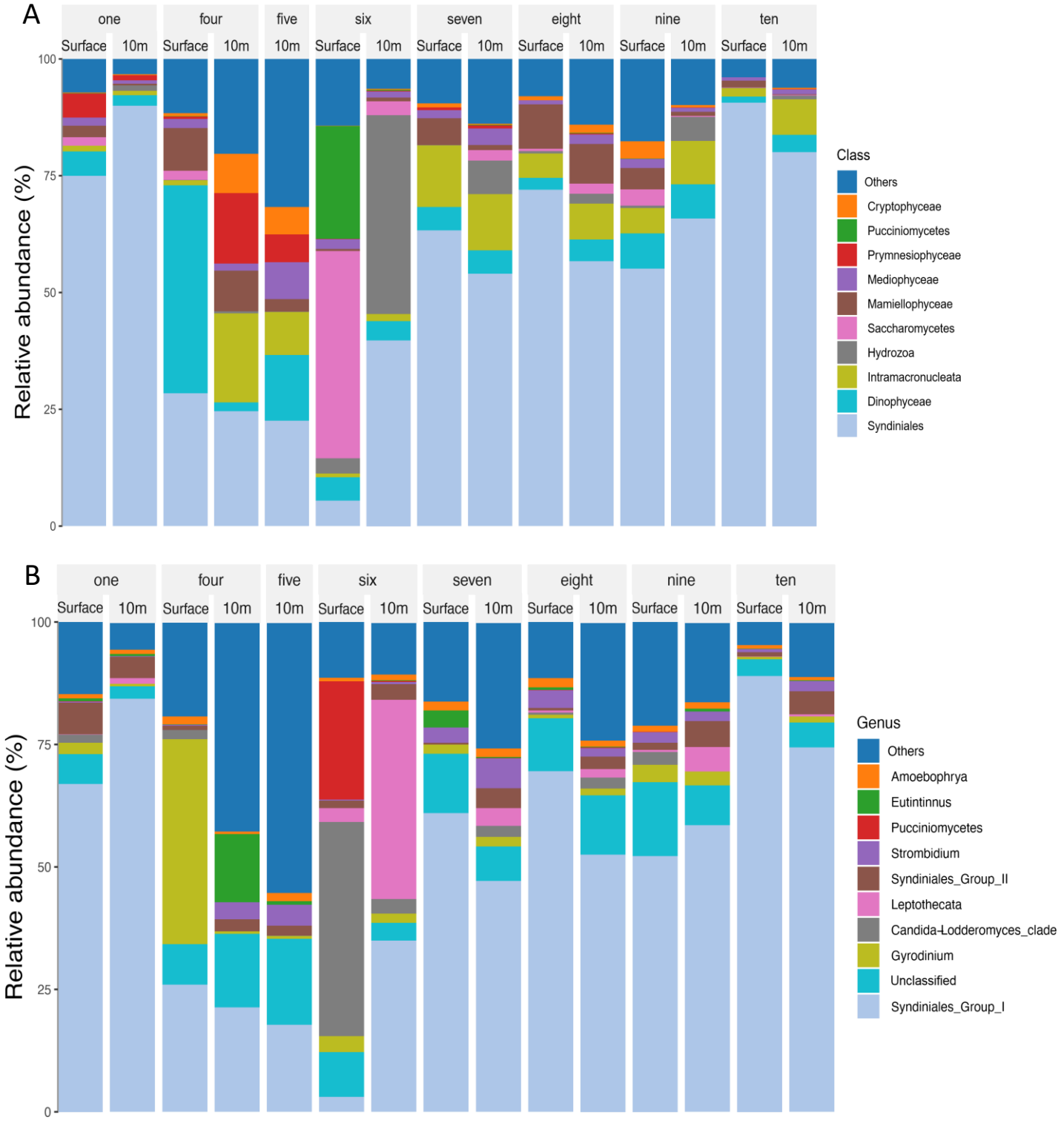

Figure 9: A:The relative abundance of 18S rRNA of eukaryotes classified down to the Class at the surface for days 1, 4 and 6-10 and at 10m depth for days 1 and 4-10. Syndiniales showcases a large proportion of the relative abundance which could be as a result of their large gene copy number. B: The relative abundance of 18S rRNA

of eukaryotes classified down to the Genus level for the same samples. The graph shows that Syndiniales I dominates the relative abundance with Syndiniales II in the minority.

Most Syndiniales ASV's belonged to group I which is contrasting to the FISH observations made via fluorescent microscopy in which case no significant difference was noted between fluorescently labeled Syndiniales group I and II (Wilcoxon statistic = 334776, p-value=0.2815). The differences noted could be due to free living dinospores not being easily detectable via microscopy. The most abundant eukaryotes (2-100µm) identified under fluorescent microscopy included *S. costatum*, species of *Radiolaria*, and an unidentified tear-shaped 1µm cell (only dominant on day 2) which could possibly be free living Syndiniales dinospores (images of the tear shaped eukaryotes are depicted in Figure 11 M-P). The filtering of ASV's for Class Syndiniales showed the presence of Syndiniales Group I which was the most abundant throughout the entire study, Group II which was the second most abundant, and Group III, Group IV, *Amoebophrya*, and Duboscuella, all in lesser abundance (Figure 10). Day 6 had a noticeable increase in Syndiniales group II abundance at the surface.

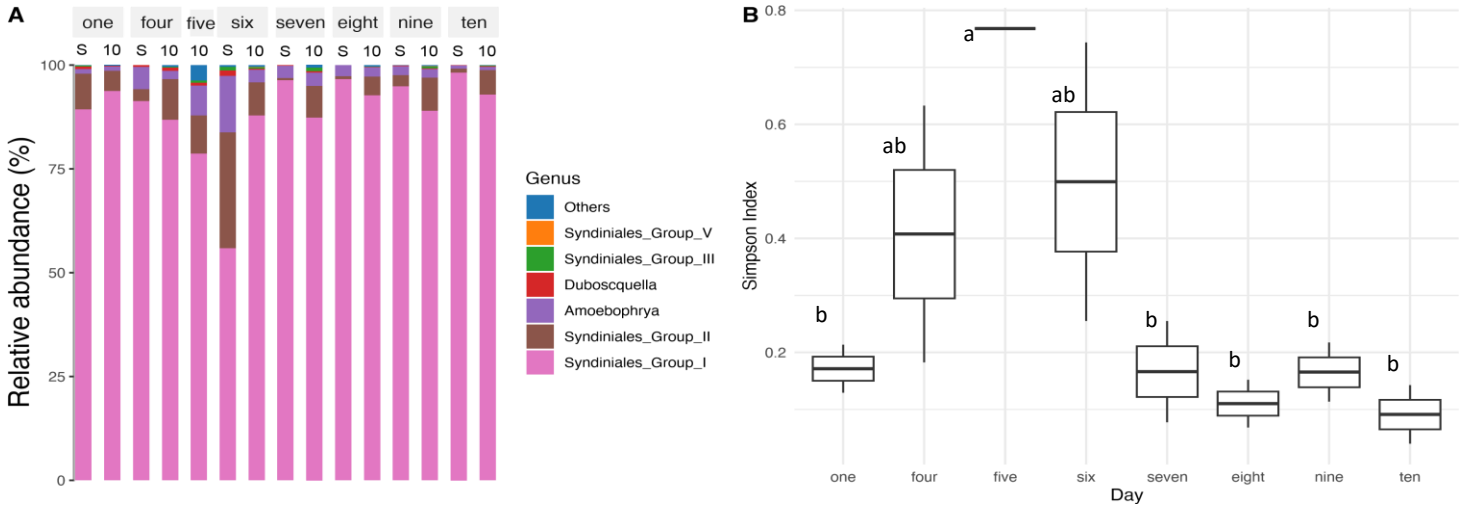

Figure 10: (A)The relative abundance of 18S rRNA for the Class Syndiniales for the samples collected at the surface and 10m depth for days 1 and 4 to 10 for the surface (S) and days 1, 4, and 6-10 for depth (10). Syndiniales Group I was the most abundant throughout the whole study. (B) The Simpson index for the Class Syndiniales over the course of the study. The groups with the same labels (a or b) do not have a significantly different Simpson index, whereas groups with different labels (a and b) show significant differences in their Simpson index. Day 4 and 6 show a higher diversity compared to day 1 and 7 - 10.

Table 1: The correlation matrix (CM) of Pearson (r) correlation coefficient and listwise deletion method for the environmental and species data taken at the surface for December 2016. The 'Total eukaryotes' represents the total eukaryotic cells (2-100µm) per ml, the 'Infected' represent the total eukaryotic cells (2-100µm) per ml infected by Syndiniales, and the 'Frequency' refers to the frequency of the infected eukaryotic cells (2-100µm). Figures in black and in brackets have a p-value < 0.05.

	Nitrate	*Nitrite*	*Ammonium*	*Phosphate*	*Silicate*	*Temperature*	*Salinity*	*Oxygen*	*Density*	*Total*	*Infected*	*Frequency*
Nitrate												
Nitrite	0.596											
	(0.069)											
Ammonium	0.777	0.364										
	(0.008)	*(0.301)*										
Phosphate	0.628	0.987	0.375									
	(0.052)	*(<.001)*	*(0.285)*									
Silicate	0.819	0.903	0.469	0.941								
	(0.004)	*(<.001)*	*(0.172)*	*(<.001)*								
Temperature	-0.95	-0.761	-0.586	-0.791	-0.94							
	(<.001)	*(0.011)*	*(0.075)*	*0.006*	*(<.001)*							
Salinity	0.558	0.279	-0.02	0.373	0.612	-0.67						
	(0.093)	*(0.435)*	*(0.957)*	*(0.288)*	*(0.06)*	*(0.034)*						
Oxygen	-0.98	-0.678	-0.672	-0.691	-0.862	0.98	-0.591					
	(<.001)	*(0.031)*	*(0.033)*	*(0.027)*	*(0.001)*	*(<.001)*	*(0.072)*					
Density	0.613	0.946	0.387	0.984	0.935	-0.765	0.405	-0.649				
	(0.059)	*(<.001)*	*(0.269)*	*(<.001)*	*(<.001)*	*(0.01)*	*(0.245)*	*(0.042)*				
Total eukaryotes	-0.628	-0.689	-0.302	-0.612	-0.645	0.721	-0.285	0.753	-0.481			
	(0.052)	*(0.028)*	*(0.396)*	*(0.06)*	*(0.044)*	*(0.019)*	*(0.424)*	*(0.012)*	*(0.16)*			
Infected	0.391	0.736	0.533	0.702	0.552	-0.424	-0.214	-0.402	0.676	-0.402		
	(0.263)	*(0.015)*	*(0.113)*	*(0.024)*	*(0.098)*	*(0.222)*	*(0.553)*	*(0.25)*	*(0.032)*	*(0.249)*		
Frequency	0.588	0.949	0.412	0.906	0.817	-0.719	0.151	-0.675	0.836	-0.776	0.843	
	(0.074)	*(<.001)*	*(0.237)*	*(<.001)*	*(0.004)*	*(0.019)*	*(0.677)*	*(0.032)*	*(0.003)*	*(0.008)*	*(0.002)*	

Table 2: The correlation matrix (CM) of Pearson (r) correlation coefficient and listwise deletion method for the environmental and species data taken at a depth of 10m for December 2016. The 'Total eukaryotes' represents the total eukaryotic cells (2-100µm) per ml, the 'Infected' represent the total eukaryotic cells (2-100µm) per ml infected by Syndiniales, and the 'Frequency' refers to the frequency of the infected eukaryotic cells (2-100µm). Figures in black and in brackets have a p-value < 0.05.

	Nitrate	*Nitrite*	*Ammonium*	*Phosphate*	*Silicate*	*Temperature*	*Salinity*	*Oxygen*	*Density*	*Total*	*Infected*	*Frequency*
Nitrate												
Nitrite	0.995 *(<.001)*											
Ammonium	0.551 *(.157)*	0.600 *(.116)*										
Phosphate	0.997 *(<.001)*	0.988 *(<.001)*	0.578 *(.134)*									
Silicate	0.982 *(<.001)*	0.958 *(<.001)*	0.437 *(.279)*	0.985 *(<.001)*								
Temperature	-0.978 *(<.001)*	-0.960 *(<.001)*	-0.365 *(.373)*	-0.968 *(<.001)*	-0.987 *(<.001)*							
Salinity	0.433 *(.284)*	0.348 *(.399)*	-0.434 *(.283)*	0.433 *(.283)*	0.582 *(.130)*	-0.593 *(.121)*						
Oxygen	-0.976 *(<.001)*	-0.975 *(<.001)*	-0.414 *(.309)*	-0.957 *(<.001)*	-0.956 *(<.001)*	0.985 *(<.001)*	-0.480 *(.228)*					
Density	0.968 *(<.001)*	0.946 *(<.001)*	0.587 *(.126)*	0.984 *(<.001)*	0.976 *(<.001)*	-0.934 *(.001)*	0.465 *(.245)*	-0.897 *(.003)*				
Total eukaryotes	-0.764 *(.027)*	-0.701 *(.053)*	-0.123 *(.772)*	-0.781 *(.022)*	-0.857 *(.007)*	0.823 *(.012)*	-0.799 *(.017)*	0.729 *(.040)*	-0.825 *(.012)*			
Infected	-0.473 *(.237)*	-0.450 *(.263)*	-0.640 *(.087)*	-0.528 *(.179)*	-0.488 *(.219)*	0.369 *(.368)*	-0.073 *(.864)*	0.302 *(.467)*	-0.629 *(.095)*	0.555 *(.153)*		
Frequency	0.313 *(.451)*	0.308 *(.458)*	-0.416 *(.305)*	0.253 *(.546)*	0.327 *(.429)*	-0.451 *(.262)*	0.505 *(.202)*	-0.488 *(.220)*	0.137 *(.747)*	-0.239 *(.569)*	0.631 *(.094)*	

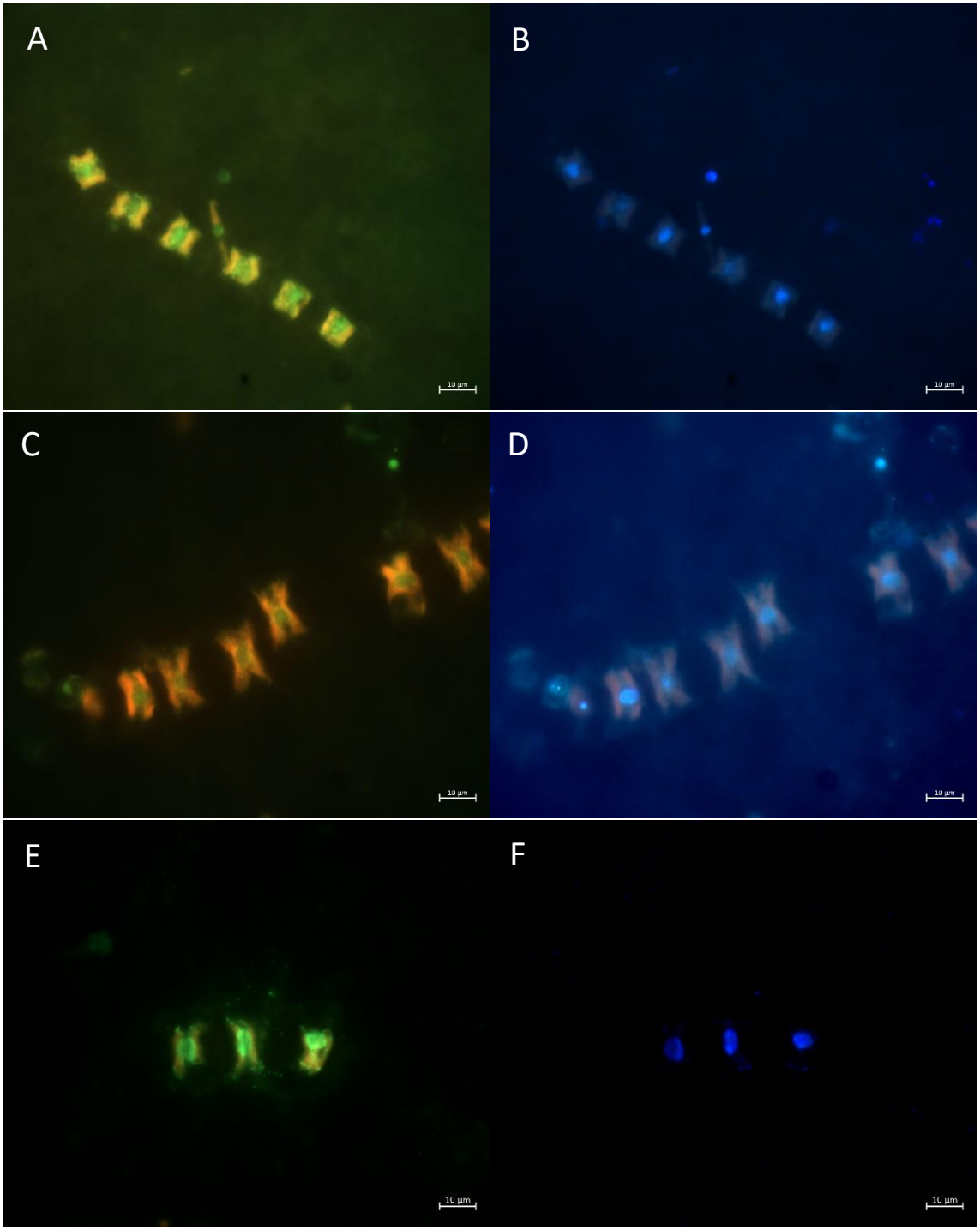
A
B
C
D
E
F
10 µm

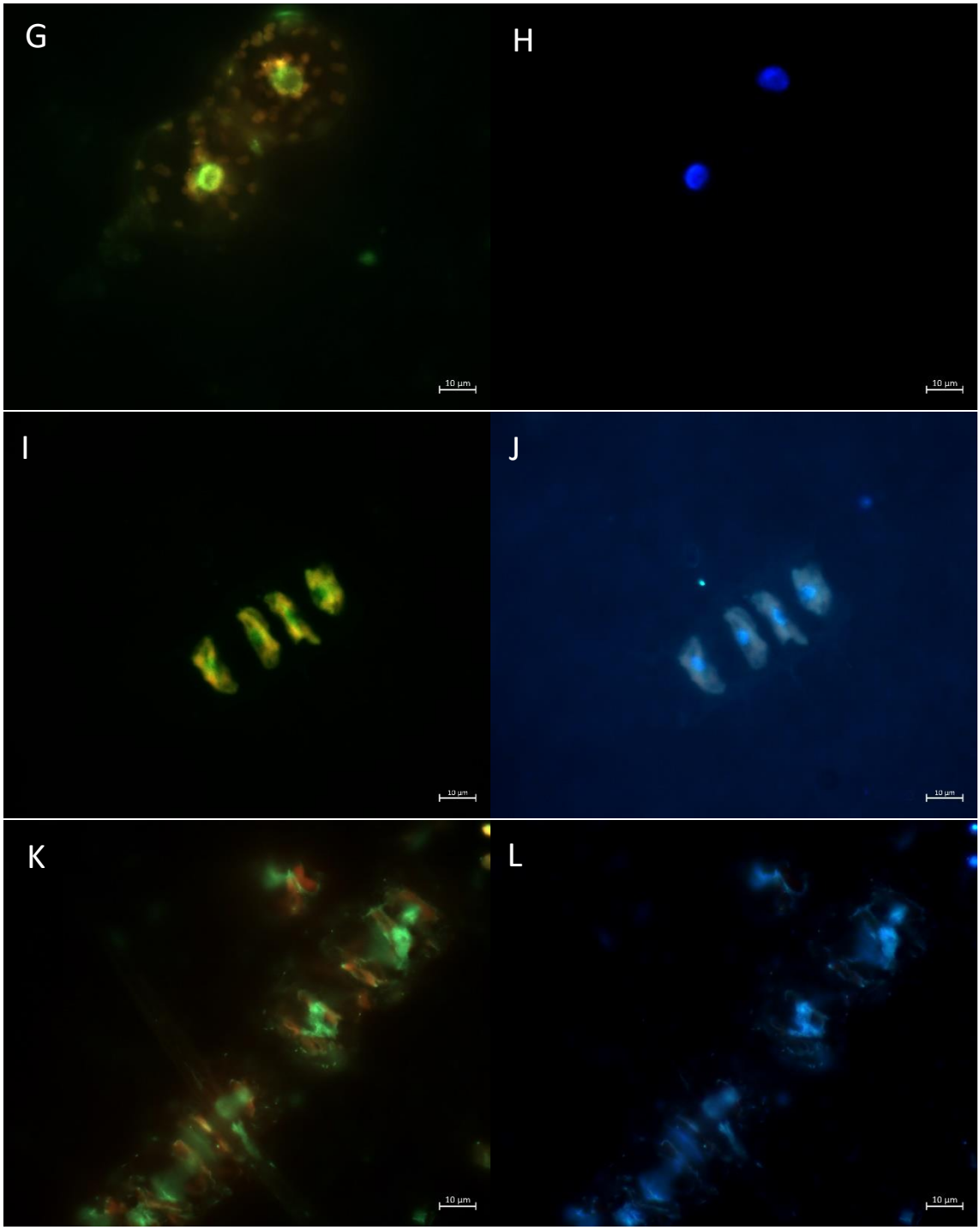
G
H
I
J
K
L
10 µm

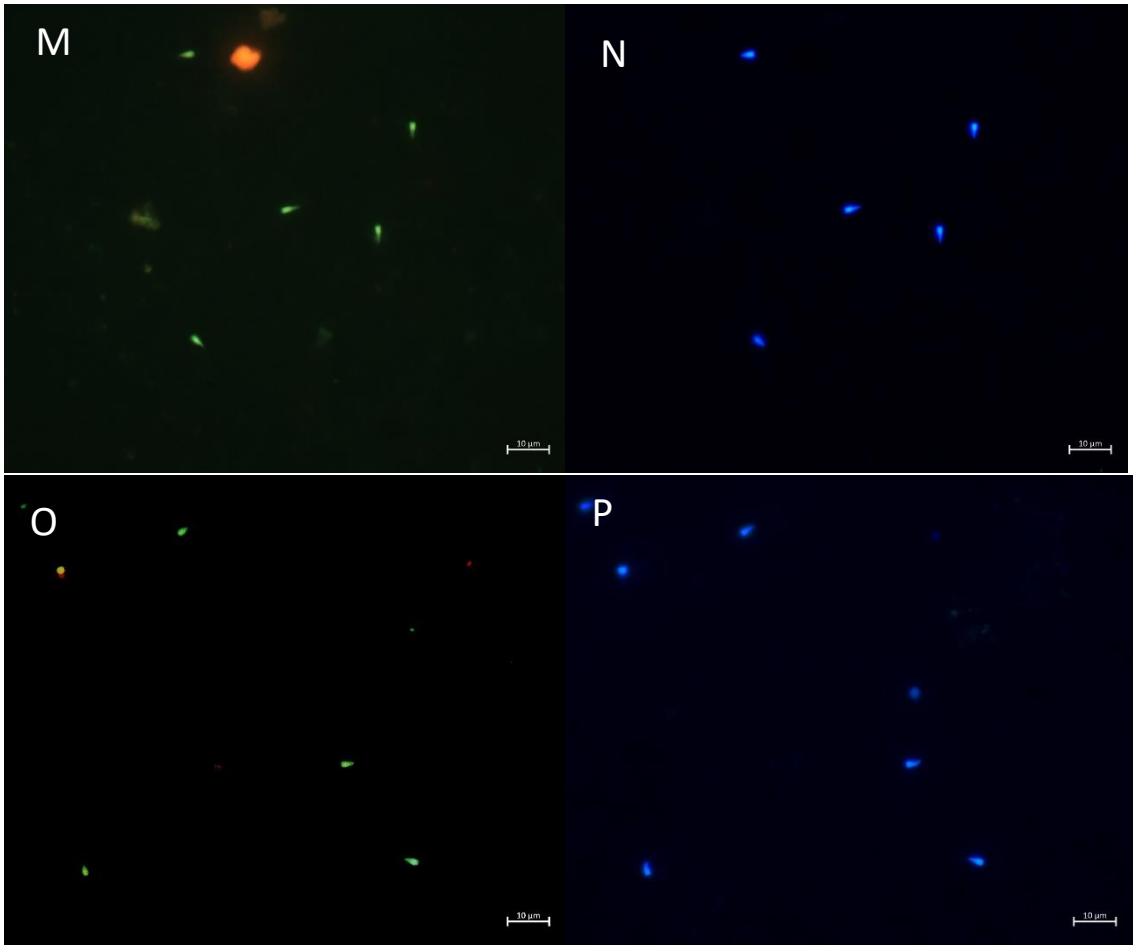

Figure 11: CARD FISH microscopy images depicting Syndiniales infected eukaryotic cells where the left image with bright green fluorescence represents the Syndiniales parasite and the right image with the blue fluorescence represent the nucleus of the eukaryotic cells. Images shown were taken from days 3 to 6 of the study, with A-D taken on day 3, E-H taken on day 4, I-J taken on day 5 and K-L taken on day 6. Images A-F and I-L depict the most abundant diatom found during the entire study period, namely Skeletonema*. Image G-H depict an infected* Radiolaria*. Image M-P depict an unidentified tear-shaped eukaryote (2-4µm), potentially Syndiniales dinospores that dominated the FISH samples on day 2.*

Canonical correspondence analysis

The CCA plot (Figure 12) used ASVs from Syndiniales and was constrained by the host *S. costatum* as well as the nutrient silicate (SiO_3). The plot depicts a separation between the samples taken during the upwelling and resting phases. The statistically significant environmental variables according to the CCA plot were silicate, nitrate and phosphate. The eigenvectors for these nutrients are negatively correlated with the samples from the relaxation phase and are directed in the general direction of the samples from the upwelling phase. Silicate is an important nutrient for the growth of diatoms as they incorporate SiO_3 into their cell walls whilst nitrate and phosphate are important nutrients for phytoplankton growth. The frequency of Syndiniales infections and the abundance of *S. costatum* are significant with the Syndiniales ASV's and are relatively close together and directed towards the upwelling samples.

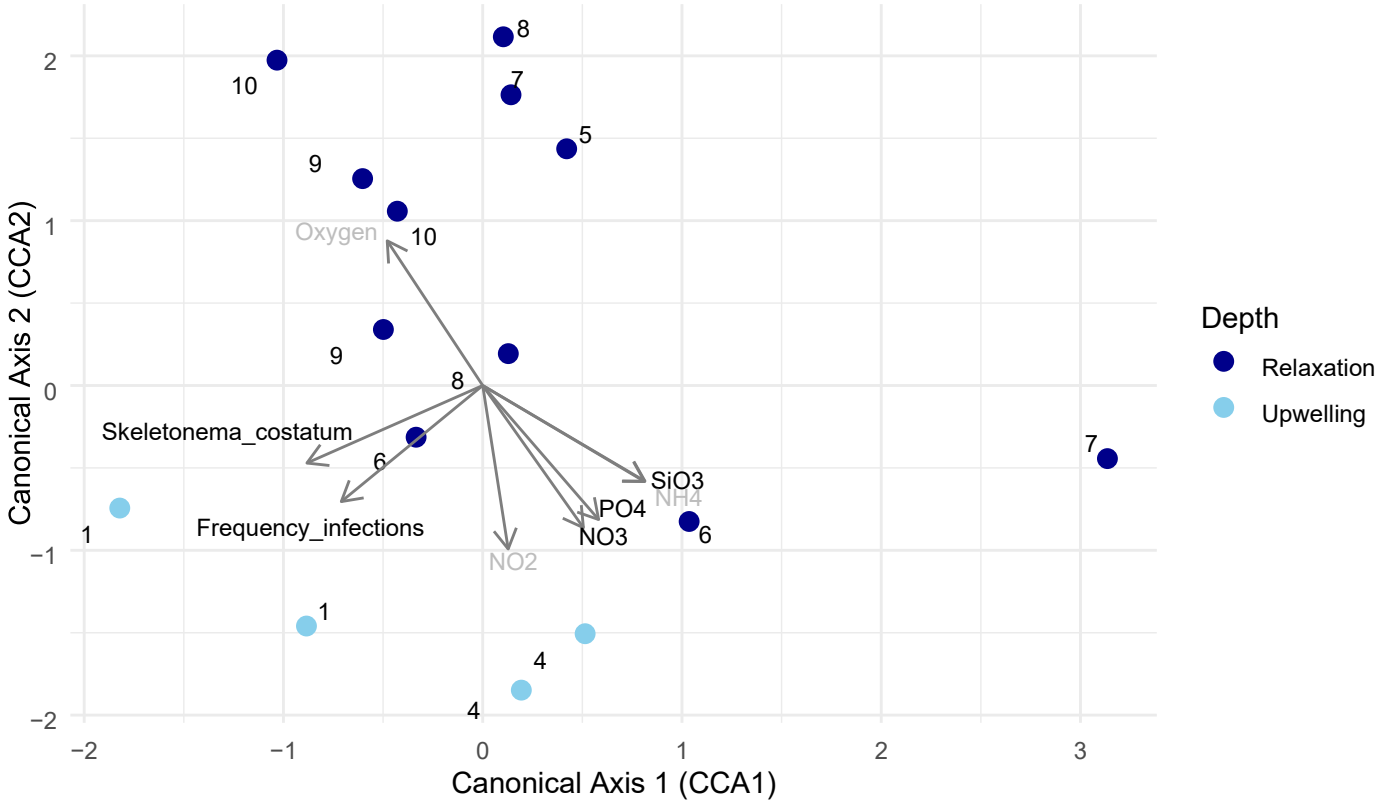

Figure 12: CCA plot using Syndiniales ASVs, constrained by the host S. costatum *and the nutrient silicate (SiO_3). The plot displays samples collected during the upwelling phase in light blue and those from the relaxation phase in dark blue. Environmental variables are shown as eigenvectors, with black labels indicating significant correlations with the Syndiniales ASVs. Numbers next to the sample points indicate the sampling day.*

Discussion

The Benguela current

The Benguela current is characterized by high net primary production caused by the persistent wind-driven upwelling of cold nutrient rich waters during spring and summer seasons (Hutchings et al., 2009), followed by wind relaxation during winter with lower productivity rates (Brown, 1984; Lutjeharms and Valentine, 1987; Shannon and Nelson, 1996; Barlow et al., 2009; Lamont et al., 2014; Flynn et al., 2018). The western coastline of southern Africa has large spatial variability leading to a variability in upwelling (Hart and Currie, 1960) confined to regions near the west coast of the Cape Peninsula, Cape Columbine, and Hondeklip Bay (Nelson and Hutchings, 1983). Due to the coast's many bays and inlets, large water-mass retention occurs, with St Helena Bay being the largest embayment on the west coast of South Africa and recognized as one of these retention zones, sustaining higher primary productivity rates and biomass compared to non-retention zones and support pelagic fish, hake, and rock lobster (Graham and Largier, 1997; Cockcroft, 2001; Cockcroft et al., 2008; Hutchings et al., 2012).

Microbial community composition

Due to their fast growth rate and ability to rapidly take up nutrients, small diatoms (e.g. *Skeletonema spp., Chaetoceros spp.*) are the first to dominate the waters post upwelling, succeeded by larger diatoms (e.g. *Thalassiosira spp., Chaetoceros spp.,* and *Nitzschia spp*.), and finally replaced by dinoflagellates (e.g. *Prorocentrum micans* and *Dinophysis spp*.) that are able to thrive in low nutrient aged, stratified water (Estrada & Blasco, 1985; Pitcher et al., 1991; Walker & Pitcher, 1991; Pitcher, Richardson & Korrubel, 1996; Álvarez-Salgado et al. 1996; Burger et al., 2020). Bloom dynamics allows fast growing phytoplankton such as diatoms to proliferate faster than they can be grazed upon by zooplankton and sinks out of the surface water layers, contributing to carbon export via the carbon pump (Painting et al., 1993; Marañón et al., 2009). As water ages and nutrients become deplete, there is a change in community composition, with small dinoflagellates starting to dominate, which in turn are grazed upon by other microbes or zooplankton, often to such an extent that there is no surplus production and little to no carbon export to deeper waters (Cushing, 1989; Painting et al., 1993; Marañón et al., 2009). The term 'quasi steady-state production' is used to describe situations were primary production and consumption occur at a similar rate, which results in minute changes in phytoplankton community structure over time (Cushing, 1989; Painting et al., 1993; Marañón et al., 2009).

Marine alveolates (MALV) are present worldwide and, according to the SSU rRNA from genetic libraries, have been shown to represent 10 to 50% of the total environmental sequences (Guillou et

al., 2008). Syndiniales is a group of marine parasites within the MALV lineages that infect and obligatory kill their hosts. This form of parasitism is essential within ecological processes as it contributes to carbon draw-down, ecosystem resilience, and acts as an evolutionary pressure on their host organisms (Blanquart et al., 2016). Based on previous studies suggesting that the parasitic dinoflagellate, Syndiniales, may lead to bloom termination via top-down pressure (Coats and Bockstahler, 1994; Coats et al., 1996; Coats and Park, 2002; Park et al., 2004; Montagnes et al., 2008; Velo-Suarez et al., 2013), I hypothesized that there will be a decrease of Syndiniales presence as the diatom relative abundance decrease and the community shifted to dinoflagellates (Álvarez-Salgado et al. 1996) during the termination of a bloom.

The water hydrography for the first 5 days of the study was indicative of a recent upwelling event (Burger et al., 2020), with nutrient rich Subantarctic Mode Water (SAMW) being the main upwelling water source to the Southern Benguela upwelling system (SBUS) (Lamont et al., 2015). The upwelling event was followed by a relaxation and stratification period for the remaining 5 days of the study (Burger et al., 2020). The lack of upwelling during this period allowed solar heating of the upper water column to establish an upper mixed layer (UML) with higher sea surface temperatures and a bottom mixed layer (BML) with lower water temperatures, with a separating thermocline (Waldron, 1985).

The euphotic zone was relatively deep during the active upwelling phase (day 1 to 5) due to vertical mixing of the water column and became shallower during the stratification/resting phase (day 6 to 10) as the water column stabilized and biomass accumulated in the UML due to phytoplankton growth (Burger et al., 2020). The chlorophyll *a* data along with microscopy observations indicated that the eukaryotic cell density between the surface and depth differed significantly, with a higher biomass at the surface where phytoplankton had a sufficient light source, one of the key factors for phytoplankton growth (Kirk, 1994). The different phytoplankton biomass is expected due to a light gradient. Over the course of the study, the eukaryotic cell density was relatively stable during the upwelling phase, consistent with a well-mixed water column where vertical mixing ensures a homogenized phytoplankton and nutrient distribution (Mellard et al., 2011). Diatoms were the dominant eukaryotic cells in these unstable upwelled waters and lower SST, similarly to other study findings (Zhang et al., 1996; Bruland et al., 2001; Smayda and Trainer, 2010), with *S. costatum* being the dominant chain forming diatom during this phase (Day 1 to 5). The cell density increased significantly during the stratified period (Day 6-10) as a two layered water system formed and water became more stable, however there was a large decrease in *S. costatum* relative abundance and a community shift occurred with an increase in *Thalassiosira spp.* as well as several dinoflagellate species as seen in Figure 6 and explained in Burger et al., (2020). On day 6 there was a noticeable shift

in community composition with an intrusion of fungi, mainly representative species of Saccharomycetes and Chytridiomycetes, indicative of an alien intrusion in the water mass before the sampling took place on day 6. The community shift from diatoms to dinoflagellates has been documented in various studies (Trigueros and Orive, 2001; Zhou et al., 2017; Spilling et al., 2018), nevertheless, the timing of these shifts and the role that parasitism amongst other biotic interactions play is still being investigated.

Eukaryotic cell (2-100µm) infections by Syndiniales MALV I and II

During the upwelling period, the frequency of infections of eukaryotic cells (2-100µm) via Syndiniales at the surface was the highest, and the most identified hosts were *S. costatum* and *Radiolaria.* The co-occurrence of Syndiniales and *S. costatum* is well documented suggesting its potential as a host for the parasitic Syndiniales (Guillou et al., 2008; Liu et al., 2017; Yan et al., 2023; Anderson et al., 2024) and microscopy images confirmed the infection of *S. costatum* which I believe is visually shown for the first time whereas many studies only recorded the parasite host co-occurrence (Guillou et al., 2008; Liu et al., 2017; Yan et al., 2023; Anderson et al., 2024).

The significant differences in the frequency of infections between the surface and 10m depth could be attributed to the higher eukaryotic cell density within the euphotic zone. Very low infection rates were noted throughout the entire study at the 10m depth samples. Similar findings were reported in the paper written by Sehein et al., (2022) showing that most of infections were concentrated at the surface where the thecate and athecate dinoflagellate hosts occurred in more oxygenated waters.

A significant difference was found for the frequency of infections at the surface between the upwelling and resting phase. This was an interesting finding as the highest frequency of infections was seen during the upwelling phase (Day 1-5) whilst the biomass nearly doubled during the resting phase (day 6-10) (Burger et al., 2020). The dominant species seen during the first phase were the small diatoms *S. costatum* and *Chaetoceros spp.*, which decreased during the resting phase as larger diatoms such as *Thalassiosira spp*. and *Coscinodiscus gigas* appeared along with dinoflagellates like *Protoperidinium spp., Gyrodinium spp.* (a known Syndiniales Group II host (Jacobson, 1987; Coats et al., 1996))*, Tripos furca, Tripos lineatum,* and *Dinophysis spp*. (Burger et al., 2020). Due to the community shift from diatom to dinoflagellates a decrease in Syndiniales infections were seen, suggesting that the specific clade of the Syndinales parasite favoured the small centric chain forming diatoms as a host, or that the shift in preferred host limited the infectivity of the dinospores. Although Syndiniales have a wide host range, this specificity for infections of certain parasite-host strains have been recorded by Cai et al. (2020). Even though dinoflagellates are well known hosts of Syndiniales, the clade found in St Helena Bay seemed to favour diatoms during the austral spring/summer season of 2016.

A recent study done by Long et al (2021) showed that resistant Dinophaceae provide extracellular defence against the parasite by excreting Anti-Parasitic Compounds (APCs) that can increase the survival of the non-resistant hosts, and can decrease the survival time, the membrane integrity, and the progeny of the free-swimming dinospores. This has shown that metabolites present in the water column affect the infection dynamics of the parasite and that higher concentrated cell patches can provide a more efficient protection against Syndiniales (Long et al., 2021). The release of these APC's could be the reason for the lower infections seen by the parasite during the resting phase in this study. Future studies on the metabolome of the water column during upwelling and resting phases is crucial to get better insight on the Syndiniales infection dynamics.

Temperature and silicate were important factors influencing the frequency of infections by Syndiniales according to the Pearson correlation matrix (Table 1), like the findings of Anderson and Harvey (2020). It is well known that abiotic factors are generally poor indicators for community composition and have less importance compared to biotic factors (Anderson and Harvey, 2020). Nevertheless, the frequency of infected eukaryotes was highly correlated with nitrite ($r = 0.949$, p-value < 0.001), phosphate ($r=0.906$, p-value<0.001), and silicate ($r=0.817$, p-value $= 0.004$). Silicate is an important growth limiting factor for diatoms (Smetacek, 1998) and the correlation of silicate with Syndiniales infections can be interpreted by the high silicate levels leading to the high abundance of diatoms where the diatom *S. costatum* was the most abundant and the main host for Syndiniales. The Canonical Correspondence Analysis (CCA) plot used Syndiniales ASV's and I constrained the model by the Syndiniales host *S. costatum* as well as the nutrient silicate required for diatom growth. The plot indicated significant correlations of silicate, nitrate, and phosphate with the samples taken at both depths during the upwelling and resting phase (Figure 10). Silicate had a positive correlation with the upwelling samples indicating that high levels of silicate allowed for high diatom biomass as was seen in the relative abundance (Figure 6), more specifically *S. costatum* biomass. Both nitrate and phosphate eigenvectors had negative correlations with the samples taken during the resting phase, indicating that the marine microbes incorporated these nutrients during phytoplankton growth. Because the biomass nearly doubled during the resting phase, this negative correlation can be explained by the increased biomass and their requirement of these nutrients to grow. Both the frequency of infected cells and the host *S. costatum* were positively correlated with the upwelling samples with their eigenvectors very close together.

Upon further inspection of the relative abundance of eukaryotes done by Burger et al., (2020), a similar profile was seen between the frequency of infected eukaryotes (Figure 5) and the relative abundance of *S. costatum* (Figure 6) over the 10-day study period. Statistical tests showed no

correlation between these values, however, upon plotting the total *S. costatum* along with the frequency of infections in Figure 8, a clear trend was observed. This graph showed a 24-hour delayed response of the host abundance according to infections, with high infections resulting in a sudden decrease in the host. The typical release time of dinospores from initiation of infection is 24 to 48 hours (Chambouvet et al., 2008; Velo-Suarez et al., 2013). During the time that the host abundance was low, the presence of infected cells decreased. This led to the hosts being able to multiply once again and become abundant, upon which the frequency of infections could increase once more within a 24-hour delay period. This gives supporting evidence that Syndiniales abundance follows that of their host, with higher infection rates during periods of high host abundances.

On day 7 there was a noticeable increase in the abundance of *S. costatum* at the surface (Figure 8). This was the day following the dramatic shift in community composition documented on day 6 due to an alien intrusion (depicted in Figures 6 and 8) which led me to believe something in the water column aided in the proliferation of these diatoms, possibly released metabolites as there was no dramatic shift or spikes in the environmental variables. The line graph (Figure 8) shows a spike in the *S. costatum* at 10m depth on day 8, which can be explained by the sinking of these diatoms present on day 7 during a resting phase when the water current fails to keep them suspended at the surface during water stratification.

The relative abundance of the 18S rRNA indicated that Syndiniales MALV I monopolized the waters over the course of the whole study (Figure 10), with MALV II only making up a small fraction of the abundance, however, is the most diverse within Syndiniales, having up to 44 unique clades gathered from environmental DNA sequences (Guillou et al., 2008). The relative abundance of Syndiniales Group I and II is contradictory to the microscopy observations showcasing the problem often encountered with gene copy numbers, leading to overrepresentation. Furthermore, many of the Syndiniales sequences could be those of their dinospore form which was not easily identifiable under the fluorescent microscope. The Simpson index showed that the Syndiniales diversity was the highest on days four to six, the transition period between the upwelling and resting phase (Figure 10B). Upwelling supports increased phytoplankton growth, favouring specific species that can rapidly respond to the influx of nutrients, typically diatoms. As these nutrients are used up and upwelling weakens, a different microbial community is established with species that can thrive under lower nutrient concentrations such as dinoflagllates (Margalef 1958; Legendre 1990; Álvarez-Salgado et al. 1996), therefore the transition period typically results in an increased biodiversity due to higher eco-niche possibilities hosting upwelling specialists and resting-phase opportunists.

A study done by Anderson et al., (2024) revealed a negative correlation between particulate organic carbon flux and Syndiniales implying that Syndiniales influences the carbon export via the breakdown of hosts' organic matter and allowing remineralization to occur in the euphotic zone, ultimately decreasing the amount of carbon that sinks to deeper depths. They also found that the amount of Syndiniales involved in vertical transport (~19%) coincides with that of primary production export from the surface to deeper water layers (10-20%) (Anderson et al., 2024). Although Syndiniales diminishes carbon flux at the surface, a proportion of the Syndiniales community do contribute to the carbon flux.

Syndiniales parasites act similar to viruses where they reroute carbon within the microbial loop to the pools of dissolved and particulate organic matter during host lysis which support bacterial growth (Yih and Coats, 2000). They are ultimately responsible for the remineralization of carbon (Anderson et al., 2024), hence playing a role in the carbon flux and biogeochemical cycle. Based on known cell concentrations and infection rates, one can create models to calculate the amount of carbon that is infected to estimate the total carbon sequestration (transport to deeper waters where it can be stored for centuries) and the carbon cycling dynamics (remineralization). This would provide crucial information on the flow of carbon in the biogeochemical cycle, especially during climate change. According to microscopy counts done by Burger et al., (2020), *S. costatum* represented 53.47% of the micro/nanoplankton cells for the first 5 days and being a host for Syndiniales are suggested to have major effects on the total particulate carbon flux attenuation within the Benguela based on the findings of Anderson et al. (2024) and can serve as carbon export biomarkers.

Chapter 3: Infection dynamics of Syndiniales within a stratified water column in St Helena Bay

The Benguela upwelling system in austral autumn/winter

The Benguela upwelling system located in the western coast of south Africa is regarded as one of the four major Eastern Boundary Upwelling systems (EBUS), along with the Canary Current, California Current, and Humboldt Current. Upwelling is most prominent during the austral spring and summer periods within the Benguela (Nelson and Hutchings, 1983) resulting in regular bloom events during that time, with diatoms being the first to dominate followed by dinoflagellate dominated blooms which could include harmful algal species that cause red tides. However, during the austral autumn and winter periods the strength of upwelling decreases due to decreased wind strengths and a shift in wind direction from southerly to northerly winds (Shannon and Nelson, 1996) resulting in a more stratified water column.

St Helena Bay is formed by the Cape Columbine and is a well-known retention zone for biomass produced in the Southern Benguela (Weeks et al., 2006). The increased residence time of the upwelled waters is distinguishable by the warmer waters and stratified water columns, which ultimately intensify phytoplankton growth, resulting in elevated production throughout the year compared to other upwelling sites in the region (Brown and Hutchings, 1987). Upwelling brings nutrient rich water masses to the surface where primary producers and heterotrophic grazers respond rapidly to the changing environmental conditions due to water mixing followed by water stratification and warming (Burger et al., 2020). Due to high productivity in stratified water, the nutrients quickly become depleted, and the phytoplankton are grazed upon or die, some of which sink to deeper water layers where they are remineralized. The remineralization occurs via aerobic respiration of bacteria as the particles sink which increase hypoxia and anoxia within deeper water layers (Pitcher and Weeks 2006; Weeks et al. 2006; Pitcher and Probyn, 2017). In aged, upwelled water where nutrients are limited, a smaller phytoplankton size (4-10µm) is favoured due to their high surface area to volume ratio (Crichton et al., 2013). Additionally larger dinoflagellates may also survive due to their vertical migration, enabling them to obtain nutrients from the underlaying water below the thermocline (Margalef, 1978; Fenchel, 1988; Pitcher et al., 1991; Kiørboe, 1993). During the austral winter, factors such as increased storm mixing, reduced upwelling and reduced sunlight, all favour the small size fraction (4-10µm) phytoplankton (Hutchings et al., 1984; Shannon et al., 1984; Pitcher et al., 2010).

An assortment of prokaryotes and eukaryotes display a parasitic lifestyle targeting various phytoplankton (Elbrächter and Schnepf., 1998). Amongst the known parasites, MALV groups I and II

are the most abundant in environmental samples and have been a topic of interest for several years to understand their role in community composition, possible top-down control, and potential biomarker for carbon flux (Coats and Bockstahler, 1994; Coats et al., 1996; Coats and Park, 2002; Park et al., 2004; Chambouvet et al., 2008; Montagnes et al., 2008; Velo-Suarez et al., 2013; Anderson et al., 2024).

This chapter aims to display the spatial and temporal distribution of Syndiniales in a stratified water column and serves as a comparison to chapter 2 to showcase the contrasting microbial and phytoplankton community dynamics and how that relates to infections from Syndiniales MALV I and II. During thermohaline stratification, the warm nutrient poor surface waters are separated from the deeper cold nutrient rich waters. Due to the absence of water mixing, the phytoplankton communities differ in composition as was demonstrated by van Schalkwyk (2021). He showed that the α-diversity differed significantly between depths but not between days, indicating that there was a stable community composition over the 5-day study period at each depth. Previous studies suggest that the parasite abundance and infection rates are mainly driven by the host density, with planktonic blooms resulting in increased infections (Park et al., 2004; Coats et al., 1996). I hypothesize that these distinct community compositions at different depths will show different proportions of Syndiniales infections. The objective was to a) quantify the total eukaryotic cell density both spatially and temporally, b) quantify the total proportion of eukaryotes infected by Syndiniales, and c) investigate how environmental variables might affect these infections.

Methods and Materials

Study area and sampling site

A 5-day anchor station study was conducted at station 6 of the Berg River transect within St Helena Bay (32.596°S; 18.043°E) on the 12th to 16th April 2019 (Pitcher et al., 2023). Five-liter water samples were collected for five consecutive days at around 9am aboard a Gemini semi-rigid inflatable craft, MA-RE (Department of Forestry, Fisheries and the Environment). Water samples were taken in triplicates at 1m, 25m, and 50m depths respectively within Niskin bottles. The water was prefiltered through a 200µm mesh before placed in 250ml black bottles. 50ml Water samples were taken from each of the depths to use for the FISH preparation by adding 37% formaldehyde with a final concentration of 1%. The water samples were then filtered out on a membrane filter with a pore size of 0.2µm and 47mm diameter. Each membrane filter was placed in a Petri dish and was stored at -80°C until further processing took place in 2024. The hydrography of the water was obtained via dispatching a handheld CTD (Sea Bird 1900 Plus) sensor from the surface to within 5m of the seafloor prior to the sampling collection.

Laboratory and microscopy work

The laboratory and microscopy work performed for the 2019 St Helena Bay FISH samples were the same as done in Chapter 2 with the exception that no CARD-FISH procedures were performed due to cost constraints.

Results

Hydrography of the water column

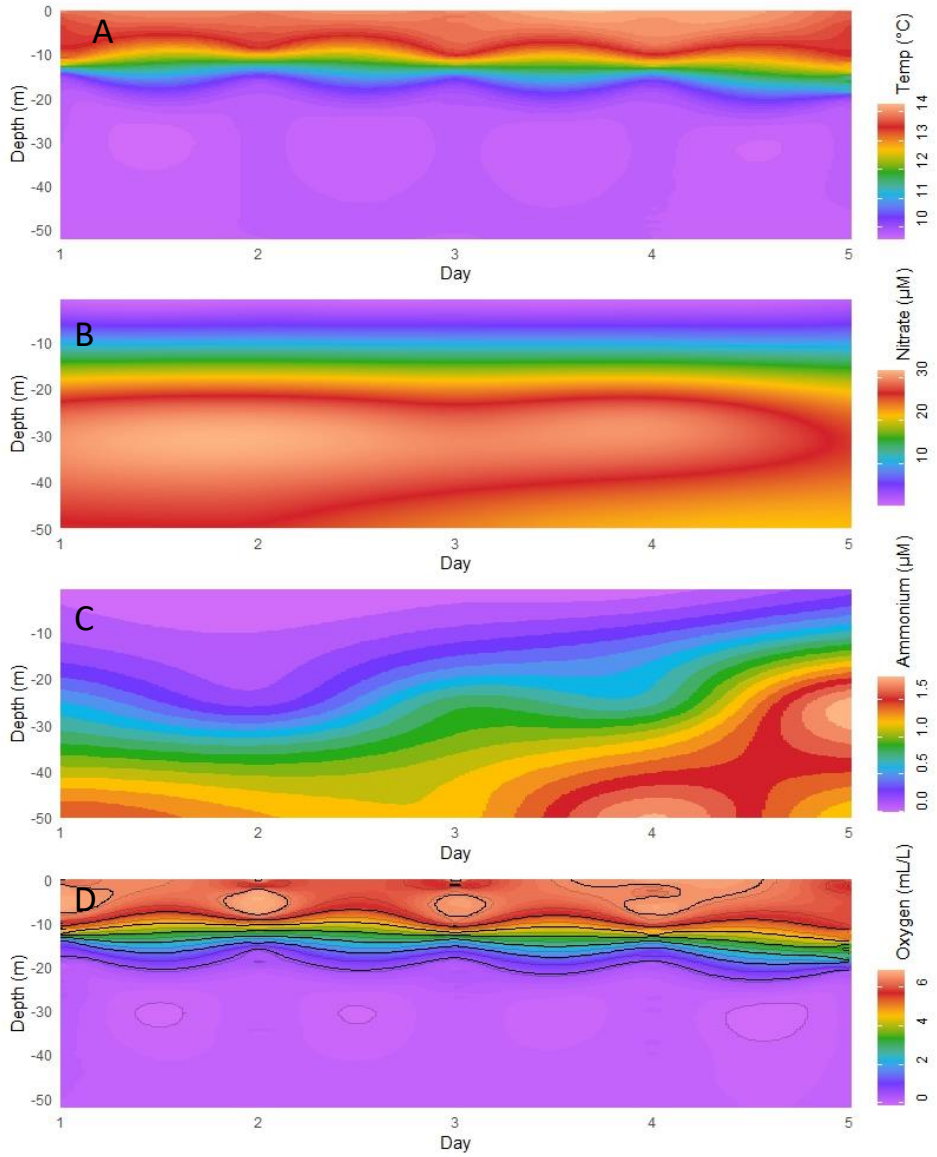

Figure 13: The hydrography of the water column over the 5 consecutive day sampling period. The major water column variables measured included the A: temperature (°C), B: Nitrate (µM), C: Ammonium (µM), and D: oxygen concentration (ml.L^{-1}). Across all 5 days the water column was stratified with the MLD around 12m from the surface.

Based on the water hydrography, the water column showed characteristics of being stratified, as is expected during the austral autumn season (Figure 13). A well-defined mixed layer depth formed with the upper euphotic zone reaching 9m deep and the bottom layer forming at 12m deep, a thermocline separated these two layers at 10m. The overall average temperature for the first 9m was 13.787°C ± 0.130°C and was highest on day 3 at 14.483° at 0m. There was a steady decrease in temperature from 13.293 ± 0.351°C to 9.878 ± 0.152°C between 10m and 20mrespectively. Day 5 displayed a slightly deeper thermocline with temperatures decreasing from 13.487°C at 13m to

9.914°C at 21m. The water column temperature from 20m downwards averaged at 9.763 ± 0.043°C for all days. Oxygen followed the same profile as the temperature with an average of 6.424±0.237 mg/L for the first 9m, with the highest recorded concentration being 6.941 mg/L on day 2 at 5m depth. From 20m onwards the oxygen concentration remained steady, averaging at 0.142±0.058 mg/L. The overall salinity for the entirety of the study at all depths were 34.756±0.029ppt, with the lowest measurement of 34.236 ppt on day 2 at 0m and the highest measurement of 34.863ppt on day 3 at 1m.

The average nitrite (NO_2^-) concentrations were 0.088±0.027 µM and 3.730±0.074 µM at 1m and 25m respectively and the nitrate (NO_3^-) concentrations were 0.853±0.150 µM and 27.792±0.333 µM at 1m and 25m respectively. The ammonium (NH_4^+) concentrations were 0.048±0.014 µM and 0.815±0.022 µM at 1m and 25m respectively. The silicate (SiO_4^-) concentration was 6.154±0.101 mg/L at the surface and increased to 34.409±0.380 mg/L at 25m whereas the phosphate (PO_4^-) concentration was 0.391±0.038 ppm at the surface and increased slightly to 2.313±0.037 ppm at 25m depth.

Eukaryotic cell density

The Shapiro wilk test was used for both the 1m and 25m depth data and indicated that the distribution of the total eukaryote cell (2-100µm) densities per ml over the 5-day study period was not normal (W= 0.79609, p-value < $2.2e^{-16}$ and W = 0.62095, p-value < $2.2e^{-16}$ respectively). The Mann-Whitney U test indicated that there was a significant difference in the distribution of the total cell densities between the two depths over the 5 days (W = 252278, p-value < $2.2e^{-16}$).

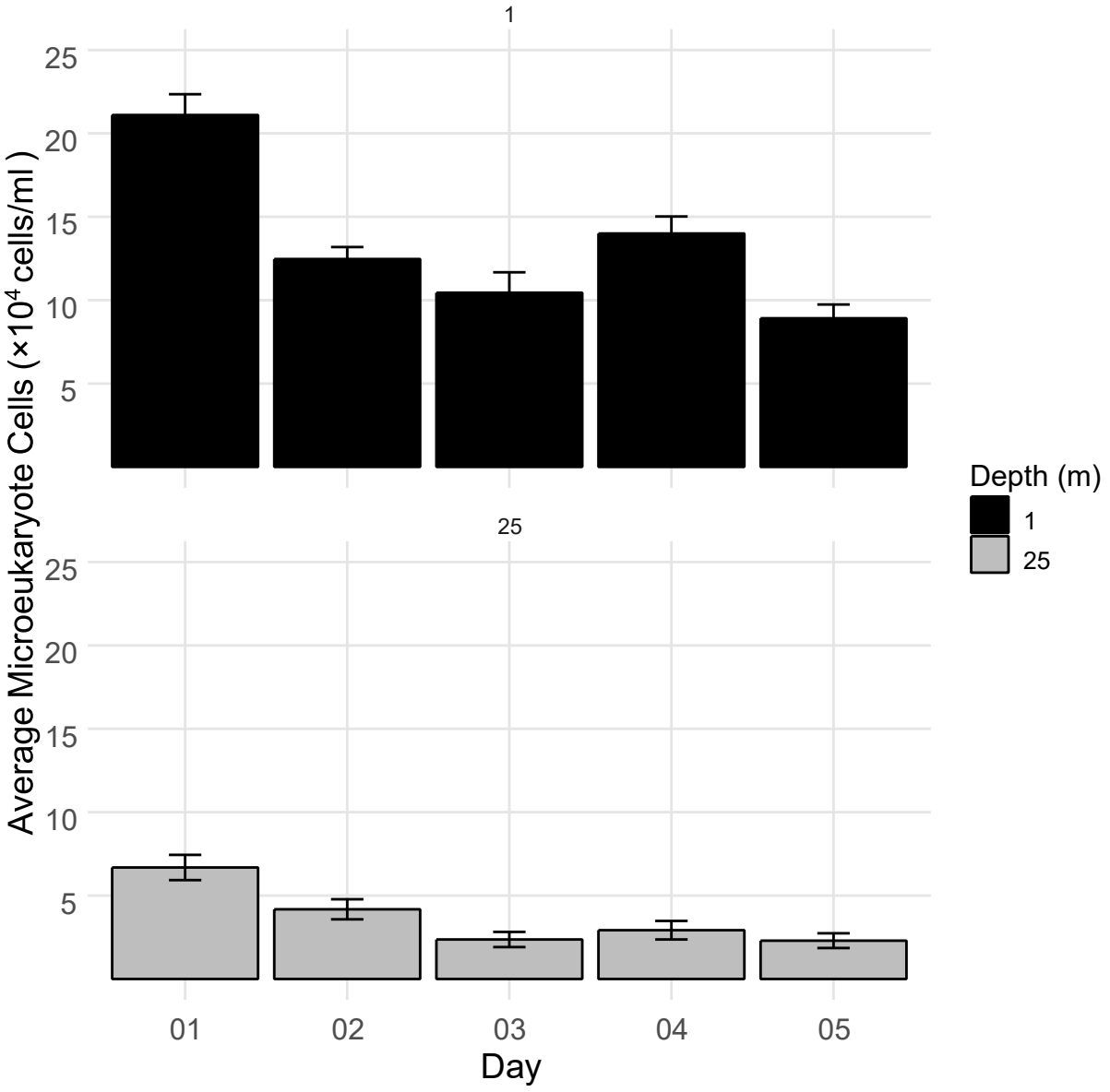

Figure 14: The average eukaryote cell (2-100µm) density per millilitre for the samples collected over 5 consecutive days from 12 to 16 April 2019. The black depicts the cell density/ml at the surface (1m) and the grey depicts the cell density/ml at a depth of 25m.

The community composition was described in detail by van Schalkwyk (2021), in summary, the α-diversity and Shannon-Wiener diversity indicated clear differences in the community composition at the two depths (FS = 42.55, $df_1 = 2$, $df_2 = 30$, $p < 0.001$ and FS = 71.04, $df_1 = 2$, $df_2 = 30$, $p < 0.001$ respectively), insufficient evidence for community composition differences amongst days for the surface (FS = 0.81, $df_1 = 4$, $df_2 = 30$, $p = 0.53$), and supporting evidence for community composition differences amongst days at 25m depth (FS = 4.91, $df_1 = 4$, $df_2 = 30$, $p = 0.003$), however, the data had insufficient power to determine which days. Furthermore, van Schalkwyk (2021) showed that the

surface had the greatest biomass, mainly made up of *Prorocentrum micans* (72.3 % of the average daily carbon biomass). This percentage is noteworthy, as *P. micans* was shown to be almost always infected by Syndiniales being a key candidate for large amounts of carbon attenuation via remineralization, playing a role in the biogeochemical cycle (Figure 15).

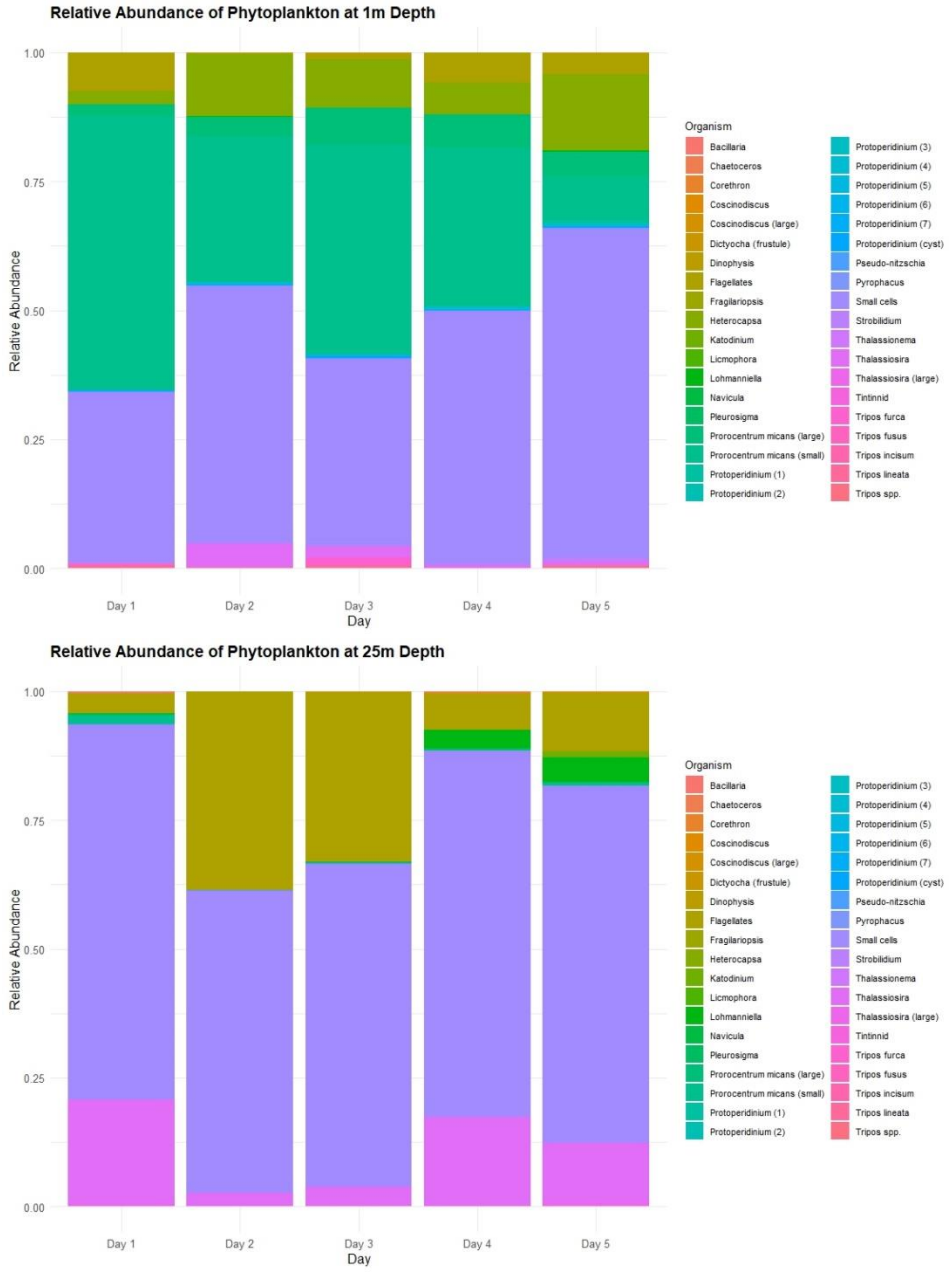

Figure 15: The relative abundance of phytoplankton identified under light microscopy by Van Schalkwyk (2021) at A) 1m and B) 25m respectfully. A) The most abundant phytoplankton at the surface included Prorocentrum micans *(small),* Prorocentrum micans *(large), Small cells, Flagellates,* Heterocapsa*, and* Thalassiosira*. B) The most abundant phytoplankton at 25m depth included small cells*, Thalassiosira*, Flagellates, and* Lohmanniella*.*

Eukaryotic cell (2-100µm) infections by Syndiniales I and II

The Wilcoxon test indicated that there were no significant differences in the frequency of infections by Syndiniales I and II (W= 153200, p-value= 0.4192). Hereafter, no distinction was made between Syndiniales I and II for statistical analyses.

The Shapiro wilk test indicated that there was a non-normal distribution of the frequency of infected eukaryotic cells at the two depths over the 5 days (W= 0.73704, p-value < $2.2e^{-16}$, and W= 0.30522, p-value < $2.2e^{-16}$ respectively). The Mann-Whitney U test indicated that there was a significant difference in the distribution of the total infected eukaryotic cell densities between the two depths over the 5 days (W= 238915, p-value < $2.2e^{-16}$) (Figure 16).

A Kruskal-Wallis test revealed significant differences in total eukaryotic cell densities at the surface across the five sampling days ($\chi^2 = 84.17$, $p < 0.001$). Post hoc analysis showed that Day 1 differed significantly from all other days, indicating a marked shift in cell abundance following the initial sampling. Although other statistically significant differences were observed (e.g., between Days 2 and 5, and Days 4 and 5), these changes were less pronounced and may not reflect ecologically meaningful variation. Similarly, at 25 m depth, significant differences were detected ($\chi^2 = 34.84$, $p < 0.001$), with Day 1 again differing from all subsequent days. These results suggest that the most ecologically relevant shift in eukaryotic cell abundance occurred between Day 1 and the remainder of the sampling period. To assess the differences in the frequency of infected eukaryotic cells at the surface, a Kruskal Wallis test was performed as the data was not normally distributed. The test indicated significant differences between the infected cells over the 5 sampling days difference ($\chi^2 = 136.038$, df = 4, $p < 0.001$) and a post hoc Dunn's pairwise comparison test was performed. This test revealed significant difference between Days 1 and 2 (Z=3.378, p-value < 0.001), 1 and 3 (Z=3.754, p-value < 0.001), 1 and 4 (Z=7.642, p-value < 0.001), 1 and 5 (Z=10.854, p-value < 0.001), 2 and 4 (4.264, p-value < 0.001), 2 and 5 (Z=7.478, p-value < 0.001), 3 and 5 (Z=3.922, p-value < 0.001), and 4 and 5 (Z=3.213, p-value < 0.001). The Kruskal Wallis test performed to assess the frequency of

infection at depth (25m) indicated no significant differences over the 5 sampling days (χ^2 = 7.895, df = 4, p = 0.095).

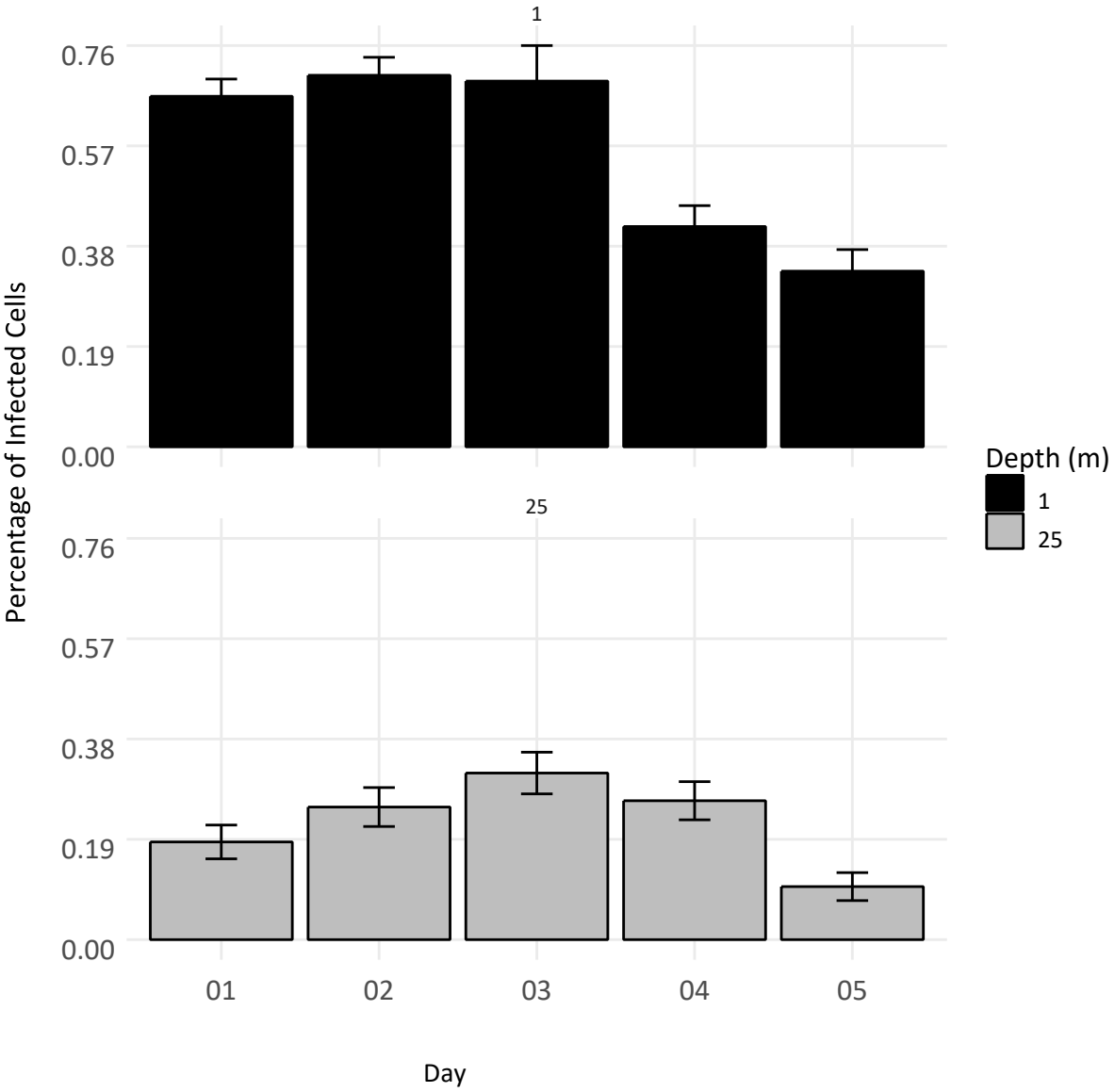

Figure 16: The percentage of eukaryote cells (2-100µm) that are infected by Syndiniales during the 5-day study period are depicted in this graph. The black depicts the percentage of infections at the surface (1m) and the grey depicts the percentage of infections at a depth of 25m.

Environmental factors and eukaryotic cell densities

A Pearson correlation matrix was created for the surface data, incorporating all the available environmental factors to identify any linear correlations between these factors and the total cells/ml as well as the frequency of infections. Based on the correlation matrix, there was no significant correlation between the environmental variables and the total eukaryote cell density per ml at the surface. The frequency of Syndiniales-infected eukaryotic cells (2-100µm) had a negative correlation

with ammonium (r = -0.658, p-value =0.039) and phosphate (r = -0.733, p-value =0.016), and a positive correlation with salinity (r=0.854, p-value = 0.002). The results are shown in Table 3.
The Pearson correlation matrix created for the samples taken at 25m yielded no significant correlations for the frequency of infected eukaryotic cell density (infected cells/total cells), however upon inspection of the total cells infected by Syndiniales, strong negative correlations with nitrite (r = -0.741, p-value = 0.014), ammonium (r = -0.717, p-value = 0.020), and temperature (r = -0.700, p-value = 0.024) was seen, and a significant positive correlation with nitrate was observed (r = 0.692, p-value = 0.027). These results are depicted in Table 4.

Table 3: The correlation matrix (CM) of Pearson (r) correlation coefficient and listwise deletion method for the environmental and species data taken at the surface (1m) for April 2019. The 'Total eukaryotes' represents the total eukaryotic cells (2-100µm) per ml, the 'Infected' represent the total eukaryotic cells (2-100µm) per ml infected by Syndiniales, and the 'Frequency' refers to the frequency of the infected eukaryotic cells. Figures in black and in brackets have a p-value < 0.05.

	Nitrate	*Nitrite*	*Ammonium*	*Phosphate*	*Silicate*	*Temperature*	*Salinity*	*Oxygen*	*Total*	*Infected*	*Frequency*
Nitrate											
Nitrite	0.968 *(<.001)*										
Ammonium	0.961 *(<.001)*	0.886 *(.001)*									
Phosphate	0.908 *(<.001)*	0.845 *(.002)*	0.969 *(<.001)*								
Silicate	0.137 *(.705)*	-0.080 *(.825)*	0.330 *(.352)*	0.228 *(.526)*							
Temperature	-0.823 *(.003)*	-0.813 *(.004)*	-0.801 *(.005)*	-0.666 *(.035)*	-0.333 *(.347)*						
Salinity	-0.520 *(.124)*	-0.438 *(.205)*	-0.531 *(.115)*	-0.639 *(.047)*	0.096 *(.791)*	-0.046 *(.899)*					
Oxygen	0.441 *(.203)*	0.253 *(.480)*	0.440 *(.203)*	0.263 *(.462)*	0.660 *(.038)*	-0.422 *(.225)*	-0.215 *(.550)*				
Total eukaryotes	-0.422 *(.224)*	-0.570 *(.085)*	-0.398 *(.254)*	-0.546 *(.103)*	0.544 *(.104)*	0.234 *(.515)*	0.321 *(.366)*	0.616 *(.058)*			
Infected	-0.539 *(.108)*	-0.587 *(.075)*	-0.550 *(.099)*	-0.710 *(.021)*	0.362 *(.304)*	0.134 *(.712)*	0.720 *(.019)*	0.311 *(.381)*	0.849 *(.002)*		
Frequency	-0.618 *(.057)*	-0.529 *(.116)*	-0.658 *(.039)*	-0.733 *(.016)*	-0.074 *(.839)*	0.179 *(.621)*	0.854 *(.002)*	-0.269 *(.452)*	0.356 *(.312)*	0.780 *(.008)*	

Table 4: The correlation matrix (CM) of Pearson (r) correlation coefficient and listwise deletion method for the environmental and species data taken at a depth of 25m for April 2019. The 'Total eukaryotes' represents the total eukaryotic cells (2-100µm) per ml, the 'Infected' represent the total eukaryotic cells (2-100µm) per ml infected by Syndiniales, and the 'Frequency' refers to the frequency of the infected eukaryotic cells. Figures in black and in brackets have a p-value < 0.05

	Nitrate	*Nitrite*	*Ammonium*	*Phosphate*	*Silicate*	*Temperature*	*Salinity*	*Oxygen*	*Total*	*Infected*	*Frequency*
Nitrate											
Nitrite	-0.976 *(<.001)*										
Ammonium	-0.961 *(<.001)*	0.963 *(<.001)*									
Phosphate	-0.478 *(.162)*	0.321 *(.366)*	0.463 *(.178)*								
Silicate	-0.947 *(<.001)*	0.897 *(<.001)*	0.890 *(.001)*	0.669 *(.034)*							
Temperature	-0.673 *(.033)*	0.758 *(.011)*	0.765 *(.010)*	-0.151 *(.677)*	0.422 *(.225)*						
Salinity	-0.101 *(.780)*	-0.109 *(.765)*	0.023 *(.950)*	0.852 *(.002)*	0.292 *(.413)*	-0.476 *(.164)*					
Oxygen	0.182 *(.615)*	-0.383 *(.274)*	-0.319 *(.369)*	0.615 *(.058)*	0.025 *(.944)*	-0.729 *(.017)*	0.920 *(<.001)*				
Total eukaryotes	0.414 *(.234)*	-0.493 *(.148)*	-0.533 *(.113)*	0.302 *(.397)*	-0.124 *(.732)*	-0.924 *(<.001)*	0.490 *(.151)*	0.693 *(.026)*			
Infected	0.692 *(.027)*	-0.741 *(.014)*	-0.717 *(.020)*	-0.082 *(.823)*	-0.572 *(.084)*	-0.700 *(.024)*	0.246 *(.493)*	0.457 *(.184)*	0.501 *(.140)*		
Frequency	0.469 *(.172)*	-0.488 *(.153)*	-0.380 *(.279)*	-0.318 *(.371)*	-0.614 *(.059)*	0.025 *(.945)*	-0.040 *(.913)*	0.003 *(.993)*	-0.337 *(.340)*	0.572 *(.084)*	

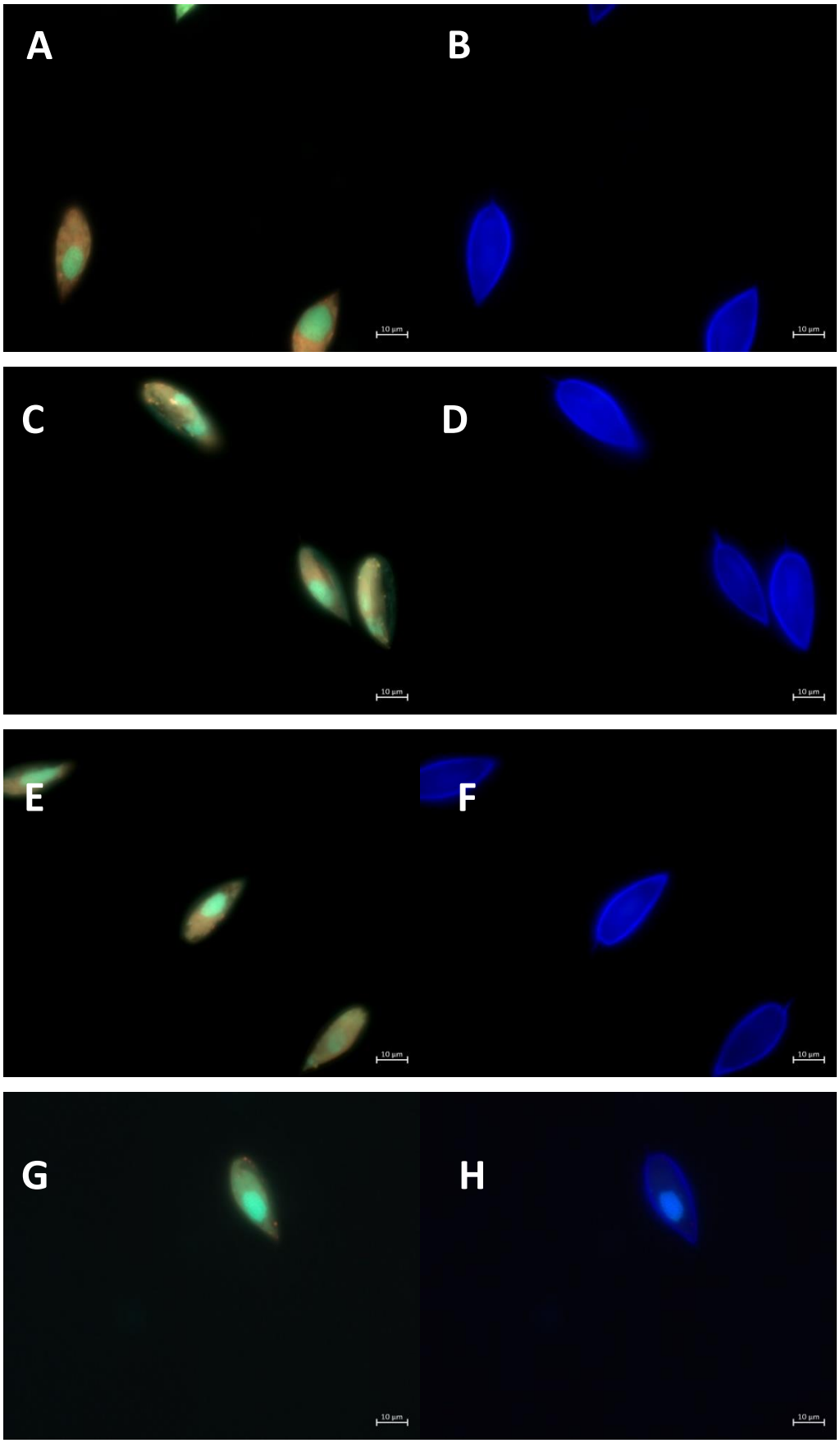
A
B
C
D
E
F
G
H

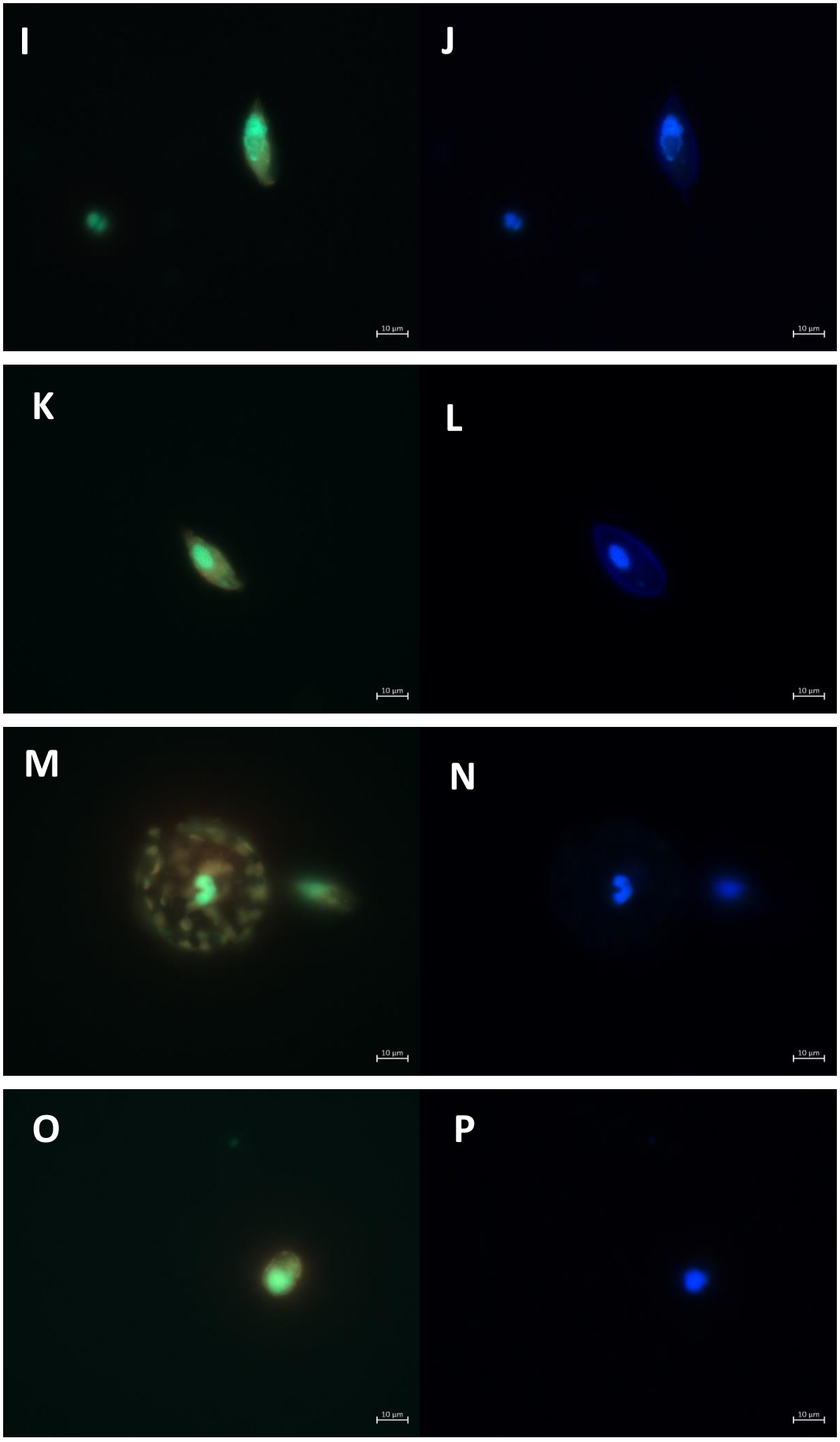
I
J
K
L
M
N
O
P
10 µm

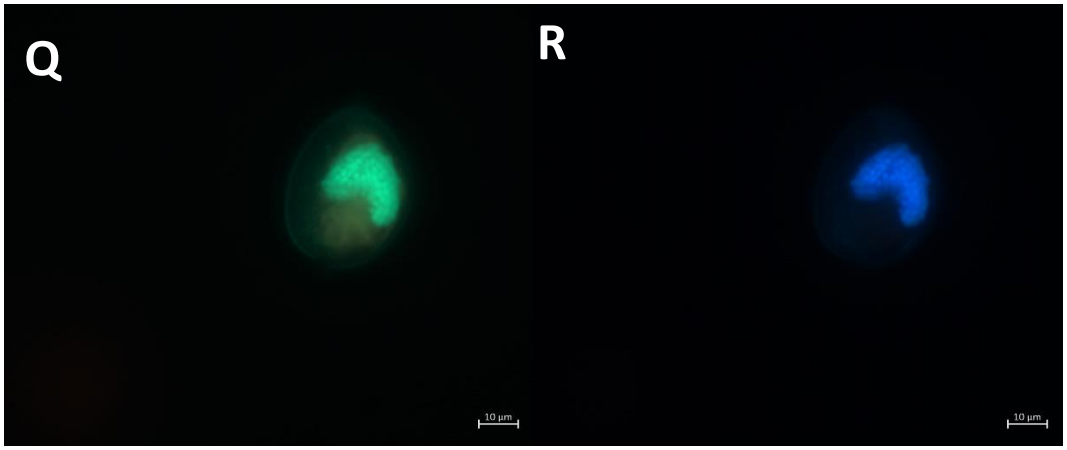
Q
R
10 µm
10 µm

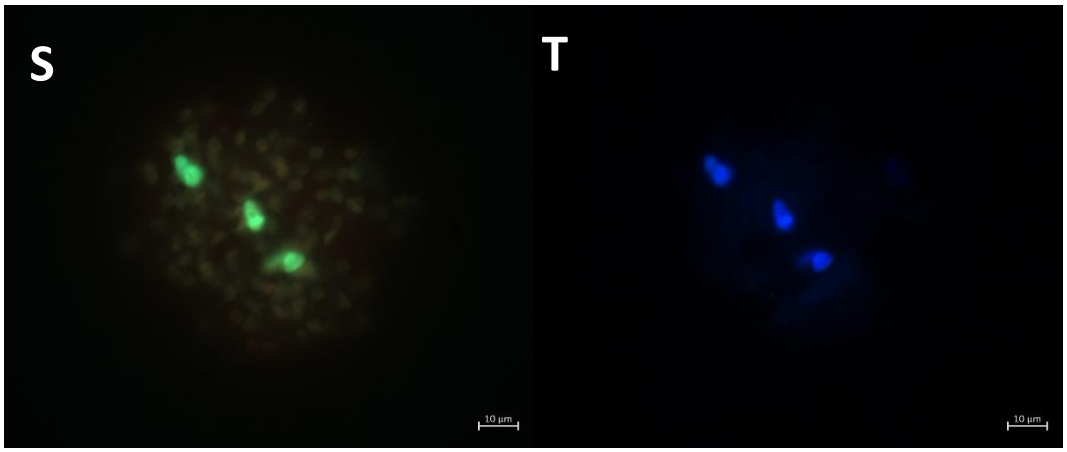
S
T
10 µm
10 µm

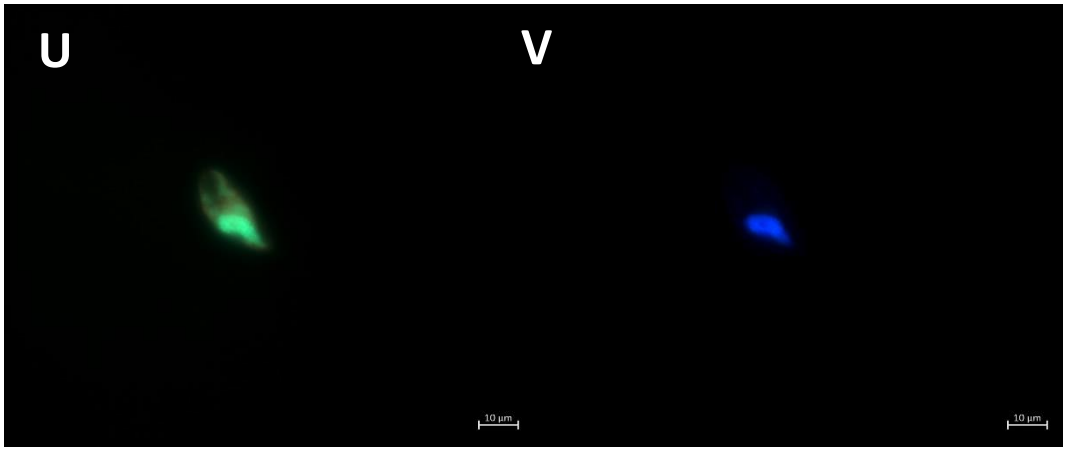
U
V
10 µm
10 µm

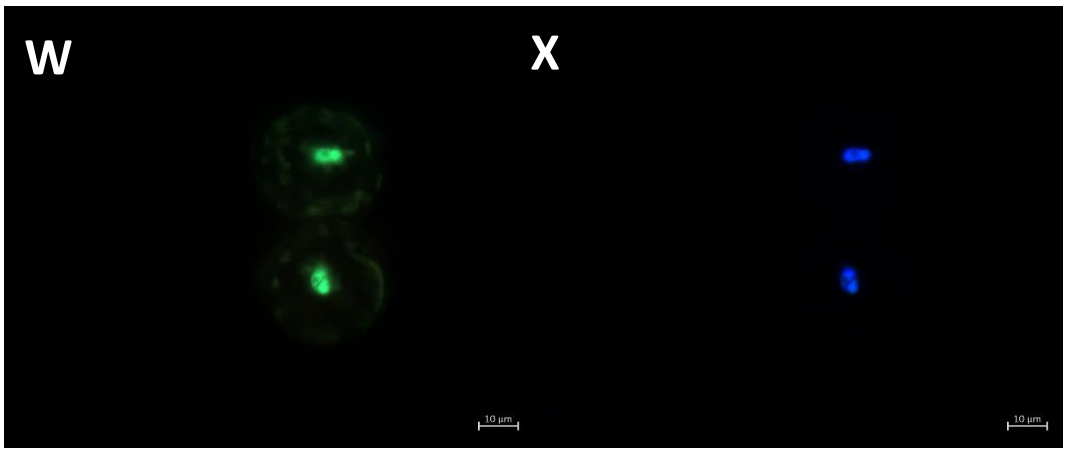
W
X
10 µm
10 µm

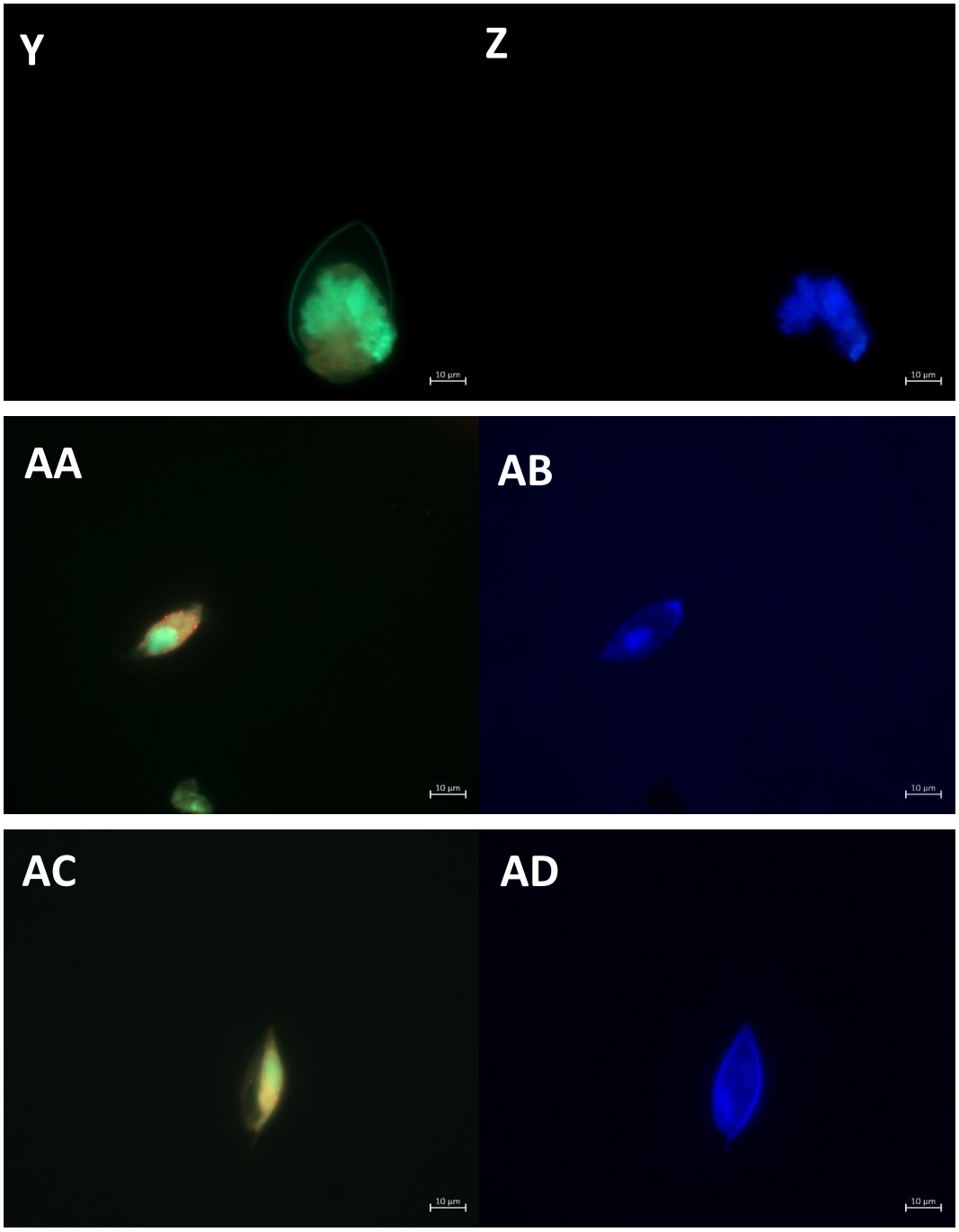
Y
Z
AA
AB
AC
AD
10 µm

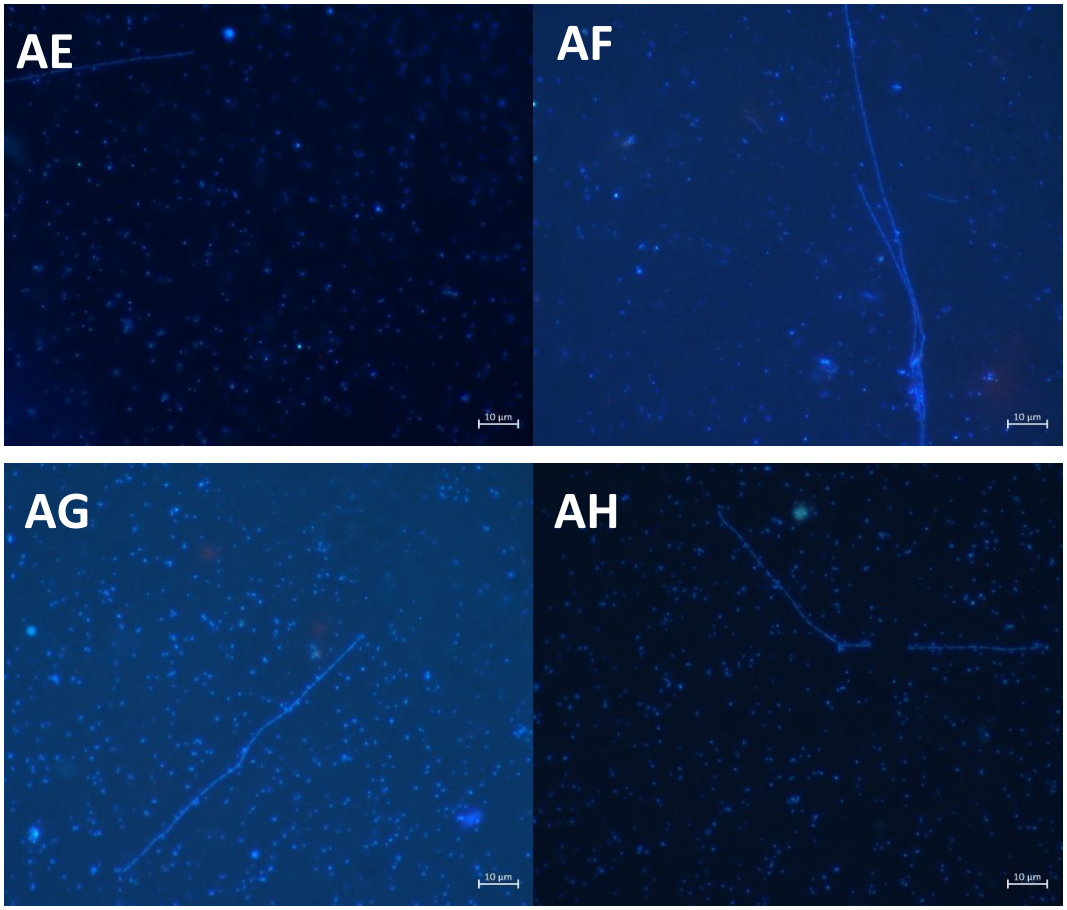

Figure 17: FISH microscopy images depicting Syndiniales infected eukaryotic cells where the left image with bright green fluorescence represents the Syndiniales parasite and the right image with the blue fluorescence represent the DNA of the prokaryotic and eukaryotic cells (cell membranes appear blue due to Calcofluor staining).Images represent samples taken at the surface for Day 1(A-J), Day 2 (K-T), Day 3 (U-Z), Day 4 (AA-AD), and at depth (25m) for Day 1 (AE-AF), and Day 2 (AG-AH). The dominant eukaryote belonged to the genus Prorocentrum *with a characteristic leaf shape (A-L, Q-R, U-V, Y-AD), rarely, the eukaryote belonging to* Radiolaria *appeared (M-N, S-T, W-X), and many unidentifiable round dinoflagellates were present (O-P). The samples taken at depth were dominated by bacteria and a very thin* Thalassiosira *chain forming diatoms (AE-AH).*

Discussion

The Benguela current

The Benguela current is part of the four major EBUS's and is arguably the most productive upwelling regions that play an important role in the marine ecosystem (Pitcher and Louw, 2021). During the austral autumn/winter periods the upwelling strength within the Benguela weakens due to the South Atlantic Anticyclone moving northward causing winds to experience a shift from southerly to northerly. This leads to the water column becoming increasingly stratified and warmer (Shannon and Nelson, 1996). The shift from upwelling to stratification is associated with microeukaryotic community shift; small diatoms are the first eukaryotes to dominate the upper mixed layer depth during upwelling periods due to their high standing stocks and is succeeded first by larger diatoms such as *Cerataulina spp., Chaetoceros spp., Lauderia spp., Coscinodiscus spp.* and *Thalassionema spp.* and finally by dinoflagellates as the phosphate and silicate become the limiting nutrients in the stratified waters (Margalef 1958; Legendre 1990; Álvarez-Salgado et al. 1996).

This chapter focused on the spatial and temporal distribution of Syndiniales MALV I and II during an austral autumn/winter period. Research have suggested that the parasite abundance and infection rates are mainly driven by the host density, with planktonic blooms/increased carbon biomass resulting in increased infections (Park et al., 2004; Coats et al., 1996). Based on the theory that parasite abundance is driven by their hosts I hypothesized that different frequencies of Syndiniales infections will be present among the two distinctly different microbial communities at the two depths within a stratified water column.

The sampling took place at the Berg River line (Station 6) labelled St Helena Bay Site B in Figure 2 which is located within the large embayment of St Helena Bay about 60km south of Elands Bay. The water hydrography showed a typical profile of a stratified water column with a thermocline forming at 10m separating the upper and bottom mixed layers. This physical separation of water breaks the water into distinct strata with the surface layer usually being well mixed and the deeper layer poorly mixed (Wuest et al., 2000). The nitrate and silicate concentrations were depleted in the surface mixed layer (0.853±0.150 µM and 6.154±0.101mg/L respectively) acting as some of the limiting nutrients for phytoplankton growth, specifically diatoms that incorporate silicate into their cell walls (Sommer, 1994). Nevertheless, according to van Schalkwyk's (2021) findings, the surface layer had the most carbon biomass and was the most variable between days, with the highest carbon biomass recorded on days 1 and 3 at the surface, and the lowest but least variable carbon biomass at 25m.

Due to the lack of upwelling these concentrations at the surface remained low over the course of the 5-day study period (Figure 13). Both the nitrate and silicate concentrations increased significantly with

depth to 27.792±0.333 µM and 34.409±0.380 mg/L respectively at 25m. The average eukaryote cell density however did not reflect increased biomass at these increased concentrations of nutrients (Figure 14). As it was a stratified period with no water mixing, the waters were most likely turbid and the high eukaryotic cell densities at the surface prevented light from penetrating deeper waters. Light is the most important factor for phytoplankton growth (Kirk, 1994) and due to the varying light levels at the various depths, phytoplankton growth rates differ (Mellard et al., 2011), which was observed in this study with higher phytoplankton biomass at the surface compared to deeper layers.

Eukaryotic community composition

The eukaryotic community within the upper mixed layer was largely dominated by dinoflagellates (eg. *Protoperidinium spp*., *Tripos spp.*) with the known Syndiniales hosts *Prorocentrum micans* (Maranda, 2001; Salomonet al., 2009) monopolizing the surface waters (Figure 15). Some ciliates (e.g., *Strobilidium spp*.) and diatoms (*Coscinodiscus spp*.) were also present. The stratified conditions (Margalef et al., 1979) along with the wide-ranging metabolic processes of dinoflagellates (Smayda and Reynolds, 2003; Kremp et al., 2008) are suggested reasons promoting dinoflagellate-dominant communities within these coastal systems during stratification. Dinoflagellates have a diverse habitat specialization but low bloom-species diversity whereas diatoms have a high bloom-species diversity but low habitat diversity (Smayda and Reynolds, 2003). These differences make the bloom behaviours of diatoms more predictable in areas with commonly available species compared to dinoflagellate blooms which relies on specific species in specific habitats (Smayda and Reynolds, 2003). The deeper water layer largely consisted of diatoms such as *Thalassiosira spp., Coscinodiscus sp. and Corethron spp.* along with some flagellates. Diatoms were the dominant phytoplankton at 25m, with species belonging to the genus *Thalassiosira* making up 58.53% of the total carbon biomass (Figure 15), likely due to high silicate levels and processes such as aggregation that led to increased sinking rates after their bloom phase in newly upwelled waters (Alldredge and Gotschalk, 1988). These diatoms therefore contribute to a large portion of the carbon flux (133314011 pg Carbon/ml over the 5-day study period) from the euphotic zone to deeper waters within the mesopelagic zone and are an important factor in the biological carbon pump (Volk and Hoffert, 1985). Other eukaryotes identified via microscopy included *Dinophysis spp*., *Coscinodiscus spp.*, *Strobilidium spp*., *Protoperidinium spp*., *Tripos sp*., and *Pyrophacus spp*.

Over the course of this study no significant changes were seen in the community composition, species diversity and richness, nor carbon biomass, indicating that the system was in a quasi-steady state with primary production and consumption likely occurring at simultaneous rates (Van Schalkwyk 2021).

The total large *P. micans* cell count over the 5-day study period was 318494 cells/ml for the surface and 1591 cells/ml for depth and had an estimated carbon content of 1989 pg C cell^{-1}, whilst the small P. micans count was 2605883 cells/ml for the surface and 6572 cells/ml for depth and had an estimated carbon content of 458 pg C cell^{-1} (Van Schalkwyk, 2021). A study by Mcnair et al., (2021) showed similar carbon content with the average cell carbon content for *P. micans* under high light conditions being 945.45±246.3 pg C cell^{-1} and under low light conditions being 618.35±58.55 pg C cell^{-1}.

Eukaryotic cell (2-100µm) infections by Syndiniales MALV I and II

The high abundance of *P. micans* (large and small), making up about 72.27% of the average daily carbon biomass at the surface (Van Schalkwyk, 2021), likely promoted the proliferation of Syndiniales dinospores, resulting in continued infections over the 5-day study period. As the host of Syndiniales remains photosynthetically active and the carbon fixing capabilities are not impaired by the first stages of infection (Decelle et al., 2022), *P. micans* can incorporate large amounts of carbon which can sink to deeper layers and contribute to carbon export. If all the *P. micans* cells (1826979565 pg C/ml) were to sink they could contribute tremendously to the carbon flux. However, Syndiniales infecting *P. micans* cause remineralization of the host's carbon and reduces the amount of carbon exported to deeper water layers.

The high abundance and carbon biomass of *P. micans* at the surface explains the higher frequency of infections seen at the surface compared to depth. This trend with higher infections seen at the surface was also noted in the study done by Sehein et al. (2022) that showed increased infections as the stratification intensified, and the biomass increased in the upper mixed layer. The diatoms present at 25m depth were extremely thin (1µm) but long (80-150µm chains) and were likely too small for Syndiniales dinospores to infect them.

Syndiniales population dynamics are complex and influenced by physical (temperature, water mixing and depth), chemical (nutrients and metabolites), and biological (host abundance) parameters (Coats et al., 1996; Parks et al., 2004; Anderson and Harvey, 2020; Long et al., 2021). The role of Syndiniales is a crucial variable to include in model development to estimate the total carbon sink versus attenuation, especially with climate change. Previous studies have estimated that the SBUS acts as an annual carbon sink of -2.02 Mt C/year in 2005 (Santana-Casiano et al., 2009; Monteiro, 2010), -1.17 mol C/m^2 per year in 2006, -3.24 mol C/m^2 per year in 2007 (González-Dávila et al., 2009), and -1.4 ± 0.6 mol C/m^2 per year in 2010 (Gregor and Monteiro, 2013). It is also reported that the average CO_2 sinks in summer (-5.8 mmol C/m^2 per day in 2010) were higher than in winter (-3.4 mmol C/m^2 per day in 2010) with autumn acting as a CO_2 source rather than a sink (1.4 mmol C/m^2 per day in 2010,

(Gregor and Monteiro, 2013)). For perspective, the average carbon uptake by the global oceans from 1990 to 2019 was –2.7 ± 0.3 Pg C year^{-1} (Gruber et al., 2023). Syndiniales could possibly be the reason for the CO_2 source during the stratified water column in autumn because it causes lysis of its host which leads to remineralization by other microorganisms such as bacteria and archaea which contributes to CO_2 release back into the water whereupon it can be released into the atmosphere. As the Syndiniales host *P. micans* accounted for 72.27% of the carbon biomass over the study period, large amounts of organic carbon could have been subjected to remineralization (Anderson et al., 2023). Remineralization also has an impact on the other nutrients in the water column. Bacteria can break down the released organic matter into inorganic nutrients such as ammonium and via nitrification, certain bacteria can convert this ammonium into nitrite and nitrate, resupplying phytoplankton with the necessary nutrients for growth (Goebel et al., 2014).

Conclusion

St Helena Bay is the largest embayment of the southwestern coast of Africa and classified as a retention zone, allowing waters to remain within the bay for longer periods of time leading to aged water that support higher primary productivity rates (Graham and Largier, 1997; Cockcroft, 2001; Cockcroft et al., 2008; Hutchings et al., 2012). This study investigated the spatial and temporal distribution of Syndiniales MALV I and II, a ubiquitous parasite (Guillou et al., 2008), within a single embayment during two different seasons which showcase different water systems in St Helena Bay. An active upwelling system followed by a relaxation period was studied from samples collected in November/December 2016 at Elands Bay. This was a classic example of 'pulsed' upwelling frequently seen during austral spring and summer periods within the embayment (Burger et al., 2020). The second system investigated the spatial and temporal distribution of Syndiniales MALV I and II during austral autumn/winter periods within a stratified aged water column from samples collected at the Berg River line Station 6 within St Helena Bay in April 2019 (Van Schalkwyk, 2021).

It was clear from the study that the different seasons supported different microbial communities with diatoms dominating the upper mixed layer post upwelling in the spring/summer seasons that eventually shifted to a dinoflagellate dominant community during stratification in austral autumn/winter, a trend that is well recorded (Álvarez-Salgado et al. 1996; Trigueros and Orive, 2001; Zhou et al., 2017; Spilling et al., 2018). The overall biomass was also much higher in the austral spring/summer period within the embayment (Vand Schalkwyk, 2021), a similar finding made by Andrews and Hutchings (1980) within the Cape Peninsula upwelling region.

The presence of Syndiniales was detected during both these events using FISH, and both chapters indicated that Syndiniales was present and was more abundant at the surface compared to depth. The

key finding of this study was the infections of the diatom *S. costatum* by Syndiniales, which as far as I'm aware is visually shown for the first time. During the shift in water hydrography in 2016 when the system switched from upwelling to resting, a noticeable decrease was seen in Syndiniales presence, contradictory to 2019's samples where the microbial community remained stable, and infections did not plummet throughout the study. This is key as there was a microbial community shift in 2016 transitioning from a diatom dominated phytoplankton community to a diatom-dinoflagellate community, whereas 2019 experienced only dinoflagellate dominance in the surface throughout the study with diatoms dominating at depth due to aggregation and sinking during water stratification.

Studies have shown that the Syndiniales abundance is controlled by their hosts, and this was the case with this study - the host-parasite coculture (*S. costatum - Amoebophrya sp.*) during the upwelling period in 2016 declined over the course of the study, leading to decreased Syndiniales presence as the host abundance decreased, and the host-parasite coculture (*Prorocentrum micans - Amoebophrya sp.*) in the 2019 study remained stable. This is evidence that the Syndiniales abundance follow that of their hosts (Park et al., 2004; Coats et al., 1996). It could also be an indication of Syndiniales host specificity as was studied by Cai et al. (2020) even though Syndiniales are known to have a broad host range.

I also noted that the increase in dinoflagellate such as *Dinophysis spp., Tripos lineatum, Tripos furca, Gyrodinium spp., and Protoperidinium spp*. during the resting phase of 2016 led to a decrease in Syndiniales presence. According to the study done by Long et al (2020), this could be because of excreted APCs from parasite resistant Dinophyceae providing protection of other potential hosts against Syndiniales or compromising the structural integrity of the dinospore membranes. In the future, it could be crucial to study the metabolite products along with DNA and environmental data, factoring in all the physical and chemical parameters and using powerful statistical tools developed for microbial ecology to get a holistic understanding of the infection dynamics of Syndiniales.

A comprehensive understanding of the role of parasites, such as Syndiniales, within the biological carbon pump is key for models predicting atmospheric CO_2 levels, ocean acidification during climate change, and to estimate the total carbon draw down within different seasons with different phytoplankton carbon biomass. Studies have shown that the SBUS is a CO_2 sink (González-Dávila et al., 2009; Santana-Casiano et al., 2009; Monteiro, 2010) with summer months having a larger contribution to the carbon sink compared to winter months (Gregor and Monteiro, 2013).

In conclusion, Syndiniales was present in both the spring/summer and autumn/winter seasons in St Helena Bay and plays a large role in the community composition and carbon fluxes, having different effects in different seasons when different hosts are present. Future studies such as that done by

Anderson et al., (2024) are required to develop a model that can be used to predict Syndiniales presence based on known host presence to possibly use Syndiniales as a putative bioindicator in order to estimate the contribution of Syndiniales to the carbon flux within the biogeochemical cycle.

Acknowledgements

I would like to thank my supervisor Dr Emma Rocke for taking me on this marine microbial journey, and who has taught me so much about marine ecology. I'd like to thank Nicole Dames, Jessica Burger and Francios van Schalkwyk for providing me with the CTD and microbial composition data. I'd also like to thank Yameen Badrodien and Sixolile Mazwane for assistance in the laboratory and R studios. This thesis was funded by the South African National Parks foundation (SANParks).

References

Alldredge, A.L. and Gotschalk, C., 1988. In situ settling behavior of marine snow 1. *Limnology and Oceanography*, *33*(3), pp.339-351.

Álvarez-Salgado, X.A., Rosón, G., Pérez, F.F., Figueiras, F.G. and Pazos, Y., 1996. Nitrogen cycling in an estuarine upwelling system, the Ria de Arousa (NW Spain). I. Short-time-scale patterns of hydrodynamic and biogeochemical circulation. *Marine Ecology Progress Series*, *135*, pp.259-273.

Amann, R.I., Ludwig, W. and Schleifer, K.H., 1995. Phylogenetic identification and in situ detection of individual microbial cells without cultivation. *Microbiological reviews*, 59(1), pp.143-169.

Anderson, D.M, Cembella, A.D., Hallegraeff, G.M. 2012. Progress in understanding harmful algal blooms: paradigm shifts and new technologies for research, monitoring, and management. *Annual Review of Marine Science*. 4: 143-176.

Anderson, D.M. 1997. Turning back the harmful red tide. *Nature*. *388*(6642): 513-514.

Anderson, D.M., 1998. Physiology and bloom dynamics of toxic *Alexandrium* species, with emphasis on life cycle transitions. *Nato Asi Series G Ecological Sciences*, *41*, pp.29-48.

Anderson, D.M., Alpermann, T.J., Cembella, A.D., Collos, Y., Masseret, E., Montresor, M. 2012. The globally distributed genus *Alexandrium*: multifaceted roles in marine ecosystems and impacts on human health. *Harmful Algae*. 14: 10-35.

Anderson, D.M., Fukuyo, Y. and Matsuoka, K., 2003. Cyst methodologies. *Manual on harmful marine microalgae, Monographs on oceanographic methodology*, *11*, pp.165-190.

Anderson, S.R. and Harvey, E.L., 2020. Temporal variability and ecological interactions of parasitic marine Syndiniales in coastal protist communities. *Msphere*, *5*(3), pp.10-1128.

Anderson, S.R., Blanco-Bercial, L., Carlson, C.A. and Harvey, E.L., 2023. Syndiniales parasites drive species networks and are a biomarker for carbon export in the oligotrophic ocean. *bioRxiv*, pp.2023-06.

Anderson, S.R., Blanco-Bercial, L., Carlson, C.A. and Harvey, E.L., 2024. Role of Syndiniales parasites in depth-specific networks and carbon flux in the oligotrophic ocean. *ISME communications*, *4*(1), p.ycae014.

Azam, F., Fenchel, T., Field, J.G., Gray, J.S., Meyer-Reil, L.A. and Thingstad, F.J.M.E.P.S., 1983. The ecological role of water-column microbes in the sea. Marine ecology progress series. Oldendorf, 10(3), pp.257-263.

Bailey, G.W. and Chapman, P., 1991. Short-term variability during an anchor station study in the southern Benguela upwelling system: Chemical and physical oceanography. *Progress in Oceanography*, *28*(1-2), pp.9-37.

Barlow, R., Lamont, T., Mitchell-Innes, B., Lucas, M. and Thomalla, S., 2009. Primary production in the Benguela ecosystem, 1999–2002. *African Journal of Marine Science*, *31*(1), pp.97-101.

Barlow, R.G., Aiken, J., Sessions, H.E., Lavender, S. and Mantel, J., 2001. Phytoplankton pigment, absorption and ocean colour characteristics in the southern Benguela ecosystem: BENEFIT Marine Science. *South African Journal of Science*, *97*(5), pp.230-238.

Belmonte, G. and Rubino, F. 2019. Resting cysts from coastal marine plankton. *Oceanography and Marine Biology*, pp.1-88.

Berdjeb, L., Parada, A., Needham, D.M., Fuhrman, J.A. 2018. Short-term dynamics and interactions of marine protist communities during the spring-summer transition. *ISME J*. 12:1907-1917.

Bjorbækmo, M.F.M., Evenstad, A., Røsæg, L.L., Krabberød, A.K., Logares, R. 2020. The planktonic protist interactome: where do we stand after a century of research? *The ISME Journal*. 14: 544-511.

Blanquart, F., Valero, M., Alves-de-Souza, C., Dia, A., Lepelletier, F., Bigeard, E., Jeanthon, C., Destombe, C. and Guillou, L., 2016. Evidence for parasite-mediated selection during short-lasting toxic algal blooms. *Proceedings of the Royal Society B: Biological Sciences*, *283*(1841), p.20161870.

Bratbak, G. and Thingstad, T.F., 1985. Phytoplankton-bacteria interactions: an apparent paradox? Analysis of a model system with both competition and commensalism. *Marine ecology progress series. Oldendorf*, *25*(1), pp.23-30.

Brown, P.C. and Hutchings, L., 1987. The development and decline of phytoplankton blooms in the southern Benguela upwelling system. 2. Nutrient relationships. *South African Journal of Marine Science*, *5*(1), pp.393-409.

Brown, P.C., 1984. Primary production at two contrasting nearshore sites in the southern Benguela upwelling region, 1977—1979. *South African Journal of Marine Science*, *2*(1), pp.205-215.

Brown, P.C., Painting, S.J. and Cochrane, K.L., 1991. Estimates of phytoplankton and bacterial biomass and production in the northern and southern Benguela ecosystems. *South African Journal of Marine Science*, 11(1), pp.537-564.

Bruland, K.W., Rue, E.L. and Smith, G.J., 2001. Iron and macronutrients in California coastal upwelling regimes: Implications for diatom blooms. *Limnology and Oceanography*, *46*(7), pp.1661-1674.

Burger, J.M., Moloney, C.L., Walker, D.R., Parrott, R.G. and Fawcett, S.E., 2020. Drivers of short-term variability in phytoplankton production in an embayment of the southern Benguela upwelling system. *Journal of Marine Systems*, 208, p.103341.

Cabello, A.M., Cornejo-Castillo, F.M., Raho, N., Blasco, D., Vidal, M., Audic, S., De Vargas, C., Latasa, M., Acinas, S.G. and Massana, R. 2016. Global distribution and vertical patterns of a prymnesiophyte–cyanobacteria obligate symbiosis. *The ISME journal*.10(3): 693-706.

Cachon, J., 1987. Parasitic dinoflagellates. *The biology of dinoflagellates*. Oxford: 571–610

Cai, R., Kayal, E., Alves-De-Souza, C., Bigeard, E., Corre, E., Jeanthon, C., Marie, D., Porcel, B.M., Siano, R., Szymczak, J. and Wolf, M., 2020. Cryptic species in the parasitic *Amoebophrya* species complex revealed by a polyphasic approach. *Scientific Reports*, *10*(1), p.2531.

Callahan, B.J., McMurdie, P.J., Rosen, M.J., Han, A.W., Johnson, A.J.A. and Holmes, S.P., 2016. DADA2: High-resolution sample inference from Illumina amplicon data. *Nature methods*, *13*(7), pp.581-583.

Caporaso, J. G., Lauber, C. L., Walters, W. A., Berg-Lyons, D., Lozupone, C. A., Turnbaugh, P. J., et al. (2011). Global patterns of 16S rRNA diversity at a depth of millions of sequences per sample. *Proceedings of the National Academy of Sciences of the United States of America 108,* 4516–4522.

Caron, D.A., Countway, P.D., Jones, A.C., Kim, D.Y., Schnetzer, A. 2012. Marine protistan diversity. *Annual Review of Marine Science.* 4: 463-493.

Caron, D.A., Goldman, J.C., Andersen, O.K. and Dennett, M.R., 1985. Nutrient cycling in a microflagellate food chain: II. Population dynamics and carbon cycling. Marine Ecology Progress Series, pp.243-254.

Carr, M.E. and Kearns, E.J., 2003. Production regimes in four Eastern Boundary Current systems. *Deep Sea Research Part II: Topical Studies in Oceanography, 50*(22-26), pp.3199-3221.

Castro, P. and Huber, M.E., 2010. *Marine biology*. McGraw-Hill.

Chambouvet, A., Alves-de-Souza, C., Cueff, V., Marie, D., Karpov, S., Guillou, L., 2011. Interplay between the parasite *Amoebophrya* sp.(Alveolata) and the cyst formation of the red tide dinoflagellate *Scrippsiella trochoidea*. *Protist*. *162*(4): 637-649.

Chambouvet, A., Laabir, M., Sengco, M., Vaquer, A. and Guillou, L., 2011. Genetic diversity of Amoebophryidae (Syndiniales) during *Alexandrium catenella/tamarense* (Dinophyceae) blooms in the Thau lagoon (Mediterranean Sea, France). *Research in microbiology*, *162*(9), pp.959-968.

Chambouvet, A., Morin, P., Marie, D., Guillou, L. 2008. Control of toxic marine dinoflagellate blooms by serial parasitic killers. *Science*. 322: 1254-1257.

Choi, C.J., Brosnahan, M.L., Sehein, T.R., Anderson, D.M., Erdner, D.L. 2017. Insights into the loss factors of phytoplankton blooms: the role of cell mortality in the decline of two inshore *Alexandrium* blooms. *Limnol Oceanogr*. 62: 1742-53.

Cleary, A.C. and Durbin, E.G., 2016. Unexpected prevalence of parasite 18S rDNA sequences in winter among Antarctic marine protists. *Journal of Plankton Research*, *38*(3), pp.401-417.

Coats, D.W. and Bockstahler, K.R., 1994. Occurrence of the parasitic dinoflagellate *Amoebophrya ceratii* in Chesapeake Bay populations of *Gymnodinium sanguineum*. *Journal of Eukaryotic Microbiology*, *41*(6), pp.586-593.

Coats, D.W., Adam, E.J., Gallegos, C.L. and Hedrick, S., 1996. Parasitism of photosynthetic dinoflagellates in a shallow subestuary of Chesapeake Bay, USA. *Aquatic Microbial Ecology*, *11*(1), pp.1-9.

Coats, D.W., Park, M.G. 2002. Parasitism of photosynthetic dinoflagellates by three strains of *Amoebophrya* (Dinophyta): Parasite survival, infectivity, generation time, and host specificity. *J Phycol*. 38: 520-528.

Cockcroft, A.C., 2001. Jasus lalandii'walkouts' or mass strandings in South Africa during the 1990s: an overview. *Marine and Freshwater Research*, *52*(8), pp.1085-1093.

Cockcroft, A.C., Van Zyl, D. and Hutchings, L., 2008. Large-scale changes in the spatial distribution of South African West Coast rock lobsters: an overview. *African Journal of Marine Science*, *30*(1), pp.149-159.

Cory, R.M., Harrold, K.H., Neilson, B.T. and Kling, G.W., 2015. Controls on dissolved organic matter (DOM) degradation in a headwater stream: the influence of photochemical and hydrological conditions in determining light-limitation or substrate-limitation of photo-degradation. *Biogeosciences*, *12*(22), pp.6669-6685.

Crichton, M., Hutchings, L., Lamont, T. and Jarre, A., 2013. From physics to phytoplankton: prediction of dominant cell size in St Helena Bay in the Southern Benguela. *Journal of plankton research*, 35(3), pp.526-541.

Cullen, J.J. and MacIntyre, J.G., 1998. Behavior, physiology and the niche of depth-regulating phytoplankton. *Nato Asi Series G Ecological Sciences*, *41*, pp.559-580.

Cushing, D.H., 1989. A difference in structure between ecosystems in strongly stratified waters and in those that are only weakly stratified. *Journal of plankton research*, *11*(1), pp.1-13.

Dai, X.F., Lu, D.D., Xia, P., Wang, H.X., He, P.X. 2012. A 50-year temporal record of dinoflagellate cysts in sediments from the Changjiang estuary, East China Sea, in relation to climate and catchment changes. Estuar. *Coast Shelf Sci*. 112: 192-197.

Dames, N.R., 2022. Short-term dynamics of nano-and picoplankton in the southern Benguela upwelling system.

De Vargas, C., Audic, S., Henry, N., Decelle, J., Mahé, F., Logares, R., Lara, E., Berney, C., Le Bescot, N., Probert, I. and Carmichael, M., 2015. Eukaryotic plankton diversity in the sunlit ocean. *Science*, *348*(6237), p.1261605.

Decelle, J., Colin, S. and Foster, R.A., 2015. Photosymbiosis in marine planktonic protists. *Marine protists: diversity and dynamics*. 465-500.

Decelle, J., Kayal, E., Bigeard, E., Gallet, B., Bougoure, J., Clode, P., Schieber, N., Templin, R., Hehenberger, E., Prensier, G. and Chevalier, F., 2022. Intracellular development and impact of a marine eukaryotic parasite on its zombified microalgal host. *The ISME Journal*, *16*(10), pp.2348-2359.

Decelle, J., Veronesi, G., LeKieffre, C., Gallet, B., Chevalier, F., Stryhanyuk, H., Marro, S., Ravanel, S., et al., 2021. Subcellular architecture and metabolic connection in the planktonic photosymbiosis between Collodaria (radiolarians) and their microalgae. *Environmental Microbiology*. 23(11): 6569-6586.

Dittmar, T. and Stubbins, A., 2014. 12.6-Dissolved organic matter in aquatic systems. Treatise on geochemistry, 2, pp.125-156.

Dougherty, E.R., Carlson, C.J., Bueno, V.M., Burgio, K.R., Cizauskas, C.A., Clements, C.F., et al. 2016. Paradigms for parasite conservation: parasite conservation. *Conserv Biol*. 30: 724-733.

Duan, P., Wei, M., Yao, L. and Li, M., 2022. Relationship between non-point source pollution and fluorescence fingerprint of riverine dissolved organic matter is season dependent. *Science of the Total Environment*, *823*, p.153617.

Dutta, P.S., Kooi, B.W. and Feudel, U., 2014. Multiple resource limitation: nonequilibrium coexistence of species in a competition model using a synthesizing unit. Theoretical ecology, 7, pp.407-421.

Elbrächter, M. and Schnepf, E., 1998. Parasites of harmful algae. In Physiological ecology of harmful algal blooms (DM Anderson, AD Cembella, GM Hallegraeff, eds) Springer, Berlin, Heidelberg (pp. 351-369).

Estrada, M. and Blasco, D., 1985. Phytoplankton assemblages in coastal upwelling areas.

Falkowski, P.G., Barber, R.T. and Smetacek, V., 1998. Biogeochemical controls and feedbacks on ocean primary production. *science*, 281(5374), pp.200-206.

Fan, L., Liu, M., Simister, R., Webster, N.S. and Thomas, T., 2013. Marine microbial symbiosis heats up: the phylogenetic and functional response of a sponge holobiont to thermal stress. *The ISME journal*, *7*(5), pp.991-1002.

Fenchel, T., 1982. Ecology of heterotrophic microflagellates. IV. Quantitative occurrence and importance as bacterial consumers. *Marine ecology progress series*, pp.35-42.

Fenchel, T., 1984. Suspended marine bacteria as a food source. *In Flows of energy and materials in marine ecosystems: Theory and practice* (pp. 301-315). Boston, MA: Springer US.

Fenchel, T., 1988. Marine plankton food chains. Annual Review of Ecology and Systematics, 19(1), pp.19-38.

Flynn, R.F., Burger, J.M., Pillay, K. and Fawcett, S.E., 2018. Wintertime rates of net primary production and nitrate and ammonium uptake in the southern Benguela upwelling system. *African Journal of Marine Science*, *40*(3), pp.253-266.

Fritz, L., Nass, M. 1992. Developemnt of the endoparasitic dinoflagellate *Amoebophrya ceratii* within host dinoflagellate species. *J Phycol*. 28: 312–320.

Fuhrma, J.A. and Suttle, C.A., 1993. Viruses in marine planktonic systems. Oceanography, 6(2), pp.51-63.

Fuhrman, J.A., Cram, J.A., Needham, D.M. 2015. Marine microbial community dynamics and their ecological interpretation. *Nat Rev Microbiol* 13: 133–146.

Gallegos, C.L., 1992. Phytoplankton photosynthesis, productivity, and species composition in a eutrophic estuary: Comparison of bloom and non-bloom assemblages. *Marine ecology progress series. Oldendorf*, *81*(3), pp.257-267.

Garcés, E., Bravo, I., Vila, M., Figueroa, R.I., Masó, M. and Sampedro, N., 2004. Relationship between vegetative cells and cyst production during *Alexandrium minutum* bloom in Arenys de Mar harbour (NW Mediterranean). *Journal of Plankton Research*, *26*(6), pp.637-645.

Goebel, N.L., Edwards, C.A., Follows, M.J. and Zehr, J.P., 2014. Modeled diversity effects on microbial ecosystem functions of primary production, nutrient uptake, and remineralization. *Ecology*, *95*(1), pp.153-163.

González-Dávila, M., Santana-Casiano, J.M. and Ucha, I.R., 2009. Seasonal variability of fCO2 in the Angola-Benguela region. *Progress in Oceanography*, *83*(1-4), pp.124-133.

Gottschling, M., Soehner, S., Zinssmeister, C., John, U., Pl¨otner, J., Schweikert, M., Aligizaki, K., Elbr¨achter, M., 2012. Delimitation of the Thoracosphaeraceae (Dinophyceae), including the calcareous dinoflagellates, based on large amounts of ribosomal RNA sequence data. *Protist* 163 (1): 15-24.

Graham, W.M. and Largier, J.L., 1997. Upwelling shadows as nearshore retention sites: the example of northern Monterey Bay. *Continental Shelf Research*, *17*(5), pp.509-532.

Gregor, L. and Monteiro, P.M., 2013. Is the southern Benguela a significant regional sink of CO2?. *South African Journal of Science*, *109*(5), pp.1-5.

Gruber, N., Bakker, D.C., DeVries, T., Gregor, L., Hauck, J., Landschützer, P., McKinley, G.A. and Müller, J.D., 2023. Trends and variability in the ocean carbon sink. *Nature Reviews Earth & Environment*, *4*(2), pp.119-134.

Guillou, L., Viprey, M., Chambouvet, A., Welsh, R.M., Kirkham, A.R., Massana, R., Scanlan, D.J. and Worden, A.Z., 2008. Widespread occurrence and genetic diversity of marine parasitoids belonging to Syndiniales (Alveolata). *Environmental microbiology*, *10*(12), pp.3349-3365.

Hahn, M.W. and Höfle, M.G., 2001. Grazing of protozoa and its effect on populations of aquatic bacteria. *FEMS microbiology ecology*, 35(2), pp.113-121.

Harris, T.F.W., and Shannon, L.V., 1979. Satellite-tracked drifter in the Benguela Current system. *South African Journal of Science*, 75(7), pp.316-317.

Hart, T.J. and Currie, R.T., 1960. The Benguela Current: Discovery Reports, v. 31.

Holden, C.J., 1985. Currents in St Helena Bay inferred from radio-tracked drifters. *South African ocean colour and upwelling experiment*.

Horstman, D.A., 1981. Reported red-water outbreaks and their effects on fauna of the west and south coasts of South Africa, 1959-1980. Fisheries bulletin; contributions to oceanography and fisheries biology-South Africa, Dept. of Agriculture and Fisheries, Sea Fisheries Institute.

Hutchings, L., Jarre, A., Lamont, T., Van den Berg, M. and Kirkman, S.P., 2012. St Helena Bay (southern Benguela) then and now: muted climate signals, large human impact. *African Journal of Marine Science*, *34*(4), pp.559-583.

Hutchings, L., Van der Lingen, C.D., Shannon, L.J., Crawford, R.J.M., Verheye, H.M.S., Bartholomae, C.H., Van der Plas, A.K., Louw, D., Kreiner, A., Ostrowski, M. and Fidel, Q., 2009. The Benguela Current: An ecosystem of four components. *Progress in Oceanography*, *83*(1-4), pp.15-32.

Iturriaga, R. and Mitchell, B.G., 1986. Chroococcoid cyanobacteria: a significant component in the food web dynamics of the open ocean. Mar. Ecol. Prog. Ser, 28(3), pp.291-297.

Jacobson, D.M., 1987. *The ecology and feeding biology of thecate heterotrophic dinoflagellates* (Doctoral dissertation, Woods Hole Oceanographic Institution).

Jamshidi, S. and Yousefi, M., 2021. Experimental evaluation of the influence of the Seawater characteristics on spatial and temporal variations of the sound speed in the southern abyssal, intermediate and shelf zones of the Caspian Sea. *Acoustical Physics*, *67*, pp.134-146.

Jardillier, L., Zubkov, M.V., Pearman, J. and Scanlan, D.J., 2010. Significant CO_2 fixation by small prymnesiophytes in the subtropical and tropical northeast Atlantic Ocean. *The ISME journal*, 4(9), pp.1180-1192.

Jephcott, T.G., Alves-de-Souza, C., Gleason, F.H., van Ogtrop, F.F., SimeNgando, T., Karpov, S.A., Guillou, L. 2016. Ecological impacts of parasitic chytrids, syndiniales and perkinsids on populations of marine photosynthetic dinoflagellates. *Fungal Ecol* 19:47–58.

Johnson, P.T.J., Preston, D.L., Hoverman, J.T., LaFonte, B.E. 2013. Host and parasite diversity jointly control disease risk in complex communities. *Proc Natl Acad Sci USA*. 110(42):16916 16921.

Johnson, P.W. and Sieburth, J.M., 1979. Chroococcoid cyanobacteria in the sea: a ubiquitous and diverse phototrophic biomass 1. Limnology and oceanography, 24(5), pp.928-935.

Kaiser, M.J., 2011. Marine ecology: processes, systems, and impacts. Oxford University Press, USA.

Karl, D.M., Church, M.J., Dore, J.E., Letelier, R.M. and Mahaffey, C., 2012. Predictable and efficient carbon sequestration in the North Pacific Ocean supported by symbiotic nitrogen fixation. *Proceedings of the National Academy of Sciences*, *109*(6), pp.1842-1849.

Kim, S., Park, M.G., KIM, K.Y., KIM, C.H., Yih, W., Park, J.S. and Coats, D.W., 2008. Genetic diversity of parasitic dinoflagellates in the genus *Amoebophrya* and its relationship to parasite biology and biogeography. *Journal of eukaryotic microbiology*, *55*(1), pp.1-8.

Kim, S., Park, M.G., Yih, W., Coats, D.W. 2004. Infection of the bloom-forming thecate dinoflagellates *Alexandrium affine* and *Gonyaulax spinifera* by two strains of *Amoebophrya* (Dinophyta). *J Phycol*. 40: 815-822.

Kiørboe, T., 1993. Turbulence, phytoplankton cell size, and the structure of pelagic food webs. *In Advances in marine biology* (Vol. 29, pp. 1-72). Academic Press.

Kirk, J.T., 1994. Light and photosynthesis in aquatic ecosystems. Cambridge university press.

Kremp, A., Tamminen, T. and Spilling, K., 2008. Dinoflagellate bloom formation in natural assemblages with diatoms: nutrient competition and growth strategies in Baltic spring phytoplankton. *Aquatic Microbial Ecology*, *50*(2), pp.181-196.

Kretschmann, J., Elbr¨achter, M., Zinssmeister, C., Soehner, S., Kirsch, M., Kusber, W.H., Gottschling, M., 2015. Taxonomic clarification of the dinophyte *Peridinium acuminatum* Ehrenb, *Scrippsiella acuminata*, comb. nov.(Thoracosphaeraceae, Peridiniales). *Phytotaxa*. 220 (3): 239–256.

Kubota, K., 2013. CARD-FISH for environmental microorganisms: technical advancement and future applications. Microbes and environments, 28(1), pp.3-12.

Lamont, T., Barlow, R.G. and Kyewalyanga, M.S., 2014. Physical drivers of phytoplankton production in the southern Benguela upwelling system. *Deep Sea Research Part I: Oceanographic Research Papers.* 90: 1-16.

Lamont, T., Hutchings, L., Van Den Berg, M.A., Goschen, W.S. and Barlow, R.G., 2015. Hydrographic variability in the St. Helena Bay region of the southern Benguela ecosystem. *Journal of Geophysical Research: Oceans*, *120*(4), pp.2920-2944.

Legendre, L., 1990. The significance of microalgal blooms for fisheries and for the export of particulate organic carbon in oceans. *Journal of Plankton Research*, *12*(4), pp.681-699.

Legendre, L., Rivkin, R.B., Weinbauer, M.G., Guidi, L. and Uitz, J., 2015. The microbial carbon pump concept: Potential biogeochemical significance in the globally changing ocean. *Progress in Oceanography*, *134*, pp.432-450.

Lévêque, C., 2001. Lake and pond ecosystems. *Encyclopedia of biodiversity*, 3, pp.633-644.

Li, C., Song, S., Liu, Y., Chen, T.2014. Occurrence of *Amoebophrya* spp. infection in planktonic dinoflagellates in Changjiang (Yangtze River) Estuary, China. *Harmful Algae*. 37: 117-24.

Li, W.K. and Platt, T., 1987. Photosynthetic picoplankton in the ocean. Science Progress (1933-), pp.117-132.

Liu, C., Cui, Y., Li, X. and Yao, M., 2021. microeco: an R package for data mining in microbial community ecology. *FEMS microbiology ecology*, *97*(2), p.fiaa255.

Liu, Y., Song, S., Chen, T. and Li, C., 2017. The diversity and structure of marine protists in the coastal waters of China revealed by morphological observation and 454 pyrosequencing. *Estuarine, Coastal and Shelf Science*, *189*, pp.143-155.

Lively, C.M., 1996. Host-parasite coevolution and sex. *Bioscience*, *46*(2), pp.107-114.

Lohrenz, S.E., Fahnenstiel, G.L. and Redalje, D.G., 1994. Spatial and temporal variations of photosynthetic parameters in relation to environmental conditions in coastal waters of the northern Gulf of Mexico. *Estuaries*, *17*, pp.779-795.

Long, M., Marie, D., Szymczak, J., Toullec, J., Bigeard, E., Sourisseau, M., Le Gac, M., Guillou, L. and Jauzein, C. 2021. Dinophyceae can use exudates as weapons against the parasite *Amoebophrya* sp.(Syndiniales). *ISME Communications*. 1(1): 34.

Lutjeharms, J.R.E. and Valentine, H.R., 1987. Water types and volumetric considerations of the South-East Atlantic upwelling regime. *South African Journal of Marine Science*, *5*(1), pp.63-71.

Ma, Y., Mao, R. and Li, S., 2021. Hydrological seasonality largely contributes to riverine dissolved organic matter chemical composition: Insights from EEM-PARAFAC and optical indicators. *Journal of Hydrology*, *595*, p.125993.

Majaneva, M., Rintala, J.M., Piisilä, M., Fewer, D.P. and Blomster, J., 2012. Comparison of wintertime eukaryotic community from sea ice and open water in the Baltic Sea, based on sequencing of the 18S rRNA gene. *Polar Biology*, *35*, pp.875-889.

Maranda, L., 2001. Infection of *Prorocentrum minimum* (Dinophyceae) by the parasite *Amoebophrya* sp.(Dinoflagellea). *Journal of Phycology*, *37*(2), pp.245-248.

Marañón, E., Steele, J., Thorpe, A. and Turekian, K., 2009. Phytoplankton size structure. *Elements of physical oceanography: A derivative of the encyclopedia of ocean sciences*, *85*.

Margalef, R., 1958. Temporal succession and spatial heterogeneity in phytoplankton. *Perspectives in Marine biology/University of California Press*.

Margalef, R., 1978. Life-forms of phytoplankton as survival alternatives in an unstable environment. *Oceanologica acta*, 1(4), pp.493-509.

María Trigueros, J. and Orive, E., 2001. Seasonal variations of diatoms and dinoflagellates in a shallow, temperate estuary, with emphasis on neritic assemblages. *Hydrobiologia*, 444, pp.119-133.

Massana, R., 2011. Eukaryotic picoplankton in surface oceans. *Annual review of microbiology*, 65, pp.91-110.

Mcnair, H., Hammond, C.N. and Menden-Deuer, S., 2021. Phytoplankton carbon and nitrogen biomass estimates are robust to volume measurement method and growth environment. *Journal of Plankton Research*, *43*(2), pp.103-112.

Mellard, J.P., Yoshiyama, K., Litchman, E. and Klausmeier, C.A., 2011. The vertical distribution of phytoplankton in stratified water columns. *Journal of theoretical biology*, *269*(1), pp.16-30.

Minor, E.C. and Oyler, A.R., 2023. Dissolved organic matter in large lakes: a key but understudied component of the carbon cycle. *Biogeochemistry*, *164*(1), pp.295-318.

Mitchell-Innes, B.A. and Walker, D.R., 1991. Short-term variability during an anchor station study in the southern Benguela upwelling system: Phytoplankton production and biomass in relation to specie changes. *Progress in Oceanography*, 28(1-2), pp.65-89.

Mitra, A., Flynn, K.J., Burkholder, J.M., Berge, T., Calbet, A., Raven, J.A., Granéli, E., Glibert, P.M., Hansen, P.J., Stoecker, D.K. and Thingstad, F., 2014. The role of mixotrophic protists in the biological carbon pump. *Biogeosciences*, 11(4), pp.995-1005.

Montagnes, D.J., Chambouvet, A., Guillou, L. and Fenton, A., 2008. Responsibility of microzooplankton and parasite pressure for the demise of toxic dinoflagellate blooms. *Aquatic Microbial Ecology*, *53*(2), pp.211-225.

Monteiro, P., 2010. Eastern boundary currents: The Benguela Current System. *Carbon and nutrient fluxes in continental margins: A global synthesis. New York: Springer*, pp.64-77.

Morran, L.T., Schmidt, O.G., Gelarden, I.A., Parrish, R.C. and Lively, C.M., 2011. Running with the Red Queen: host-parasite coevolution selects for biparental sex. *Science*, *333*(6039), pp.216-218.

Muyzer, G., de Waal, E. C., and Uitterlinden, A. G. (1993). Profiling of complex microbial populations by denaturing gradient gel electrophoresis analysis of polymerase chain reaction-amplified genes coding for 16S rRNA. *Applied and Environmental Microbiology* 59, 695–700.

Nelson, G. and Hutchings, L., 1983. The Benguela upwelling area. Progress in Oceanography, 12(3), pp.333-356.

Newell, G.E. and Newell, R.C., 1970. Marine plankton: a practical guide.

Painting, S.J., Lucas, M.I., Peterson, W.T., Brown, P.C., Hutchings, L. and Mitchell-Innes, B.A., 1993. Dynamics of bacterioplankton, phytoplankton and mesozooplankton communities during the development of an upwelling plume in the southern Benguela. *Marine Ecology Progress Series*, pp.35-53.

Park, M.G., Cooney, S., Yih, W., Coats, D. 2002. Effects of two strains of the parasitic dinoflagellate *Amoebophrya* on growth, photosynthesis, light absorption, and quantum yield of bloom-forming dinoflagellates. *Mar Ecol Prog Ser*. 227: 281-292.

Park, M.G., Yih, W. and Coats, D.W., 2004. Parasites and phytoplankton, with special emphasis on dinoflagellate infections 1. *Journal of Eukaryotic Microbiology*, *51*(2), pp.145-155.

Paseka, R.E., White, L.A., Van de Waal, D.B., Strauss, A.T., González, A.L., Everett, R.A., et al. 2020. Disease-mediated ecosystem services: pathogens, plants, and people. *Trends Ecol Evolut*. 35: 731-743.

Pitcher, G.C. and Louw, D.C. 2021. Harmful algal blooms of the Benguela eastern boundary upwelling system. *Harmful Algae*. 102: 101898.

Pitcher, G.C. and Probyn, T.A., 2017. Seasonal and sub-seasonal oxygen and nutrient fluctuations in an embayment of an eastern boundary upwelling system: St Helena Bay. *African Journal of Marine Science*, *39*(1), pp.95-110.

Pitcher, G.C. and Weeks, S.J., 2006. 7 The variability and potential for prediction of harmful algal blooms in the southern Benguela ecosystem. In *Large marine ecosystems* (Vol. 14, pp. 125-146). Elsevier.

Pitcher, G.C., du Randt, A., Seanego, K.G. and Tsanwani, M., 2023. Variability and controls of the ocean acidification metrics pH and pCO2 in a large embayment of an Eastern Boundary Upwelling System (EBUS). *Estuarine, Coastal and Shelf Science*, *292*, p.108473.

Pitcher, G.C., Figueiras, F.G., Hickey, B.M. and Moita, M.T., 2010. The physical oceanography of upwelling systems and the development of harmful algal blooms. *Progress in oceanography*, *85*(1-2), pp.5-32.

Pitcher, G.C., Walker, D.R., Mitchell-Innes, B.A. and Moloney, C.L., 1991. Short-term variability during an anchor station study in the southern Benguela upwelling system: phytoplankton dynamics. *Progress in Oceanography*, *28*(1-2), pp.39-64.

Pitcher, G.C., Richardson, A.J. and Korrubel, J.L., 1996. The use of sea temperature in characterizing the mesoscale heterogeneity of phytoplankton in an embayment of the southern Benguela upwelling system. *Journal of Plankton Research*, *18*(5), pp.643-657.

Probyn, T.A., Pitcher, G.C., Monteiro, P.M.S., Boyd, A.J. and Nelson, G., 2000. Physical processes contributing to harmful algal blooms in Saldanha Bay, South Africa. South African Journal of Marine Science, 22(1), pp.285-297.

Rohde, K., 1984. Zoogeography of marine parasites. *Helgoländer Meeresuntersuchungen*, *37*, pp.35-52.

Rose, J.M., Caron, D.A. 2007. Does low temperature constrain the growth rates of heterotrophic protists? Evidence and implications for algal blooms in cold waters. *Limnol Oceanogr.* 52: 886-895.

Ryabov, A.B. and Blasius, B., 2011. A graphical theory of competition on spatial resource gradients. *Ecology Letters*, 14(3), pp.220-228.

Salomon, P.S., Granéli, E., Neves, M.H. and Rodriguez, E.G., 2009. Infection by *Amoebophrya* spp. parasitoids of dinoflagellates in a tropical marine coastal area. *Aquatic Microbial Ecology*, *55*(2), pp.143-153.

Salomon, P.S., Stolte, W. 2010. Predicting the population dynamics in *Amoebophrya* parasitoids and their dinoflagellate hosts using a mathematical model. *Mar Ecol Prog Ser*. 419: 1-10.

Santana-Casiano, J.M., González-Dávila, M. and Ucha, I.R., 2009. Carbon dioxide fluxes in the Benguela upwelling system during winter and spring: A comparison between 2005 and 2006. *Deep Sea Research Part II: Topical Studies in Oceanography*, *56*(8-10), pp.533-541.

Sassenhagen, I., Irion, S., Jardillier, L., Moreira, D. and Christaki, U., 2020. Protist interactions and community structure during early autumn in the Kerguelen region (Southern Ocean). Protist, 171(1), p.125709.

Sehein, T.R., Gast, R.J., Pachiadaki, M., Guillou, L. and Edgcomb, V.P., 2022. Parasitic infections by Group II Syndiniales target selected dinoflagellate host populations within diverse protist assemblages in a model coastal pond. *Environmental Microbiology*, 24(4), pp.1818-1834.

Shilo, M. 1967. Formation and mode of action of algal toxins. *Bacteriol. Rev*. 31:180.

Siano, R., Alves-de-Souza, C., Foulon, E., Bendif, E.M., Simon, N., Guillou, L. and Not, F., 2011. Distribution and host diversity of Amoebophryidae parasites across oligotrophic waters of the Mediterranean Sea. Biogeosciences, 8(2), pp.267-278.

Sieburth, J., 1979. McN.: Sea microbes, 491 pp.

Smayda, T.J. 1997. Harmful algal blooms: their ecophysiology and general relevance to phytoplankton blooms in the sea. *Limnol. Oceanogr*. 42: 1137–1153.

Smayda, T.J. 2002. Turbulence, watermass stratification and harmful algal blooms: an alternative view and frontal zones as "pelagic seed banks". *Harmful Algae*. 1:95–112.

Smayda, T.J. and Reynolds, C.S., 2003. Strategies of marine dinoflagellate survival and some rules of assembly. *Journal of Sea Research*, *49*(2), pp.95-106.

Smayda, T.J. and Trainer, V.L., 2010. Dinoflagellate blooms in upwelling systems: Seeding, variability, and contrasts with diatom bloom behaviour. *Progress in Oceanography*, *85*(1-2), pp.92-107.

Smetacek, V., 1998. Diatoms and the silicate factor. *Nature*, *391*(6664), pp.224-225.

Sommer, U., 1994. The impact of light intensity and daylength on silicate and nitrate competition among marine phytoplankton. *Limnology and Oceanography*, *39*(7), pp.1680-1688.

Spilling, K., Olli, K., Lehtoranta, J., Kremp, A., Tedesco, L., Tamelander, T., Klais, R., Peltonen, H. and Tamminen, T., 2018. Shifting diatom—dinoflagellate dominance during spring bloom in the Baltic Sea and its potential effects on biogeochemical cycling. *Frontiers in Marine Science*, 5, p.327.

Stockner, J.G. and Antia, N.J., 1986. Algal picoplankton from marine and freshwater ecosystems: a multidisciplinary perspective. *Canadian journal of fisheries and aquatic sciences*, 43(12), pp.2472-2503.

Stoeck, T., Bass, D., Nebel, M., Christen, R., Jones, M. D. M., Breiner, H. W., et al. (2010). Multiple marker parallel tag environmental DNA sequencing reveals a highly complex eukaryotic community in marine anoxic water. *Molecular Ecology* 19, 21–31.

Stukel, M.R. and Ducklow, H.W., 2017. Stirring up the biological pump: Vertical mixing and carbon export in the Southern Ocean. *Global Biogeochemical Cycles*, *31*(9), pp.1420-1434.

Sundquist, E.T., and Visser Ackerman, K., 2013. The geologic history of the carbon cycle. In K. Turekian and H. Holland (eds.), Treatise on Geochemistry, 2nd ed., pp. 361-398, New York: Elsevier.

Suttle, C.A., 1994. The significance of viruses to mortality in aquatic microbial communities. *Microbial ecology*, 28, pp.237-243.

Suttle, C.A., 2007. Marine viruses—major players in the global ecosystem. *Nature reviews microbiology*, 5(10), pp.801-812.

Thompson, A.W., Foster, R.A., Krupke, A., Carter, B.J., Musat, N., Vaulot, D., et al. 2012. Unicellular cyanobacterium symbiotic with a single-celled eukaryotic alga. *Science*. 337: 1546–1550.

Thornton, D.C., 2014. Dissolved organic matter (DOM) release by phytoplankton in the contemporary and future ocean. *European Journal of Phycology*, *49*(1), pp.20-46.

Tilman, D., 1982. Resource competition and community structure. Princeton university press.

Tilstone, G.H., Miguez, B.M., Figueiras, F.G. and Fermín, E.G., 2000. Diatom dynamics in a coastal ecosystem affected by upwelling: coupling between species succession, circulation and biogeochemical processes. *Marine Ecology Progress Series*, *205*, pp.23-41.

Toft, C.A. and Karter, A.J., 1990. Parasite-host coevolution. *Trends in Ecology & Evolution*, *5*(10), pp.326-329.

Van Schalkwyk, F., 2021. Phytoplankton community dynamics during autumn in St Helena Bay.

Vaulot, D., Eikrem, W., Viprey, M. and Moreau, H., 2008. The diversity of eukaryotic marine picophytoplankton. FEMS Microbiol. Rev, 32, pp.795-820.

Velo-Suárez, L., Brosnahan, M.L., Anderson, D.M., McGillicuddy, D.J. 2013. A Quantitative assessment of the role of the parasite *Amoebophrya* in the termination of *Alexandrium fundyense* blooms within a small coastal embayment. *PLoS ONE*. 8(12): 81150.

Vincent, F. and Bowler, C., 2022. An integrated view of diatom interactions. *The Molecular Life of Diatoms*, pp.59-86.

Vincent, F. and Vardi, A., 2023. Viral infection in the ocean—A journey across scales. PLoS biology, 21(1), p.e3001966.

Volk, T. and Hoffert, M.I., 1985. The Carbon Cycle and Atmospheric CO2: Natural Variations Archean to Present, chap. Ocean carbon pumps: Analysis of relative strengths and efficiencies in oceandriven atmospheric CO2 changes., 99–110. *Geophys. Monogr. Ser*, *32*.

Waldron, H.N., 1985. Influences on the hydrology of the Cape Columbine/St. Helena region.

Walker, D.R. and Peterson, W.T., 1991. Relationships between hydrography, phytoplankton production, biomass, cell size and species composition, and copepod production in the southern Benguela upwelling system in April 1988. *South African Journal of Marine Science*, *11*(1), pp.289-305.

Walker, D.R. and Pitcher, G.C., 1991. The dynamics of phytoplankton populations, including a red-tide bloom, during a quiescent period in St Helena Bay, South Africa. *South African Journal of Marine Science*, 10(1), pp.61-70.

Wang, Z., Tsementzi, D., Williams, T.C., Juarez, D.L., Blinebry, S.K., Garcia, N.S., Sienkiewicz, B.K., Konstantinidis, K.T., Johnson, Z.I. and Hunt, D.E., 2021. Environmental stability impacts the differential sensitivity of marine microbiomes to increases in temperature and acidity. *The ISME Journal*, *15*(1), pp.19-28.

Weeks, S.J., Barlow, R., Roy, C. and Shillington, F.A., 2006. Remotely sensed variability of temperature and chlorophyll in the southern Benguela: upwelling frequency and phytoplankton response. African Journal of Marine Science, 28(3-4), pp.493-509.

Willey, J.M., Sherwood, L.M. and Woolverton, C.J., 2011. Epidemiology and public health microbiology: Nosocomial infections. Willey JM, Sherwood LM and Woolverton CJ. edited Prescott's Microbiology. 8th Edition, New York. The McGraw Hill Companies. International Edition. pp, pp.873-884.

Williams, P.M. and Druffel, E.R., 1987. Radiocarbon in dissolved organic matter in the central North Pacific Ocean. *Nature*, 330(6145), pp.246-248.

Worden, A.Z. and Not, F., 2008. Ecology and diversity of picoeukaryotes. *Microbial ecology of the Oceans*, 2, pp.159-205.

Worden, A.Z., Follows, M.J., Giovannoni, S.J., Wilken, S., Zimmerman, A.E., Keeling, P.J. 2015. Rethinking the marine carbon cycle: factoring in the multifarious lifestyles of microbes. *Science*. 347: 1257594.

Wu, X., Li, L., Lin, S., 2022. Energy metabolism and genetic information processing mark major transitions in the life history of *Scrippsiella acuminata* (Dinophyceae). *Harmful Algae*. 116: 102248.

Wüest, A., Piepke, G. and Van Senden, D.C., 2000. Turbulent kinetic energy balance as a tool for estimating vertical diffusivity in wind-forced stratified waters. *Limnology and Oceanography*, *45*(6), pp.1388-1400.

Wyatt, T. and Jenkinson, I.R., 1997. Notes on *Alexandrium* population dynamics. *Journal of Plankton Research*, *19*(5), pp.551-575.

Yan, Y., Lin, T., Xie, W., Zhang, D., Jiang, Z., Han, Q., Zhu, X. and Zhang, H., 2023. Contrasting mechanisms determine the microeukaryotic and Syndiniales community assembly in a eutrophic bay. *Microbial Ecology*, *86*(3), pp.1575-1588.

Yih, W. and Coats, D.W., 2000. Infection of *Gymnodinium sanguineum* by the dinoflagellate *Amoebophryasp*.: effect of nutrient environment on parasite generation time, reproduction, and infectivity. *Journal of Eukaryotic Microbiology*, *47*(5), pp.504-510.

Zhang, Y. and Prepas, E.E., 1996. Regulation of the dominance of planktonic diatoms and cyanobacteria in four eutrophic hardwater lakes by nutrients, water column stability, and temperature. *Canadian Journal of Fisheries and Aquatic Sciences*, *53*(3), pp.621-633.

Zhou, Y., Zhang, Y., Li, F., Tan, L. and Wang, J., 2017. Nutrients structure changes impact the competition and succession between diatom and dinoflagellate in the East China Sea. *Science of the Total Environment*, 574, pp.499-508.

Zingone, A. and Enevoldsen, H.O., 2000. The diversity of harmful algal blooms: a challenge for science and management. *Ocean Coast. Mange*. 43: 725-748.